HARDING (ANNOTATED)

US Department
of Transportation

**Federal Railroad
Administration**

Maglev Severe Segment Test Report

Office of Research and
Development
Washington, D.C. 20590

MAGLEV SYSTEM CONCEPT DEFINITION

**Foster-Miller, Inc.
350 Second Avenue
Waltham, MA 02154-1196**

DOT/FRA/ORD-92/01

November 1992
FINAL REPORT

MAGLEV SEVERE SEGMENT TEST REPORT

MAGLEV SYSTEM CONCEPT DEFINITION

Foster-Miller, Inc.
350 Second Avenue
Waltham, MA 02154-1196

November 1992

Final Report

Technical Report Documentation Page

1. Report No.	2. Government Accession No.	3. Recipient's Catalog No.
4. Title and Subtitle MAGLEV SYSTEM CONCEPT DEFINITION SEVERE SEGMENT TEST REPORT		5. Report Date November 1992 6. Performing Organization Code 30233
7. Author(s) See Preface		8. Performing Organization Report No.
9. Performing Organization Name and Address Foster-Miller, Inc. 350 Second Avenue Waltham, MA 02154-1196		10. Work Unit No. (TRAIS) 11. Contract or Grant No. DTFR53-92-C-00002
12. Sponsoring Agency Name and Address U.S. Dept. of Transportation, Federal Railroad Administration Office of Procurement Services, RAD-30, 400 Seventh St., SW Room 82222, Washington, DC 20590		13. Type of Report and Period Covered Final 11-01-91 through 10-31-92 14. Sponsoring Agency Code 5028-1
15. Supplementary Notes U.S. Department of Transportation, Transportation Systems Center Kendall Square, Cambridge, MA 02142		

This report presents Foster-Miller Maglev system performance results and cost analysis for the Severe Segment Test (SST) stipulated by the government.

The route design procedures are described and the resulting SST route geometries are defined for the two sets of requirements on ride quality ("Design Goal" and "Minimum Required"). Maglev vehicle performance in terms of speed, acceleration, trip time and power consumption is assessed for each of the two levels of ride quality. The effects of available power and ride quality on the overall system performance are evaluated in a parametric study.

Four very severe segments of the SST route are identified for detailed analysis. In these segments, passenger comfort is evaluated using a previously developed multi degree-of-freedom dynamic model which incorporates the guideway geometry, lateral and vertical irregularities and the primary and secondary vehicle suspensions.

Detailed cost analyses are presented to assess all capital, depreciation, operating and maintenance costs of the Maglev system for the SST route. At-grade and elevated guideway design options are evaluated to determine their impact on system cost.

Based on this work, several conclusions of practical interest are drawn, which include the following: travel times of 2 hr are achievable for the 800 km route; overall capital costs are on the order of $9.11 million per kilometer; and operation and maintenance costs, including depreciation, are on the order of 6.6 cents per passenger-kilometer.

17. Key Words	18. Distribution Statement
Maglev, Severe Segment Test, Ride Quality, Cost	

19. Security Classif. (of this report)	20. Security Classif. (of this page)	21. No. of Pages	22. Price
UNCLASSIFIED	UNCLASSIFIED	173	

SI* (MODERN METRIC) CONVERSION FACTORS

APPROXIMATE CONVERSIONS TO SI UNITS

Symbol	When You Know	Multiply By	To Find	Symbol
	LENGTH			
in	inches	25.4	millimeters	mm
ft	feet	0.305	meters	m
yd	yards	0.914	meters	m
mi	miles	1.61	kilometers	km
	AREA			
in^2	square inches	645.2	*millimeters squared*	mm^2
ft^2	square feet	0.093	meters squared	m^2
yd^2	square yards	0.836	meters squared	m^2
ac	acres	0.405	*hectares*	ha
mi^2	square miles	2.59	kilometers squared	km^2
	VOLUME			
fl oz	fluid ounces	29.57	milliliters	ml
gal	gallons	3.785	liters	l
ft^3	*cubic feet*	0.028	*meters cubed*	m^3
yd^3	cubic yards	0.765	meters cubed	m^3
	MASS			
oz	ounces	28.35	grams	g
lb	pounds	0.454	kilograms	kg
T	short tons (2000 lb)	0.907	megagrams	Mg
	TEMPERATURE (exact)			
°F	Fahrenheit temperature	5(F-32)/9 or (F-32)/1.8	Celcius temperature	°C
	ILLUMINATION			
fc	foot-candles	10.76	lux	l
fl	*foot-Lamberts*	3.426	*candela/m^2*	cd/m^2
	FORCE and PRESSURE or STRESS			
lbf	poundforce	4.45	newtons	N
psi	poundforce per square inch	6.89	kilopascals	kPa

NOTE: Volumes greater than 1000 l shall be shown in m^3.

APPROXIMATE CONVERSIONS FROM SI UNITS

Symbol	When You Know	Multiply By	To Find	Symbol
	LENGTH			
mm	millimeters	0.039	inches	in
m	*meters*	3.28	feet	ft
m	meters	1.09	yards	yd
km	kilometers	0.621	miles	mi
	AREA			
mm^2	millimeters squared	0.0016	square inches	in^2
m^2	meters squared	10.764	square feet	ft^2
m^2	meters squared	1.195	square yards	ac
ha	hectares	2.47	acres	mi^2
km^2	kilometers squared	0.386	square miles	
	VOLUME			
ml	milliliters	0.034	fluid ounces	fl oz
l	liters	0.264	gallons	gal
m^3	meters cubed	35.71	cubic feet	ft^3
m^3	meters cubed	1.307	cubic yards	yd^3
	MASS			
g	grams	0.035	ounces	oz
kg	kilograms	2.202	pounds	lb
Mg	megagrams	1.103	short tons (2000 lb)	T
	TEMPERATURE (exact)			
°C	Celcius temperature	1.8C + 32	Fahrenheit temperature	°F
	ILLUMINATION			
lx	lux	0.0929	foot-candles	fc
cd/m^2	candela/m^2	0.2919	foot-Lamberts	fl
	FORCE and PRESSURE or STRESS			
N	newtons	0.225	poundforce	lbf
kPa	kilopascals	0.145	poundforce per square inch	psi

* SI is the symbol for the International System of Units

(Revised January 1992)

PREFACE

This report presents the work performed by Foster-Miller and its team on the Maglev System Concept Definition Contract (No. DTFR53-93-C-00002) awarded by the Federal Railroad Administration under the National Maglev Initiative (NMI)). Mr. Michael Coltman of Volpe National Transportation System Center (VNTSC) in Cambridge, MA is the Contracting Officer's Technical Representative for the project, and Dr. John Harding of FRA is the chief scientist of NMI. In addition to these individuals several government personnel from U.S. Corps of Engineers, Department of Energy, Argonne National Laboratory and Department of Transportation were involved in review of the project.

The program manager of the Maglev System Concept Definition is Dr. Gopal Samavedam. The Principal Investigator of Severe Segment Test Studies is Mr. Steven Kokkins of Foster-Miller. Other Foster-Miller technical staff who contributed to this report are Messrs. Prem Pradhan, Doug Thomson and Adam Purple.

Significant contributions to this report are also made by our consultants Dr. Fred Blader, Mr. Larry Ishler and Mr. Robert Fowler.

Major contributions to this report on Train Performance Calculations and Costing have been made by our subcontractor, Parsons DeLeuw, under the overall direction of Mr. Duncan Allen, P.E.. Mr. Udayan Khan of Parsons DeLeuw has made significant technical inputs to this report.

TABLE OF CONTENTS

TABLE OF CONTENTS (Continued)

TABLE OF CONTENTS (Continued)

TABLE OF CONTENTS (Continued)

Section **Page**

LIST OF ILLUSTRATIONS

LIST OF ILLUSTRATIONS (Continued)

LIST OF ILLUSTRATIONS (Continued)

LIST OF ILLUSTRATIONS (Continued)

LIST OF TABLES

LIST OF TABLES (Continued)

LIST OF TABLES (Continued)

1. INTRODUCTION

The Severe Segment Test (SST), formerly known as the Hypothetical Route, was defined by the government to be used as a benchmark evaluation tool for the Maglev systems developed under the System Concept Definition programs. Parameters such as system performance, construction cost, and operating costs were evaluated for this route which contains various sequences of curves, grades, station stops and tunnel. The route was described in schematic form only, with detailed curve design and integration of ride comfort parameters left to the system contractor. Although the route as a whole is not intended to duplicate an actual transportation corridor end-to-end, many of the most demanding operating situations that could be encountered over such a route are included, hence the designation "Severe Segment Test."

The subject matter of the complete report is organized into three different areas:

- Part I - Route Design and System Performance.
- Part II - Vehicle Dynamics on Route Segments.
- Part III - System Capital and Operating Costs.

Part I of the report covers a major aspect of the effort which included the evaluation of system performance over the actual route. Since the route in turn was defined only in terms of overall schematic alignment, substantial work by the contractor was required to derive an actual path in three dimensions which limited the g-loads, jerk, roll rates, etc. to those contained in the standards used for ride quality (1-1). This effort consisted primarily of defining the spiral curve transitions and minimum arc segments needed for the smooth negotiation of the route. This was then followed by use of a Train Performance Calculator (TPC) program, especially developed by Parsons De Leuw, Inc. (PDI) for Maglev applications. (PDI is a major subcontractor to Foster-Miller for the Maglev development program.) The TPC was used to apply the system performance capabilities to Maglev consists traveling over the detailed route alignment developed by Foster-Miller, Inc. Results included time, speed, and energy consumption, as well as continuous plots of vehicle speed, acceleration and power used.

Foster-Miller developed two full sets of guideway curve geometries, each optimized for different ride quality levels. These groups of ride quality parameters had been determined at a Ride Quality Workshop held by the government in December of 1991, with participation of Foster-Miller and the other SCD contractors. The two principal ride classifications were intended to represent a "design goal" (comfortable) ride quality, and a "minimum acceptable" ride quality (less comfortable, but permitting higher speeds and accelerations).

The Foster-Miller curve design procedure, using both sets of ride quality definitions, took full advantage of the banking capability in the tilting bogie suspension of the Foster-Miller vehicle, which produced the highest possible speeds by utilizing the full "envelope" of the several ride quality parameters in each of the two cases above. Superelevation of the guideway, within limits deemed appropriate for safety in emergencies and maintenance, was also utilized.

The TPC was developed by PDI using advanced transit models as a starting point, then modified for Maglev application by incorporating new train resistance and braking scenarios, higher speed and accel/decel capability, etc. Comparisons were then made of all performance parameters over the SST route with different maximum electrical power levels and the two ride comfort levels.

Overall results when the procedures above are used show that trip times can be brought under 2 hr for the 800 km SST route with acceptable ride quality, and that Design Goal ride quality can be achieved with a trip time increase of only 7 or 8 min.

In Part II of the report, detailed dynamic analyses of the actual ride over four specific sections of the SST route were made by Dr. Fred Blader. These sections had been identified by the government specification for the Hypothetical Route activity. This dynamic modeling incorporated the complete set of suspension design parameters for the car bodies traveling in consist, including both the primary electrodynamic levitation/guidance/propulsion system (EDS), and the onboard tilting secondary suspension systems.

Results show the ISO ride quality levels are met with projected guideway deflections, and that the vehicles will safely negotiate even severe guideway irregularities, in some cases on the order of 25 mm (1 in.).

Part III of the report contains a summarized capital and operating cost analysis of the Foster-Miller Maglev system. In the case of capital costs for the guideway system (the major cost element), the cost breakdowns are first made in the SI format common to the existing Foster-Miller Final System Concept Definition Report, and then are reformulated referencing the Parsons Brinckerhoff (PBQ&D) Maglev Capital Costing Report, which used English units and also contained additional cost categories for highly route-specific items not directly associated with the Maglev system itself. The Foster-Miller costs are clearly identified as to where they fit in the PBQ&D format.

Also, an at-grade guideway design is costed in addition to the elevated guideway, so that where future route conditions permit, additional cost savings could be effected. Finally, costs for pile-type footings for use in poor soil conditions are included, to allow cost factoring where these might be required along a route.

Bottom line costs show that the completed two-way elevated guideway system, including all electrical, signal and power components (with substations) can be installed for $9.11 million per km on an average prepared ROW. The at-grade guideway, where appropriate, could save an additional $1.6 million per two-way km.

Direct operating and maintenance costs over the route are shown to be 2.8 cents per passenger-km before depreciation, and 6.6 cents/psgr-km including depreciation of all the capital equipment. This is very competitive with other high-speed transport modes.

The 75-passenger vehicles will average $6.5 million each, including full amenities, secondary suspension with tilting capability, and meeting all safety requirements.

In summary, the Foster-Miller Maglev system has successfully addressed the goals of the Severe Segment Test requirements, achieving high levels of performance and safety at low capital and operating cost.

References

1-1. U.S. Army Corps of Engineers, Huntsville Division, Hypothetical Route for Maglev System Concept Definition.

PART I

SST CURVE DESIGN AND PERFORMANCE EVALUATION

2. OVERVIEW OF SST CURVE DESIGN AND PERFORMANCE ANALYSIS

The major task in the physical definition of the route alignment consists of modifying the original, schematic route description furnished by the government so that smooth transitions take place continuously through the tangents and curves, allowing the highest possible speed over the route. The original route description, discussed in the subsections below, contained only constant radius turns through prescribed deviation angles, connected by tangents. Therefore, spiral transitions from tangent to the minimum radius curve were optimized for each individual turn, based on two different levels of multiple ride quality parameters cited in the previous section. These were the "Design Goal," the milder set, and "Minimum Required," a more aggressive set. These parameters will be detailed in the subsections that follow.

The important ground rules here were that the resulting curve had to include a section at the original minimum radius, and that the total deviation angle through the resulting turn would equal that of the original. Therefore, the overall alignment over the right of way would be equivalent to that of the original, except for the slight "pulling in" of the points of intersection (PIs), typical of normal surveying practice.

Foster-Miller developed computerized procedures to relate multiaxial interior vehicle "g" levels to speed and bank angle, as well as incorporating the simultaneous effects of vertical curves which appeared at intervals in the route. This not only enabled rapid determination or checking of speed limits at any points in the curve, but was also incorporated in a larger procedure to optimize the speed-bank angle relationship in order to take maximum advantage of the ride quality "envelope." This envelope included not only multiaxial "g" in the vehicle, but also vector sum combinations. These are quasi-steady state g-levels for a body moving on the route alignment. A later section of the report also shows a detailed dynamic analysis of the Maglev consist over certain sections of the SST route, and also over selected guideway deflections and irregularities.

Since the two different sets of ride quality parameters resulted in a slightly different optimum curve geometry for each turn, two full SST routes were generated in detail. This enabled a comparison to be made of the best possible performance for each level of ride quality, rather than over a single route geometry which might compromise performance in places for one or the other level of ride quality.

Also, an important feature of the Foster-Miller vehicles is the incorporation of up to 12 deg of tilt capability, which allows much greater freedom in allocating appropriate portions of the overall bank angles to both the vehicle and guideway. This had significant advantages over a non-tilting scheme:

- It minimized maximum superelevation of the fixed guideway to the 18 deg range, since the 30 deg bank angle limits for the "Min Required" ride quality case could be achieved by adding body tilt. This permits safe guideway maintenance activity and also use of the guideway for some modes of emergency egress.

- It permitted a much wider range of acceptable speeds through banked curves. In particular, if lower speeds through superelevated curves would be required either due to system congestion

or some degraded operating mode, these lower speeds would not result in unacceptable high inward lateral "g" since the car body could be "untilted" an appropriate amount.

The resulting curves, described by detailed point-by-point speed "gates," together with horizontal and vertical curve geometry, were then used as input to a multifunctional train performance calculation program (TPC), developed by Parsons De Leuw specifically for Maglev applications. All train operating characteristics are included: accel/decel capability, train weight, power consumption (including regeneration), and train resistance, including that due to magnetic, aerodynamic and multimode applied braking. The TPC was repeatedly run and checked over the complete SST route for several different maximum power levels, and for both sets of ride quality. Note that this latter really entailed running over the two individually optimized routes, each containing curve geometries optimized for the particular set of ride quality parameters.

The overall procedure, carried out at both Foster-Miller, Inc. facilities in Waltham, MA, and Parsons De Leuw, Inc., in Washington, D.C. is depicted graphically in Figure 2-1.

2.1 SST Route Description

The SST route was specified by the government (2-1) using a set of tangents linked at points of intersections (PIs) representing curves, and forming a 800 km long route. There are 52 horizontal and 59 vertical curves in the complete route. The minimum radius (R) and deflection angle (I) are specified for each of the curves in the horizontal plane. Each vertical curve is defined using a length of vertical curve (LVC). A major task effort in the SST evaluation consists of designing actual curve layouts for each of these PIs that maximize both speed and ride quality.

There are two in-line station stops. For the purposes of this analysis no dwell time has been allowed. Thus, the route consists of three segments. Each of the segments has characteristically different severity.

Segment 1 is 400 km long with 47 horizontal curves. This segment has 400m to 1,000m radii curves and -10 percent to 10 percent grades with a maximum grade change in the vertical plane of 10 percent. After completion of the curve design, or "characterization," this segment develops into a total of 345 arcs, spirals and tangents. Segment 2 is 70 km long with five horizontal curves. The segment has 1,200m to 10,000m radii curves and -1 percent to 1 percent grades. After characterization this segment develops into 37 arcs, spirals and tangents. Segment 3 is 330 km long with no horizontal curves. This segment includes a 5 km long tunnel.

2.2 Ride Quality Specifications

Three curve performance criteria representing differing levels of passenger ride quality were also specified by the government (2-2):

- "Design Goal."
- "Minimum Required."
- "Seat/Belt."

These specifications are listed in Table 2-1.

2.3 Headway

A traffic plan of vehicle consists and headway was developed which can handle a movement of 9,600 passengers per hour in each direction. For an eight-car consist with 75 seats per car, this requires maintaining an average headway, or departure interval, of 225 sec. For a four-car consist, average headway (departure interval) becomes 112 sec.

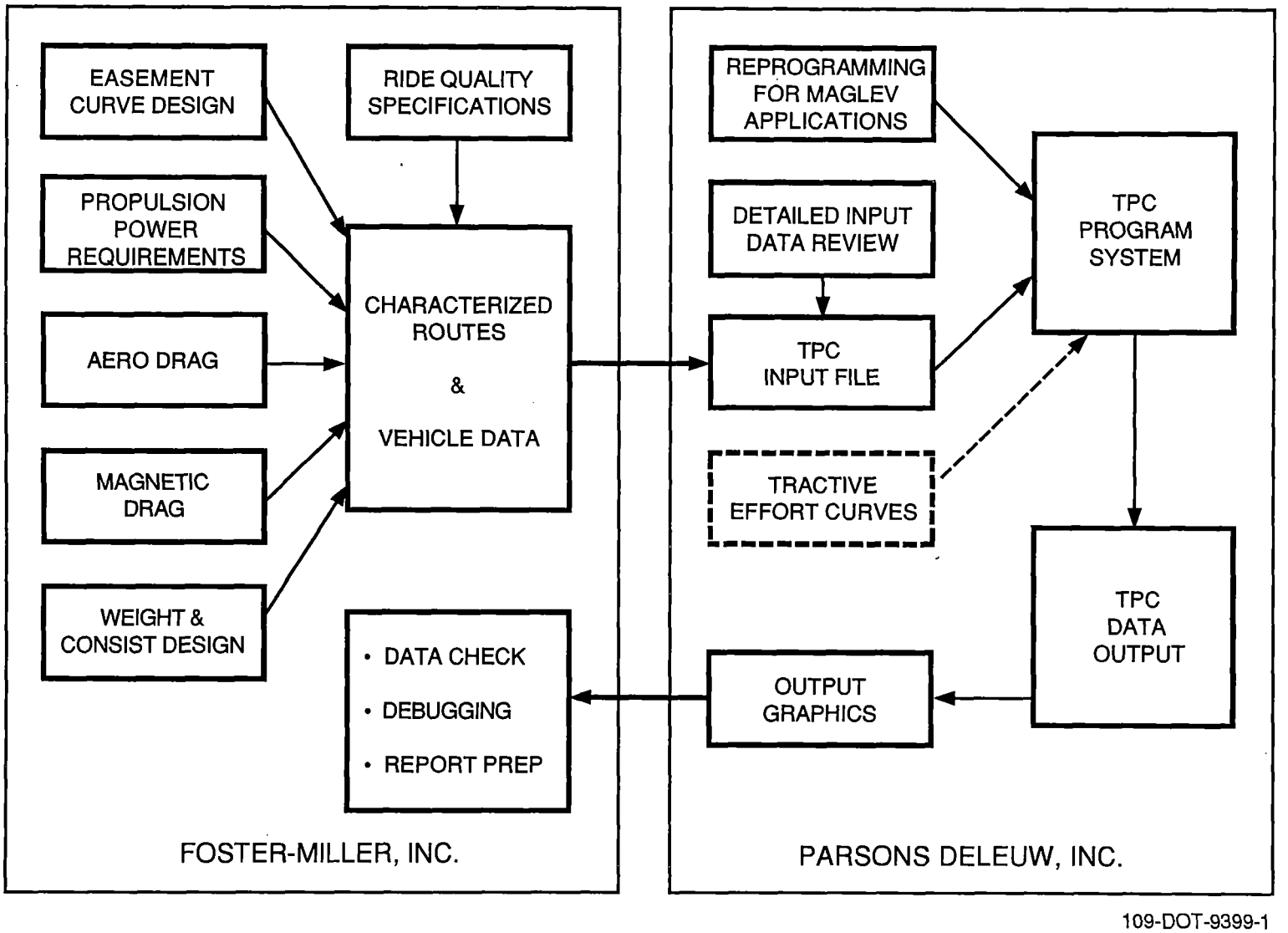

Figure 2-1. Curve Design and Performance Analysis Procedures and Management

Table 2-1. Curving Performance Table

Curving Performance (Average value for event for spiral or curve)			
Specifications	Design	Minimum Requirement	Seat/Belt
Lateral Curves			
Bank angle	24	30	45
Roll rate (deg/s)	5		10
Roll acceleration (deg/sec^2)	15		
Lateral Accelerations (Gs)	0.1	0.16	0.2
Vertical Accelerations			
Vertical (up)	0.05	0.1	0.1
Vertical (down)	0.02	0.3	0.4
Accelerations and Braking			
Normal	0.16	0.2	0.6
Vector Combinations			
Lateral/Longitudinal	0.2	0.3	0.6
Lateral/Vertical	0.2	0.3	0.4
Total	0.24	0.36	0.6
Jerk Rates (Gs/sec filtered at 0.3 hr) or JOLT (peak to peak Gs in 1 sec)			
Lateral	0.07	0.25	0.25
Vertical	0.1	0.3	0.3
Longitudinal	0.07	0.25	0.25

Actual headways enroute based on the maximum closure rate of succeeding consists can be shorter under certain conditions and will be explored later in the report.

2.4 Summary and Outline of SST Curve Design and Performance Analysis

The methods, original route description, design specifications and performance analyses mentioned above are detailed in the following sections of this report:

- First, the procedures for developing easement curves are described in Section 3.
- The detailed curve designs for Design Goal ride quality and Minimum Required ride quality specifications are then described in Section 4. The detailed characterized route is presented in the Appendix.

- The vehicle and consist performance over the complete route, including the power, speed and acceleration profiles are then incorporated in the TPC simulation. The TPC overview is given in Section 5 and the results from the simulation efforts are then described in Section 6.

- Tradeoff analyses are then performed by comparing the effects of changes in power, ride quality and vehicle consist. Section 7 discusses the results of these tradeoffs, and also includes recommendations for further improvements in route analysis.

- Finally, the Appendix contains all intermediate route analysis data, such as the route description and route characterization.

References

2-1. "Hypothetical Route for Maglev System Concept Definition Contract, DTFR53-92-C-00002," Transmittal Letter dated January 28, 1992 from Mr. Michael Coltman, COTR, FRA/VNTSC.

2-2. "Minutes of December 16, 1991 Ride Quality Workshop," Transmittal Letter dated January 10, 1992 from Mr. Michael Coltman, COTR, FRA/VNTSC, and Dr. John Harding, Chief Scientist, NMI/FRA.

3. EASEMENT CURVE GENERATION PROCEDURE

3.1 Overview

The development of the easement curves is described in the following subsections. First, some examples of the specified route data are presented. Then, the geometric components (points, tangents, bank angles, spirals, and arcs) of the easement curves to be developed are defined. The design of the easement curve (spirals) and the minimum radius curves (arcs) is based on the target ride quality of the system. The equations used to evaluate these ride quality parameters in the spirals and the arcs are then presented. Lastly, the chosen curve design procedure used to develop the given route data is described.

3.2 Description of the Specified Route Data

The SST route specification (3-1) gives the surveying stations for the horizontal and vertical points of intersection of tangents which develop the route. The horizontal points of intersection (PI) have data defining the minimum radius at the curve (R in meters) and deflection angle (I, in degrees) between the surveyed tangents. Table 3-1 gives an example of the specified horizontal data, in terms of running station (in meters), shown in a tabular form. For complete details of these specifications, see (3-1) and Tables 17 and 18 in Appendix A.

For the vertical transitions of various segments, the station of point of vertical intersection (PVI), elevation (EL in meters), segment grade (in percent), and length of the vertical curves (LVC in meters) are provided in the specifications. Some examples of specifications are shown in Table 3-2.

Figure 3-1 shows data for a typical horizontal PI. The dotted line shows the curve developed to allow a smooth transition between the tangents.

3.3 Geometric Entities in Easement Curves

During the process of developing the easement curves the following sections are defined:

- A transition spiral (SPIRAL 1) is introduced near the end of the first tangent (TANGENT 1). SPIRAL 1 has an infinite radius near TANGENT 1, which reduces to the given minimum radius R (as in Table 3-1) near its end.

- A minimum radius curve with constant route data specified radius (ARC) is added at the end of the SPIRAL 1.

- A second transition spiral (SPIRAL 2) is introduced at the end of the ARC connecting near the end of the second tangent (TANGENT 2). SPIRAL 2 begins at the minimum radius and increases to an infinite value as it approaches TANGENT 2.

Table 3-1. Examples of Specification of Horizontal PIs

PI No.	Station	R	I	PI No.	Station	R	I
1	9,000	400	40	27	231,000	800	70
2	16,000	500	20	28	238,000	900	65
3	22,000	700	30	29	243,000	600	30
-	-	-	-	-	-	-	-
-	-	-	-	-	-	-	-
-	-	-	-	-	-	-	-
23	206,000	500	35	49	420,000	3,000	15
24	212,000	700	15	50	434,000	5,000	10
25	217,000	800	10	51	449,000	8,000	15
26	221,000	1,000	20	52	469,000	10,000	10

Table 3-2. Examples of Specification of Vertical Intersections

Station	EL	LVC	Grade	Station	EL	LVC	Grade
0.0	1,680	0	3.5	236,000	1,865	500	-1.5
10,000	2,050	700	-2.0	245,000	1,730	200	0.0
17,000	1,910	600	2.5	257,000	1,730	500	-3.5
25,000	2,110	600	1.0	262,000	1,555	400	-1.0
-	-	-	-	-	-	-	-
-	-	-	-	-	-	-	-
-	-	-	-	-	-	-	-
215,000	2,085	200	-1.0	459,000	1,490	8,000	1.0
222,000	2,015	200	0.0	475,000	1,650	20,000	0.0
230,000	2,015	400	-2.5				

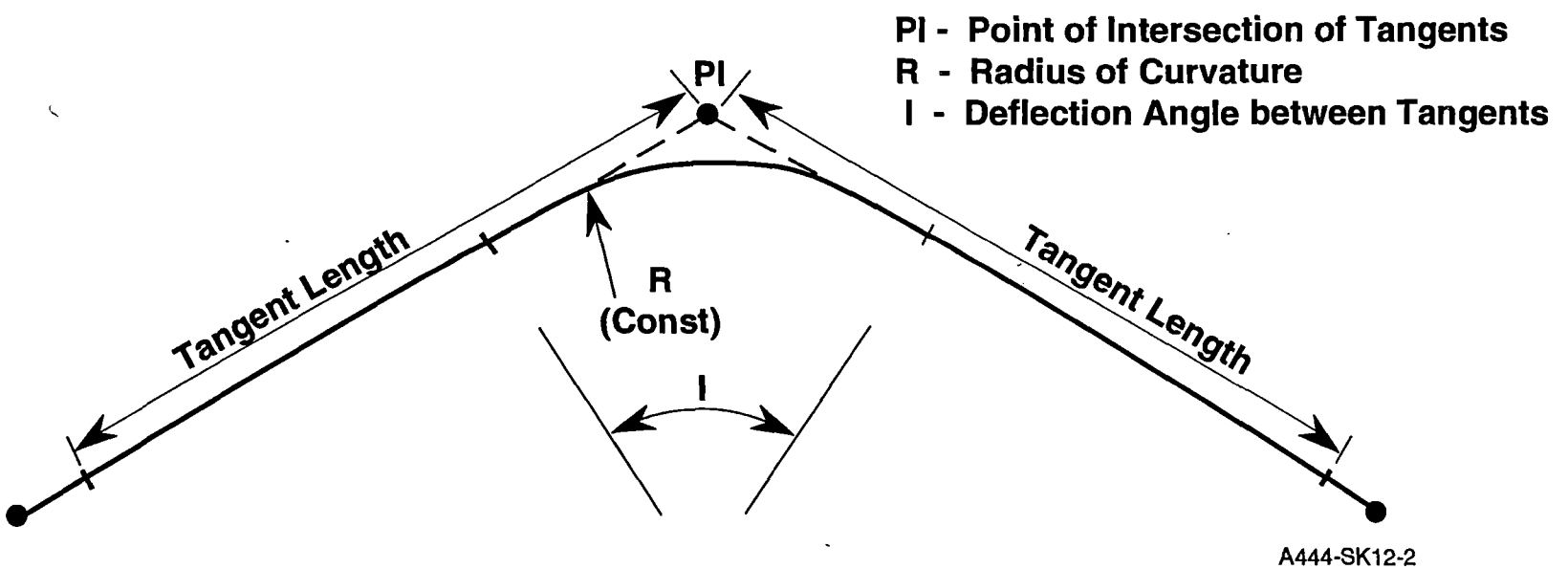

Figure 3-1. Typical Point of Intersection Specification

The specification requires maintaining the minimum radius at each PI. The above procedure forces the easement curve design to maintain the radii specified in the Hypothetical Route Drawing (3-1) (see also Table 18 in Appendix A). The original TANGENT 1 and TANGENT 2 are slightly shortened to accommodate the spirals and the ARC. The following points are also defined to clarify the geometry:

- TS - Point between TANGENT 1 and SPIRAL 1.
- SC - Point between SPIRAL 1 and ARC.
- CS - Point between ARC and SPIRAL 2.
- ST - Point between SPIRAL 2 and TANGENT 2.

Figure 3-2 shows the geometric entities, TS, SC, CS, ST, TANGENT 1, SPIRAL 1, ARC, SPIRAL 2 and TANGENT 2 which constitute each of the PIs after developing the easement curves. Each assembly of these entities is termed an Easement curve (or Transition curve) in this report.

Loss of Stationing

There is a loss of stationing (distance) at each PI due to the rounding of the corner. The sum of segments shown in Figure 3-2 will be slightly smaller than the sum of tangents shown in Figure 3-1. This loss is considered in defining the stationing of all points defining the easement curves. The cumulative loss of stationing totals a few kilometers in length for the characterized SST routes.

3.4 Normal Speeds and Accelerations in Easement Curves

To negotiate the easement curves, the vehicle is decelerated ahead of the TS point within the first tangent segment (TANGENT 1). The vehicle enters the SPIRAL 1 with V_{ts} speed at point TS. The deceleration continues until the vehicle reaches the point SC where its speed is V_{sc}. In the ARC the speed is maintained at V_{sc} until the point ST is reached. The vehicle then accelerates to its full speed of 134.1 m/sec. Due to the curve design procedure used, the speed at point ST automatically reaches V_{ts}. Figure 3-3 shows typical speed and acceleration profiles in an easement curve.

3.5 Description of the Bank Angles

To achieve the specified acceleration limits for passenger comfort while maximizing vehicle performance, the vehicle requires banking at each curve. This banking is achieved by a combination of vehicle tilting and guideway superelevation as shown in Figure 3-4. The lateral and vertical accelerations are functions of this total bank angle.

Typically, the guideway easement curves are designed such that there is no guideway banking in the tangent sections. Banking starts as the vehicle enters the easement curves. The ride comfort limited roll and roll acceleration rates are maintained during the transition. The vehicle reenters the tangent section after transition, with zero bank angle. The exceptions to this rule are severe curves with small deflection angles (I). In these locations a banking of the vehicle in the tangent section is required to traverse the sharp radius at maximum speed.

In situations where the given curve radius is small, the required bank angle is high. If deflection angles required for such curves are also small, then the route design will exceed the specified deflection in the distance required to complete banking and unbanking. A solution to this type of problem is to introduce some vehicle tilting prior to the TS point. In tangent sections the vehicle can be banked to 5.7, 9.2 or 11.5 deg without violating "Design," "Min Reqd," or "Seat-belt" acceleration limits, respectively. This banking of the vehicle in the tangent segment before entry to the spiral

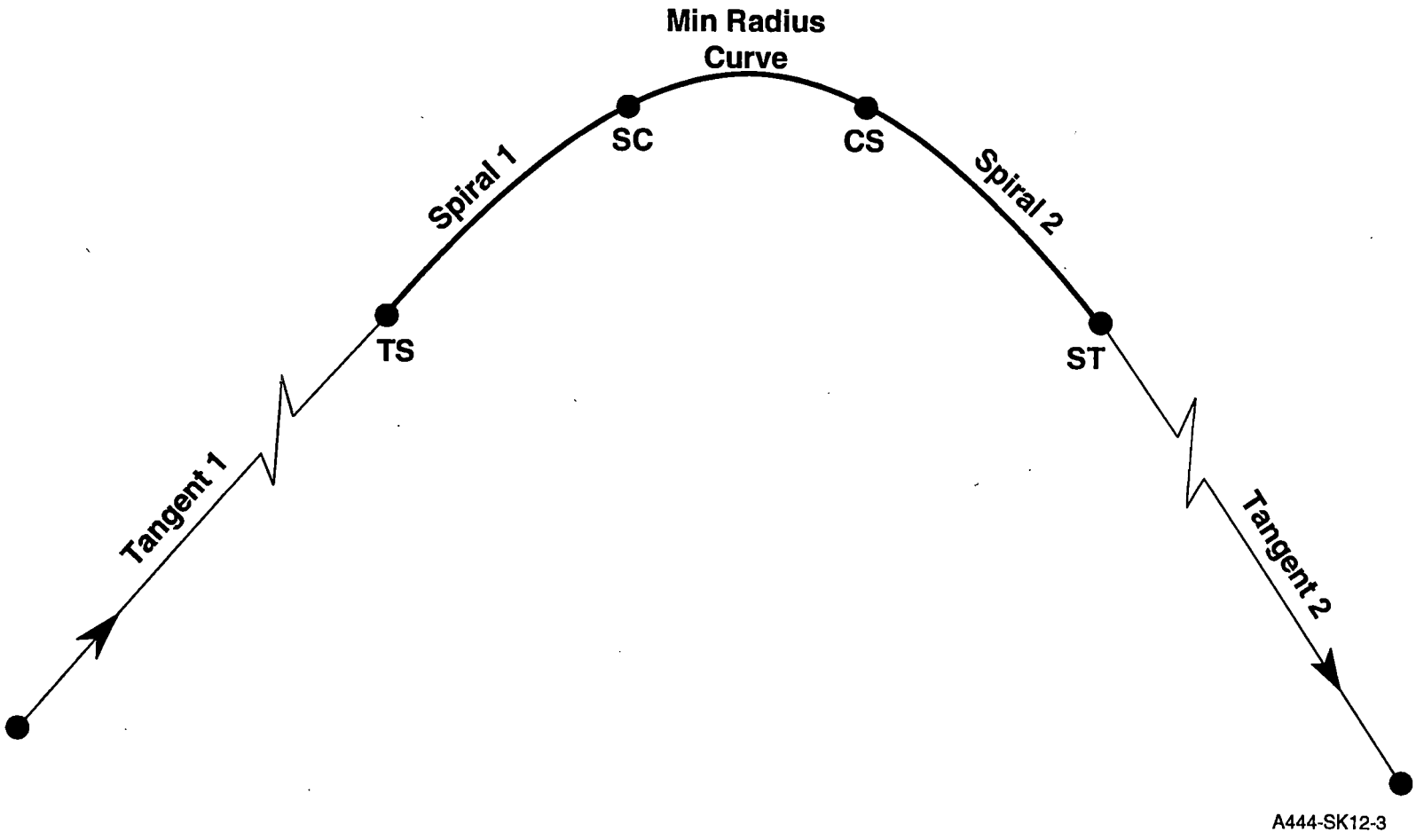

Figure 3-2. Geometric Entities of an Easement Curve

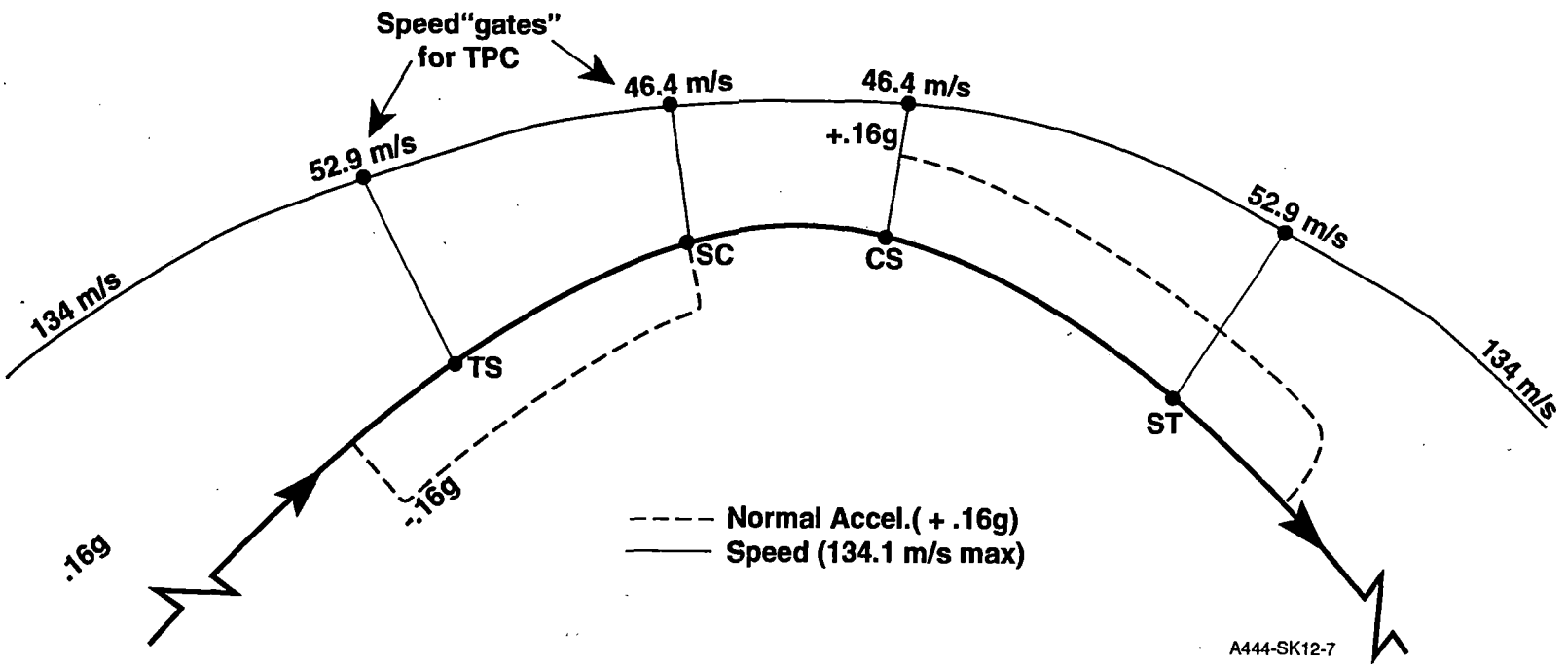

Figure 3-3. Typical Speed and Acceleration Profiles in an Easement Curve

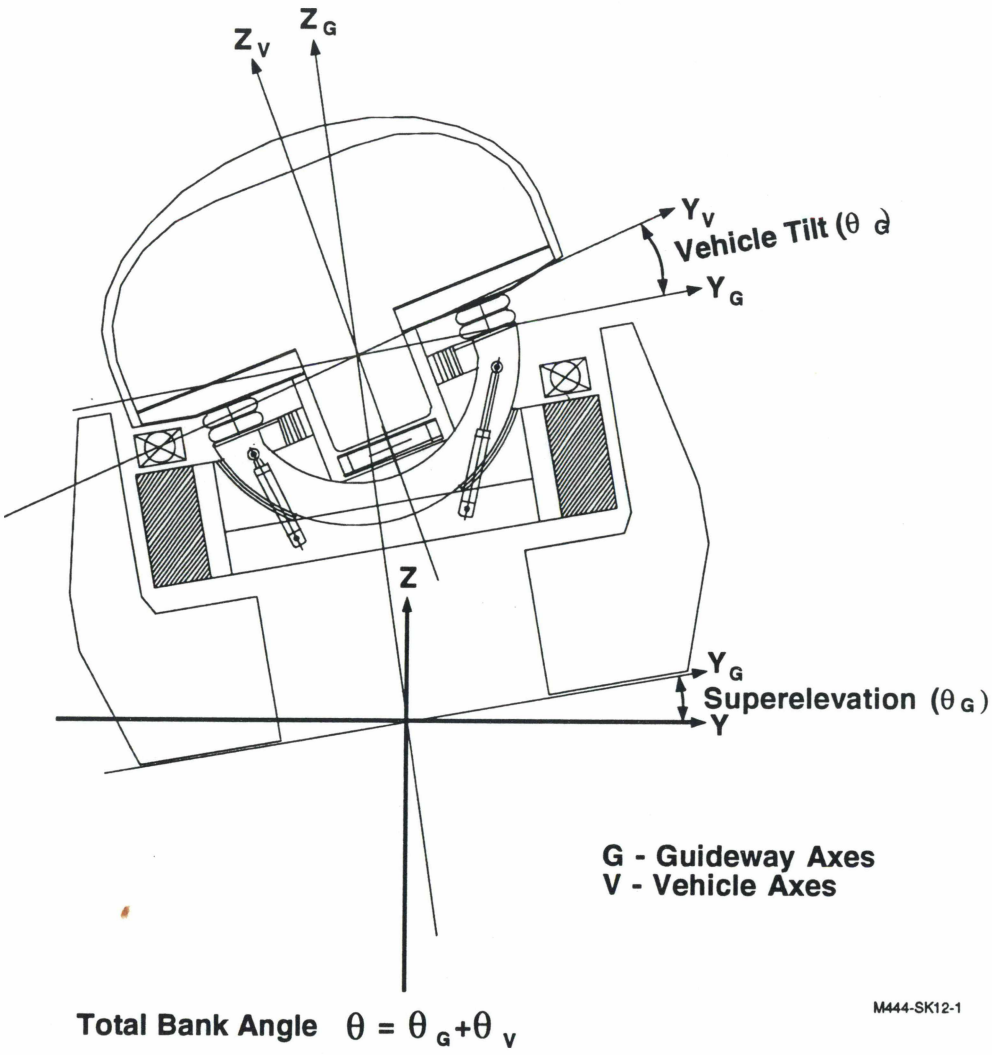

Figure 3-4. Banking of Vehicle and Guideway

is termed "prebanking" here. Figure 3-5 shows the effect of using prebank to reduce the deflection angle.

If the vehicle is prebanked before entry into a transition spiral, then the rolling required in the spiral section is reduced. This reduces the transition spiral length, which reduces the deflection angle in a curve, as shown in Figure 3-5. The disadvantage of prebanking is the introduction of several changes in sign in the lateral accelerations during easement curve negotiation. This may deteriorate the ride quality and hence may not be satisfactory, unless maximizing the V_{sc} is the main goal. Prebanking has been introduced in many instances of curve design in the SST route characterization, because of the severe nature of many curves.

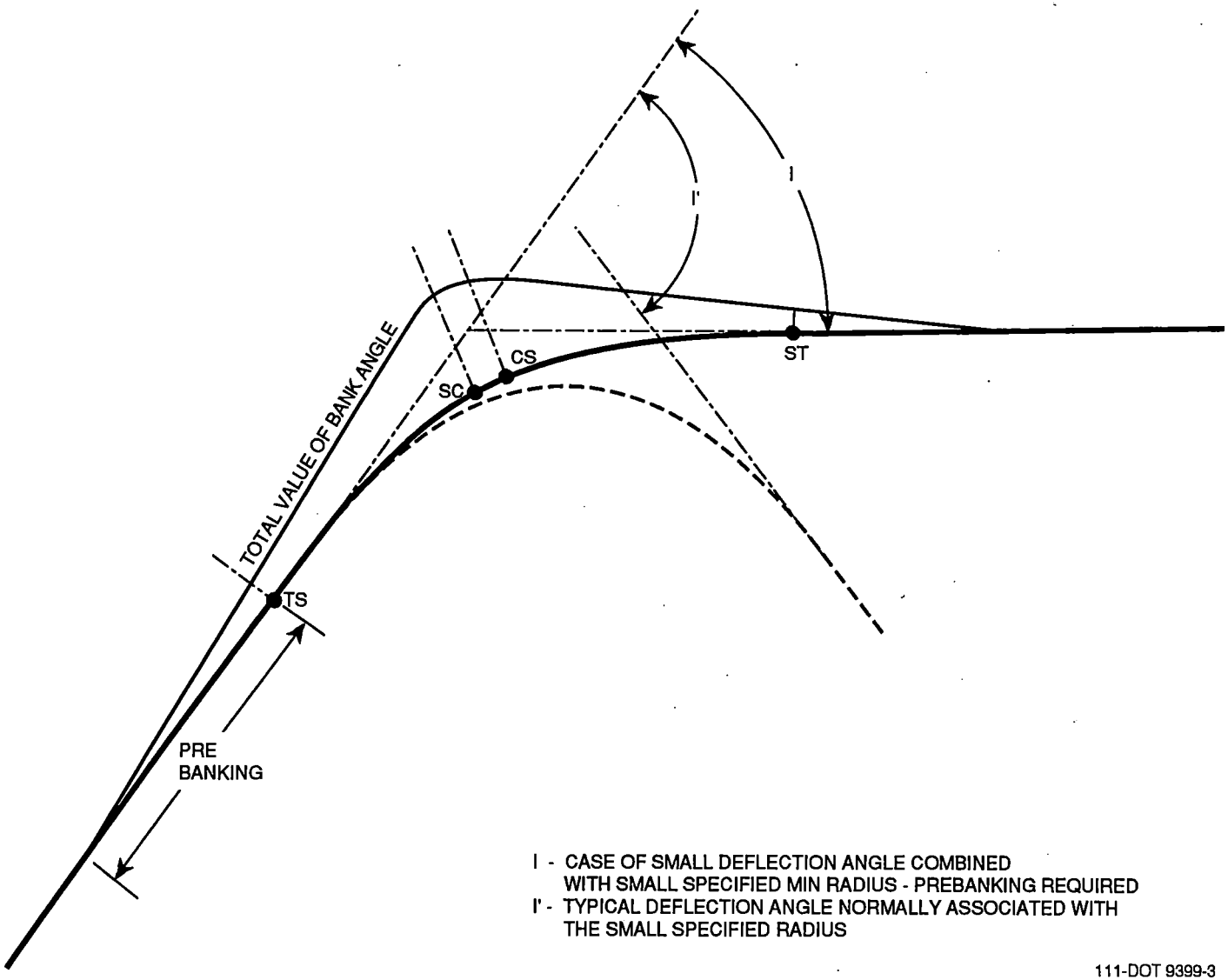

Figure 3-5. Reducing Deflection Angle Using Prebanking

3.6 Description of Spirals

Symmetric cubic parabolas (3-2) have been used to develop entry and exit spirals in the easement curves. The cubic parabola commonly used in railroad design has following convenient points for measuring and laying out the geometry in the field:

- Offsets from tangents vary as the cube of distance.
- Midordinates increase at a constant rate.
- Deflection angles vary as square of distance.
- Degree of spiral increases at a uniform rate.

It is assumed that to develop the easement curve geometry "analysis of a point in motion" will be acceptable. It is also assumed that the two way traffic may be required at all curves and thus they need to be symmetric in design. In addition to the curve design ride quality checks, a detailed vehicle motion ride quality analysis is performed (see Part II). In actual practice the passenger comfort level can be improved using the vehicle control system.

In traditional railroad engineering the bank angles are small. The more easily measurable parameter is the superelevation (difference in height of rails). This is not a convenient measure in the Maglev concept because of the detailed analysis required for evaluating acceleration components at all locations in the curve. To evaluate the acceleration components at all points in the spiral, bank angles are more convenient parameter for Maglev guideway design.

3.7 Evaluation of Acceleration in Curves

Easement curves are analyzed for ride quality using equations of circular motion. For the purposes of curve development it is assumed that at any point in the transition curve the bank angle and the vehicle speed are fixed.

Figure 3-6 shows the forces acting on a body (passenger) while in a turn. A right handed 3-D coordinate system is used to evaluate the forces. Positive Z is considered the direction of vehicle motion. The following symbols are used:

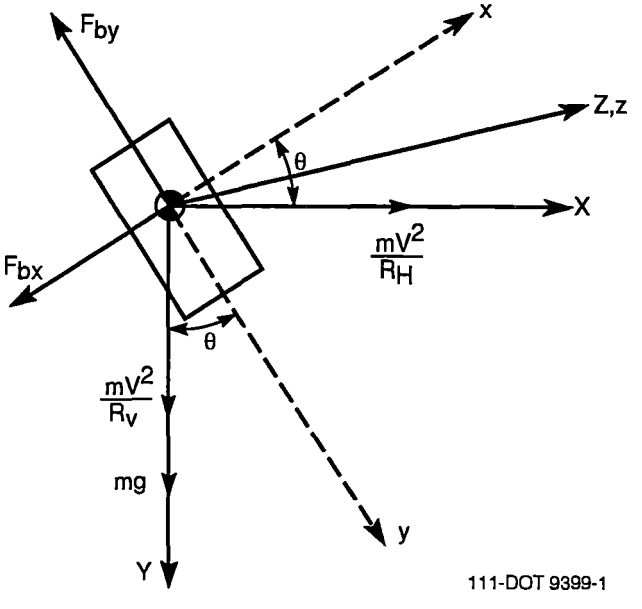

Figure 3-6. Forces Acting on a Passenger in a Curve

θ = Ivstantaneous bank angle
R_H = Instantaneous horizontal radius
R_V = Instantaneous vertical radius
m = Passenger mass
g = Accel due to gravity
XYZ = Global coordinate system
xyz = Rotating coordinate system
A_{lat} = Lateral accelerations in G's
A_{vert} = Vertical accelerations in G's.

In the state of equilibrium the sum of component forces, which is zero, can be written as:

$$\Sigma F_x = -mg \sin\theta + \frac{mV^2}{R_H}\cos\theta - F_{bx} - \frac{mV^2}{R_V}\sin\theta = 0$$

$$\Sigma F_y = -F_{by} + mg \cos\theta + \frac{mV^2}{R_H}\sin\theta + \frac{mV^2}{R_V}\cos\theta = 0$$

From the above equations, the components of accelerations acting on the passenger can be determined from the seat forces Fbx and Fby) acting on the passenger. The lateral acceleration in G's is

$$A_{lat} = \frac{\ddot{x}}{g} = -\sin\theta + \frac{v^2}{gR_H}\cos\theta - \frac{v^2}{gR_V}\sin\theta$$

The vertical acceleration in G's is

$$A_{vert} = \frac{\ddot{y}}{g} = + \cos\theta + \frac{v^2}{gR_H}\sin\theta + \frac{v^2}{gR_V}\cos\theta$$

These equations consider the sign convention of R_V to be negative cresting. If the sign convention of R_V is taken positive cresting then the above acceleration equations can be written as:

$$A_{lat} = -\sin\theta + \frac{v^2}{gR_H}\cos\theta + \frac{v^2}{gR_V}\sin\theta$$

$$A_{vert} = \cos\theta + \frac{v^2}{gR_H}\sin\theta - \frac{v^2}{gR_V}\cos\theta$$

Both sign conventions are commonly used by various disciplines. Since the hypothetical route drawing only specifies LVC and grades, any sign convention can be used.

The acceleration along z-axis is termed normal acceleration (A_{norm}). The ride quality evaluation needs computing all three acceleration components individually and A_{lat}/A_{norm}, A_{lat}/A_{vert} and the vector sum of all three components. Checks are required at all curves during transition curve design to permit maximum vehicle speed while maintaining the ride quality specified in the guidelines. The speed-bank angle-acceleration relationships described in this subsection were incorporated as an integral part of the computerized route design process.

The desired Maglev performance requirements of high speed with acceptable levels of passenger comfort generally require very large radius turns and/or large total bank angles. Large bank angles may be required to satisfy both the performance and ride quality requirements even with radii in the range found in the SST route.

Generally, however, these bank angle requirements cannot be satisfied by superelevation alone. A large superelevation (20 deg or more) becomes difficult for maintenance vehicles and personnel to negotiate safely, and requires a high minimum vehicle speed for passenger comfort. Further, high superelevation can adversely affect the vehicle's stability and safety of egress when stopped on a turn.

Design studies were undertaken to determine the effects on performance of combined superelevation and vehicle tilting, using the following practical limits for bank angle:

- Guideway superelevation limited to 12 to 18 deg.
- Vehicle tilting to supply an additional 10 to 12 deg, yielding an upper limit for total bank angle of approximately 30 deg.

The preceding equations were used to then illustrate the relationship between speed, bank angle and acceleration. The results of this study are shown in Figures 3-7 to 3-9, which plot the acceleration levels achieved in turn radii of 500m, 1,000m and 2,000m, respectively. The results show, for example, that in a 500m radius turn with the "Design Goal" ride quality limits, the maximum speed at 30 deg of bank is limited to less than one half the design cruise speed of 134 m/s. At greater speeds, the passenger acceleration levels become unacceptable. Even in the larger radius turns, the cruise speed cannot be maintained without violating one or more of the desired limits on passenger acceleration. The minimum turn radius required to maintain cruise speed at 30 deg of bank without exceeding the "Design Goal" levels of passenger comfort is approximately 2,825m (9,367 ft).

It is interesting to note that further increases in bank angle beyond 30 deg do not appreciably increase the allowable vehicle speed. For example, based on the vector sum limit of 0.2g the maximum speed in the 2,000m turn at 30 deg of bank is approximately 113 m/sec. Increasing the bank angle to get to the maximum speed allowed by the 0.2g vector sum limit (at 33.6 deg) will

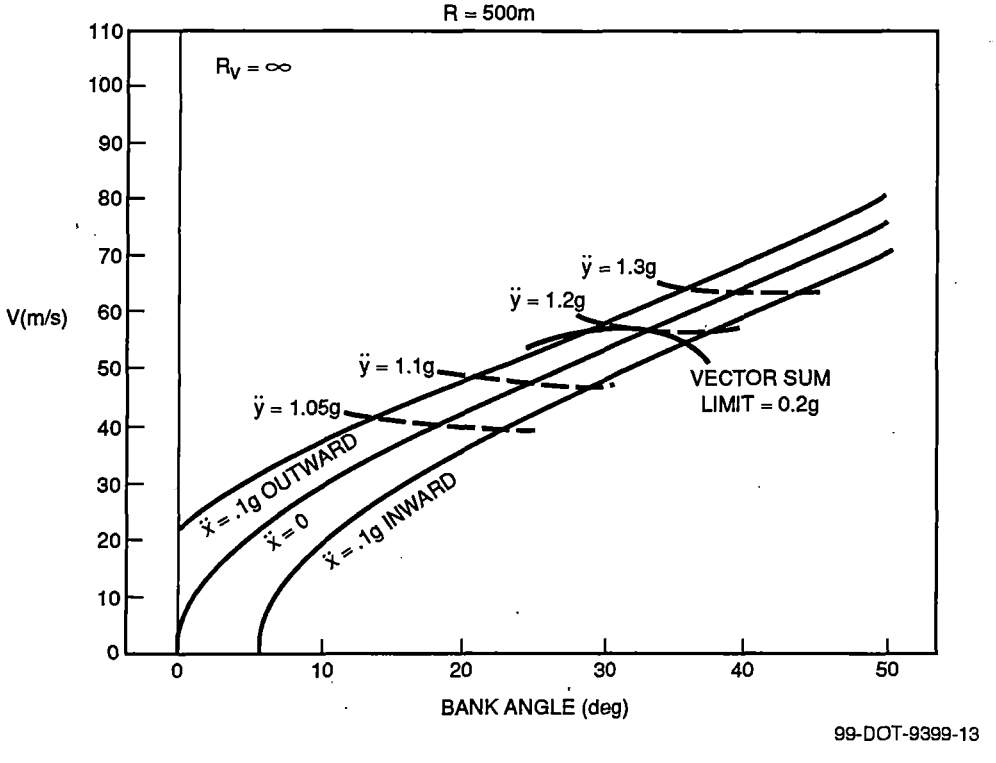

Figure 3-7. Relationship between Speed, Bank Angle and G-Load, R = 500m

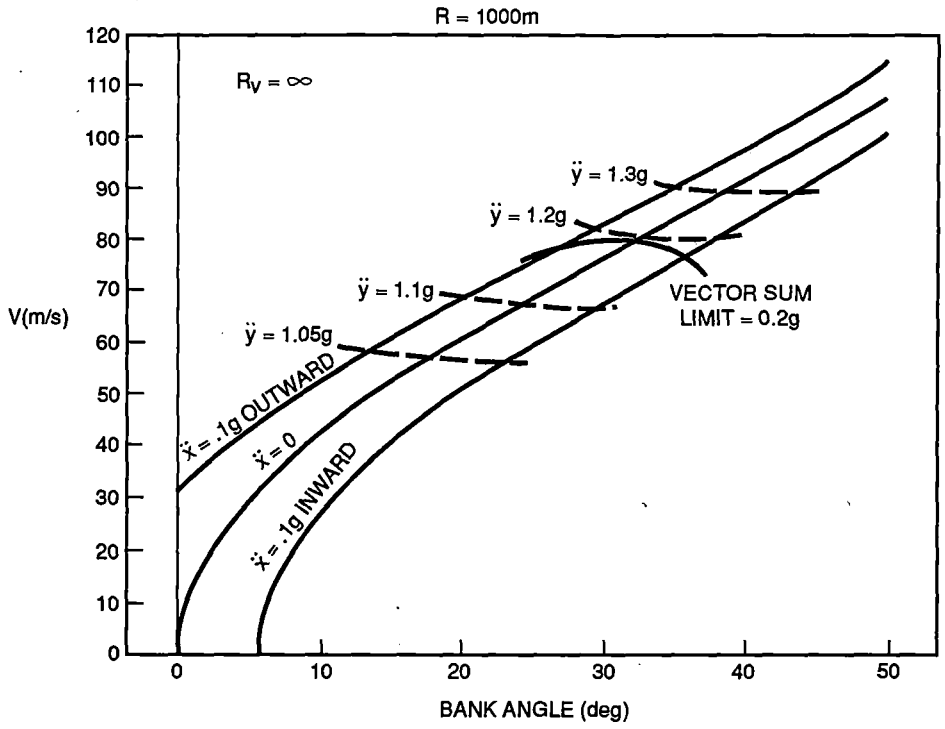

Figure 3-8. Relationship between Speed, Bank Angle and G-Load, R = 1,000m

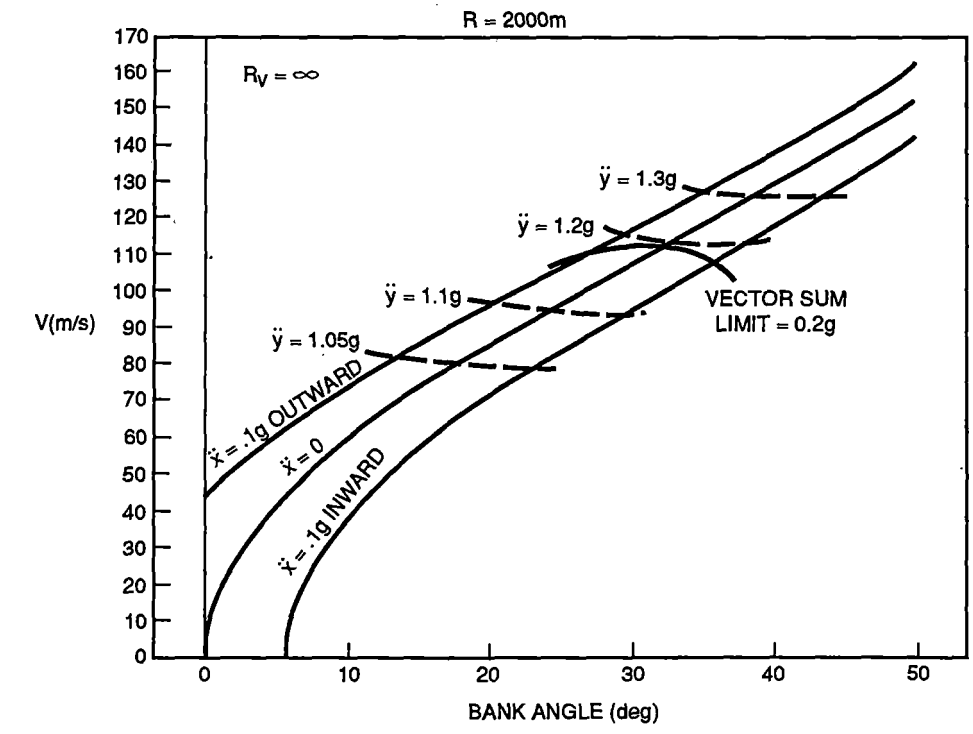

Figure 3-9. Relationship between Speed, Bank Angle and G-Load, R = 2,000m

increase the maximum speed to only 114 m/sec, a change of less than 1 percent. Any further increases in speed would come at the expense of passenger comfort. Similar results are obtained at other turn radii.

3.8 Ride Quality Parameters

The ride quality specifications impose geometric limitations on the guideway design, particularly due to the limits on the bank angles. The bank angles and subsequently, the spirals and arc at each PI will be geometrically unique for each different ride quality level. Separate routes were designed for each ride quality (see Table 2-1). This permitted tradeoff analyses for system performance and construction cost estimations. The following two ride qualities were used to design the curves for SST simulation.

"Design Goal" Ride Quality

When the design goal ride quality specifications, as listed in Table 2-1, are used as limits, the guideway bank angle is limited to 24 deg. This limit is reached in most cases except where the deflection angles are very small, or in situations where prebanking was introduced to achieve better performance. The roll rate reaches 5 deg/sec in the spiral during entry and exit. This is further controlled by the roll acceleration limit of 15 deg/sec^2. In negative g situations the vertical g is limited to 0.95g (0.05g up). In positive g situations the vertical g is limited to 1.2g (0.2g down). Both the lateral and vertical jerk limits were checked to be consistent with the Design Goal ride quality specifications. Normal acceleration and deceleration of 0.16g is used for maximizing spiral performance. A jerk limit of 0.07g is used during TPC runs.

"Minimum Required" Ride Quality

When the minimum required ride quality specifications, as listed in Table 2-1, are used as limits, the guideway bank angle is limited to 30 deg. The roll rate reaches 10 deg/sec in the spiral during entry and exit. This is controlled by the roll acceleration limit of 30 deg/sec^2. This limit was introduced for consistent design approach, though not required in the specifications. In negative g situations the vertical g is limited to 0.9g (0.1g up). In positive g situations the vertical g is limited to 1.3g (0.3g down). Both the lateral and vertical jerk limits were checked to be consistent with the Minimum Required ride quality specifications. Normal acceleration and deceleration of 0.2g is used for maximizing spiral performance. Jerk limits of 0.07g and 0.25g are used during TPC runs.

Curves Comparison

The curves for individual ride qualities have different maximum bank angles, different roll rates and also different roll acceleration rates. The spiral entry and minimum curve speeds are also different in each ride qualities category. Each curve is designed semiautomatically using human interactive optimization approach. Figure 3-10 shows the plan view of two horizontal curves for Design Goal ride quality (noted with superscript 0) and Minimum Required ride quality (noted with superscript 1) specifications. In general, it has been found that the more aggressive ride quality results in shorter spirals and longer arc section at the easement curve.

3.9 Easement Curve Design Procedure

The easement curve design steps can be summarized as:

- Designing the blending spirals (SPIRAL 1 and SPIRAL 2).
- Developing the required minimum radius curve (ARC).

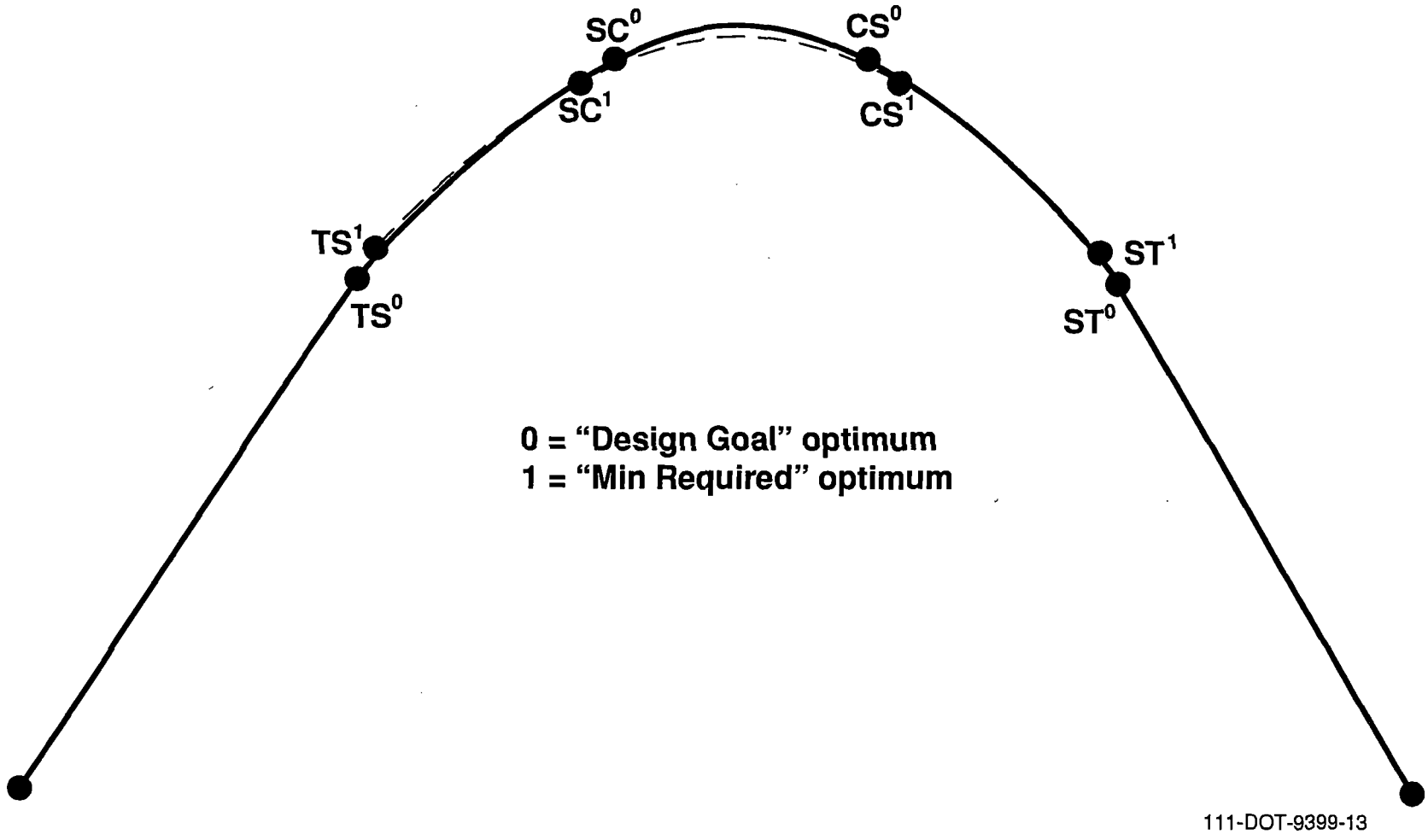

Figure 3-10. Comparison of Schematic Curves Layouts Optimized for Ride Quality

- Optimizing the easement curve for maximum vehicle speed within the allowable ride quality guidelines.

3.10 Spiral Design Procedure

The spiral design procedure can be divided into the following three simpler steps.

- Find curve bank angle ranges for all curve speeds, and select a bank angle and a speed for each curve.
- Determine the time to complete banking to the selected curve bank angle.
- Calculate spiral length and spiral entry speed, given the spiral exit speed and the time to negotiate the spiral.

Bank Angle Ranges

In the first step, using the desired acceleration limits, the allowable vehicle speed and bank angles are evaluated. This is done using uniform circular motion equations. The effect of the vertical radius is also considered wherever necessary, such as PI No. 5 at station 40,000 where both vertical and horizontal transitions occur. This study summarizes the speed range allowed for any given bank angle.

Time to Complete Banking

In the second step, the maximum curve bank angle (θ_{max}) and maximum vehicle speed for a curve (V_{sc}) are selected. From the roll rate ($\dot{\theta}$) and roll accel ($\ddot{\theta}$) limits, the time (t_s) to complete maximum banking (θ_{max}) is evaluated. This controls the minimum length allowed for the transition spiral for the selected banking angle (θ_{max}). This minimization of the spiral length is important as the cost of laying out a curved section will be higher than the cost of laying out a tangent section. Thus, the t_s will be:

$$t_s = t_1 + t_2 + t_3$$

where:

t_1 = Time to reach max roll rate ($\dot{\theta}$) using the roll accel ($\ddot{\theta}$)

t_2 = Time to roll at $\dot{\theta}$ to achieve θ_{max}

t_3 = Time to decrease roll rate to zero, using the roll accel ($\ddot{\theta}$)

Figure 3-11 shows the roll rates and roll acceleration profiles used to achieve the required bank angle at each curve:

The roll rates of Figure 3-11 define the profile of the bank angles in the easement curve as shown in Figure 3-12.

Spiral Length and Spiral Entry Speed

Having known the maximum speed (V_{sc}) in the minimum specified radius portion of the curve and the time required to traverse the spiral (t_b), the spiral entry speed (V_{ts}) can be evaluated for a given normal acceleration (a_n):

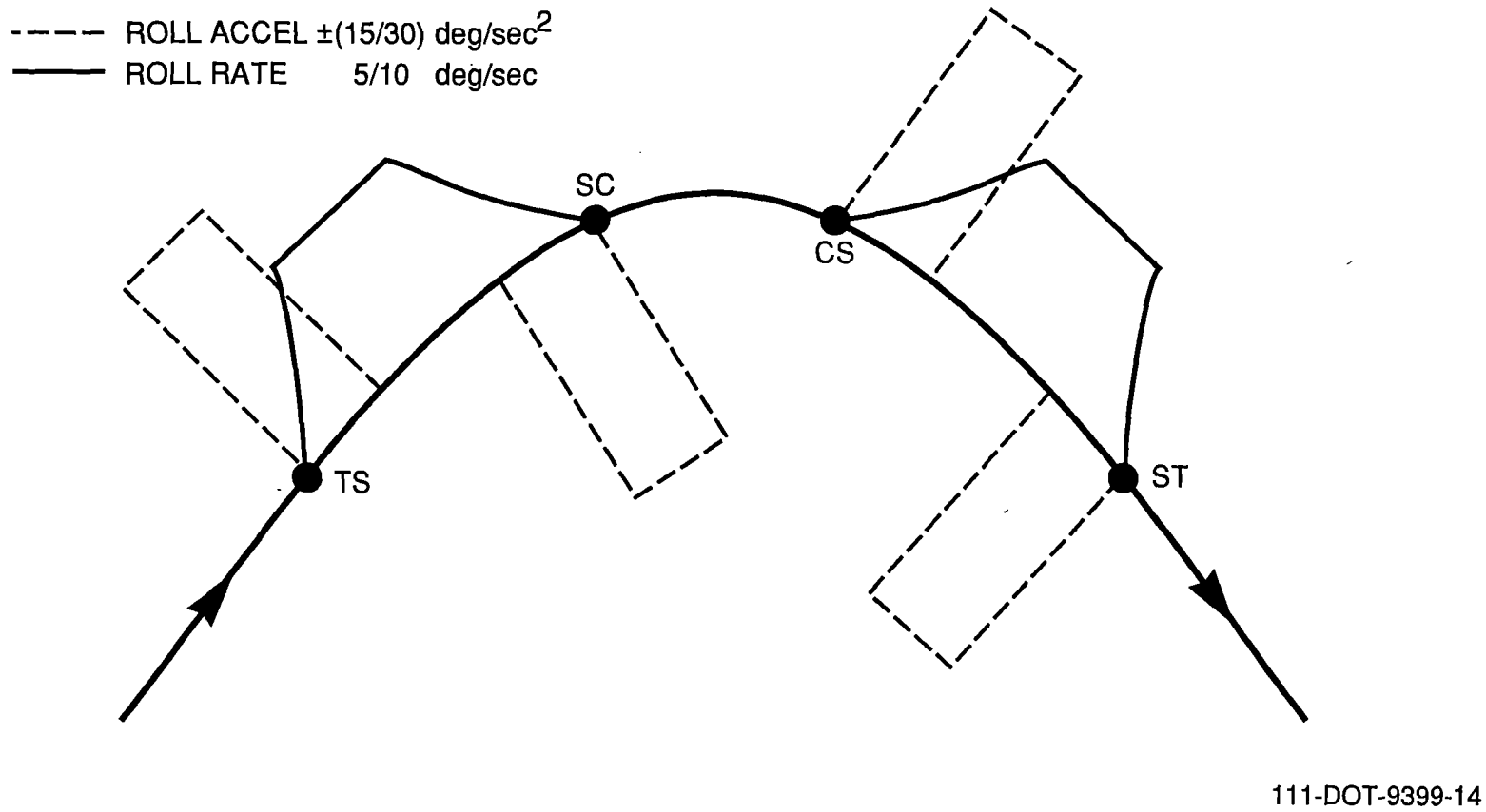

Figure 3-11. Typical Roll Rates and Roll Accel Profiles

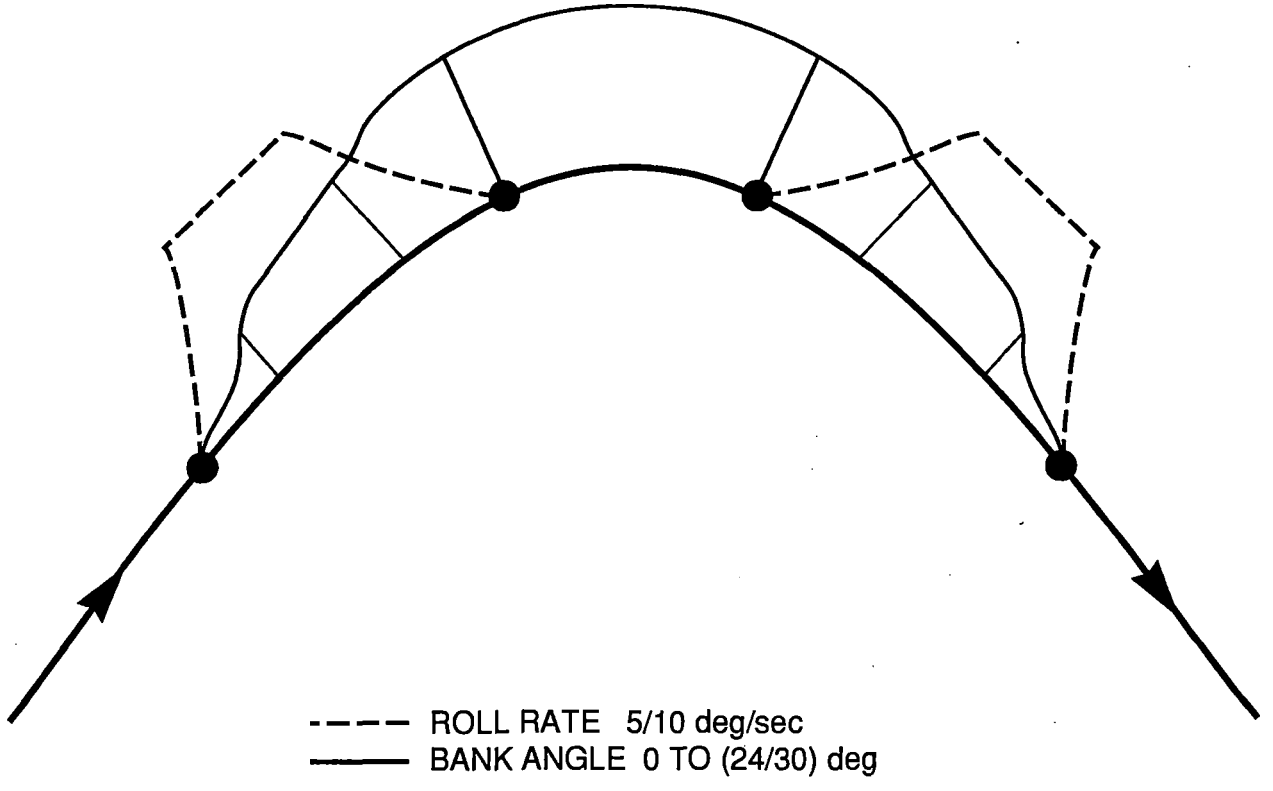

Figure 3-12. Typical Roll Rates and Bank Angle Profiles

$V_{ts} = V_{sc} + a_n \bullet t_b$.

The three steps above provide the initial curve design. The following data are now evaluated:

- Minimum Spiral (at minimum R_h) speed (V_{sc}).
- Maximum vehicle bank angle (q_{max}).
- Length of the transition spiral (L_s).
- Spiral entry vehicle speed (V_{ts}).

3.11 Arc Design Procedure

At each curve the spirals are connected with an arc whose radius is the minimum radius defined in (3-1) (Hypothetical Route Drawing). The length of this arc determines the total deflection angle required at each PI. The guideway is banked to a constant angle equalling the maximum angle of the connecting spiral. The theoretical speed of the vehicle is deemed to be constant while traversing the arc. From the design of the spiral described above, the following arc parameters are known:

- The allowable vehicle speed (V_{sc}).
- The maximum vehicle bank angle (q_{max}).

This set of data is sufficient to use well-known easement curve equations of W. Hay (3-2) for evaluating the arc length (L_C) when deflection angle (I) is known. Once L_S and L_C are known the stationing loss due to the use of an easement curve is also known.

3.12 Optimizing Curves for Maximum Speed

In many PIs the above procedure is sufficient to design the spirals and arc within the given constraints. A check is nevertheless required to see if any of the accelerations limits (Table 2-1) are violated. Any such violations are nullified by reducing the arc speed (V_{SC}). Any adjustment in V_{SC} also changes V_{ts}. In some instances, adjustments in the bank angle are also required to achieve the given deflection angle (I). These adjustments change all parameters of the easement curves including lengths, speeds, accelerations and jerk. Hence, to achieve maximum speed at any easement curve, developing an optimized curve design becomes necessary. Some or all of the following data may be reevaluated when the above adjustments are completed:

- Revised maximum bank angle (q_{max}).
- Revised Arc Speed (V_{sc}).
- Revised Spiral Energy Speed (V_{ts}).
- Revised Spiral Length (L_s).
- Revised Arc Length (L_c).
- Revised Lost Stationing (L_l).

These revised data constitute the parameters of the completed easement curve. From the above data one can plot the speed and acceleration profiles for each easement curve. A semiautomatic procedure has been developed to speed this iterating design process.

3.13 Curving Performance Analysis

The curving performance analysis is done in two parts, as clarified earlier. The first part involves checking the specified ride qualities are not exceeded during the curve design phase. The second part involves carrying out detailed ride quality analysis using MAGSIM software for four sections of the characterized route. The first part of carrying out the specified ride quality checks during initial spiral design phase are illustrated here using two examples.

Example 1

Each curve must have accelerations and jerks/jolts within the curving performance limits defined in Table 2-1. This is checked during the initial spiral design phase. The analyses are carried out using uniform circular motion equations described earlier. The radius at any point in the spiral has been taken to be inversely proportional to its distance from TS, which is a standard practice in evaluating easement curve geometry. The speeds are dictated by the normal acceleration limits. Figure 3-13 shows one of such checks carried out at PI No. 10 for Minimum Required ride quality specifications.

This example studies the traversal of the vehicle from the minimum radius point at CS to the tangent section ST while traversing the SPIRAL 2 in the easement curve. Such checks have been carried out at all points of interest for both ride quality specifications. It can be observed that all accelerations are within that specified in the Minimum Required ride quality.

Example 2

Another example of such static study done at PI 26 for Design Goal ride quality is presented in the tabular form below. This example also studies the traversal of the vehicle from the minimum radius point to the tangent section while traversing the spiral in the easement curve. Table 3-3 shows the change in distance in meters, horizontal radius in meters, bank angle in degrees, speed in m/sec, lateral acceleration in g's, vertical acceleration in g's, vector combinations of lateral and longitudinal accelerations in g's, combination of lateral and vertical accelerations in g's, total acceleration in g's, lateral jerk in g's/sec, and vertical jerk in g's/sec. It shows the radius variation from 1,000 to 36,633m in 5 sec, and the speed changes from 73 to 80.8 m/sec during that period. The bank angle decreases to almost zero in 5 sec.

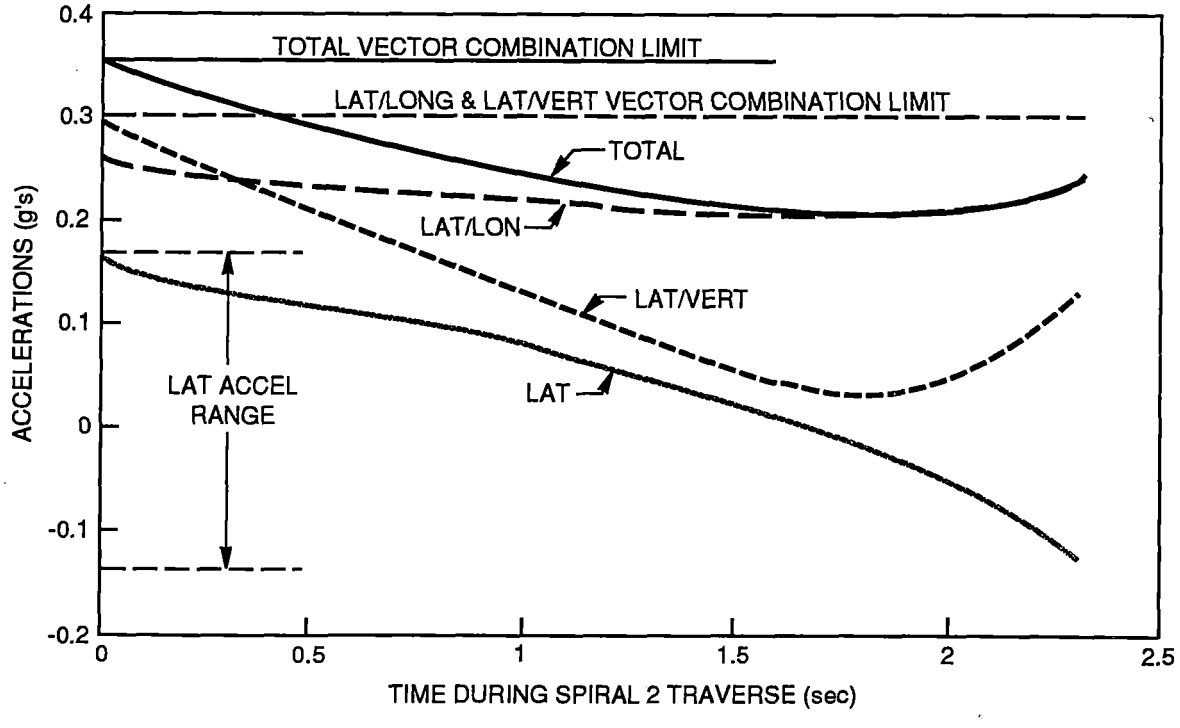

Figure 3-13. Example of Time versus Accels in a Spiral

Table 3-3. Example of a Curving Parameters Check (PI26)

Time (sec)	Distance (m)	RH (m)	Bank (deg)	Speed (m/sec)	Accel Lat (g)	Accel Ver (g)
0	0	1,000.0	24	73	0.078	0.159
1	73.8	1,229.4	19.8	74.6	0.085	0.124
2	149.1	1,605.6	14.8	76.1	0.092	0.089
3	226.1	2,334.9	9.8	77.7	0.084	0.061
4	304.6	4,352.0	4.8	79.3	0.060	0.041
5	384.6	36,633.1	0.5	80.8	0.009	0.033

Time (sec)	Accel Lt/Ln (g)	Accel Lt/Vt (g)	Accel Total (g)	Jerk Lat (g/sec)	Jerk Ver (g/sec)
0	0.178	0.178	0.239	-	-
1	0.181	0.150	0.219	0.007	-0.035
2	0.185	0.128	0.205	0.007	-0.035
3	0.181	0.103	0.190	-0.008	-0.028
4	0.171	0.072	0.176	-0.024	-0.020
5	0.160	0.035	0.164	-0.051	-0.008

Among the comfort parameters, the lateral acceleration is always within the stipulated 0.1 G's. The maximum lateral acceleration is felt in the middle of the spiral. The vertical acceleration is also within the stipulated 0.2 G's. The maximum value vertical acceleration is felt at the minimum radius portion of the curve. All the vector combinations of accelerations are also within limits. The jerks in both lateral and vertical directions are within the specified limits. Figure 3-14 is the graphical representation of some of the data in Table 3-3.

It is possible that the dynamic study (see Part II) will reveal problems in comfort level due to the dynamic evaluation of jerk rates. In such cases, corrections in vehicle banking and damping should rectify the problems. In worst cases, some local corrections in the curve design might be essential. The effect of such changes in the TPC simulation runs will be negligible. Several test runs were carried out using slight changes in accelerations. These runs revealed that the effects in the vehicle performance due to such adjustments will be less than 1 percent in trip time.

In addition to adjustment in guideway geometry, the bank angles can also be actively controlled. This will improve the jerk values without changing the vehicle speed/time performance. The details of such studies were considered to be beyond the scope of current simulation requirements. However, the longitudinal jerk limits were automatically controlled during TPC simulations.

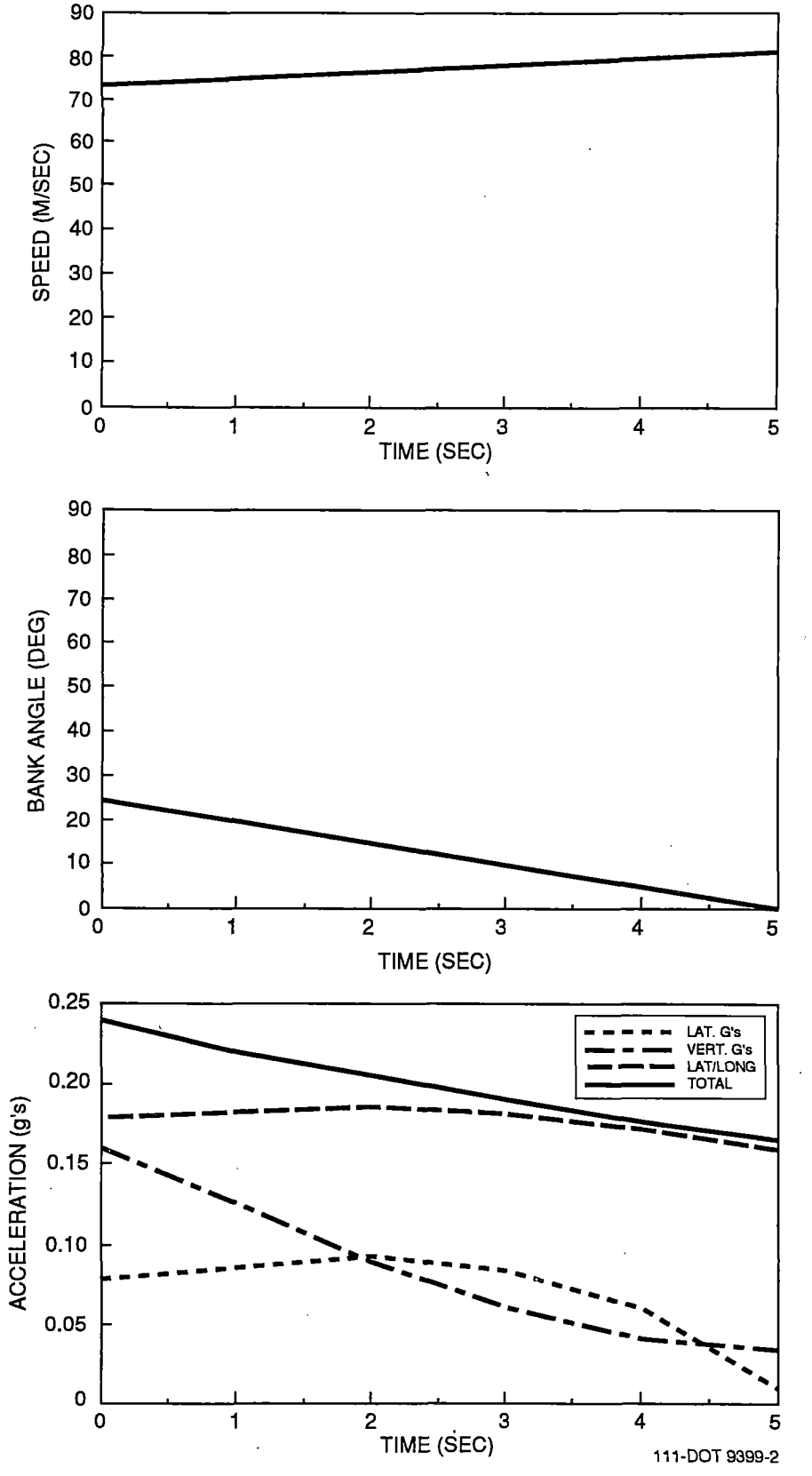

Figure 3-14. Time versus Spiral Ride Quality Parameters at PI26

3.14 Summary

The complete procedure used to develop PIs into easement curves has been described. The standard procedure described by W. Hay to develop easement geometry in railway engineering has been used to evaluate arc lengths for given deflection angles. The difference here is in the use of bank angles, roll rates, and roll accelerations required in traversing the spirals and evaluation of comfort level during curve traversing. The procedure to use these parameters has also been described in detail. Finally, the acceleration/jerk/jolt checks have been done using semi-automated analysis by solving equations of circular motion listed earlier. The ride quality analyses were done using the MAGSIM simulation program of Dr. F. Blader, using dynamic modeling methods. The detailed studies of the four sections of the route required by the Government and carried out by Dr. Blader are presented in Part II of the report. The detailed geometric properties of the spirals and the arcs designed using the procedure described earlier is presented in the next section.

References

3-1. U.S. Army Corps of Engineers, Huntsville Division, Hypothetical Route for Maglev, System Concept Definition.

3-2. Hay, W.W., *Railroad Engineering*, John Wiley & Sons, 1982.

4. ROUTE CHARACTERIZATION

The route characterization involves breaking up the SST route into individual segments whose geometric characteristics, grades, and speed profiles are defined by numeric input for the TPC simulation program. The segments consist of tangents, spirals and arcs. The procedures discussed in the preceding section are followed to design the segments.

Though a generalized SST route could be designed for all three ride comfort specifications, the route would not be optimized for maximum performance for any of the given specifications. Thus, a separate set of transition curves were developed for each of the curving performance requirements.

The route characterization procedure is broken into the following steps:

- Horizontal curve outlining.
- Horizontal detailing.
- Vertical detailing.
- Combining the horizontal and vertical details.
- Converting the data to the TPC input format.

4.1 Horizontal Curve Outlining

To carry out the horizontal outlining, detailed transition curves have been designed for each of the points of intersection in the SST route. This outline, detailing final geometric and speed data required for each PI, for Design Goal ride quality requirements is tabulated in Table 4-1. The units are in meters, degrees, and m/sec. A similar tabulation for Minimum Required ride quality specifications is shown in Table 4-2.

4.2 Horizontal Detailing

Horizontal detailing was carried to generate the individual segments from the Horizontal outline. The specified stations are converted to the actual distance to be traveled by the vehicle. Table 4-3 shows the data generated for first three points of intersections from the curve outlining for design goals ride quality specifications. The symbols used in these tables refer to the following:

R	Minimum curve radius
I	Deflection angle
L_S	Spiral length
L_C	Minimum radius curve (arc) length
L_1	Stationing loss due to curve introduction
V_{ts}	Spiral entry speed
V_{sc}	Spiral exit speed
θ_p	Prebank angle in degrees
θ_{max}	Maximum banking in spiral

Table 4-1. Curve Outlining for Design Goal Specifications

PI#	Station	R	I	L_s	L_c	L_l	V_{ts}	V_{sc}	B_p	B_{max}
1	9000	400	40	205.2	74.1	7.3	52.9	46.4	5.0	19.0
2	16000	500	20	165.4	9.1	1.2	52.2	47.0	5.7	15.0
3	22000	700	30	281.2	85.2	5.4	68.3	61.5	4.0	20.0
4	33000	1000	50	333.2	539.4	32.0	80.3	73.5	4.0	20.0
5	40000	600	90	309.7	632.8	135.1	64.4	56.3	0.0	24.0
6	54000	800	40	353.8	204.7	14.0	73.0	64.9	0.0	24.0
7	62000	600	10	97.4	7.3	0.2	47.4	44.0	4.0	9.0
8	72000	900	50	375.4	410.0	29.8	77.2	69.1	0.0	24.0
9	81000	1000	40	395.4	302.7	17.0	81.1	73.0	0.0	24.0
10	96000	600	20	209.2	0.2	1.5	56.3	50.1	0.0	18.0
11	101000	500	50	279.9	156.4	17.7	58.6	50.5	0.0	24.0
12	107000	600	85	306.6	583.5	110.4	63.8	55.7	0.0	24.0
13	117000	800	20	240.3	39.0	1.9	64.2	58.0	0.0	18.0
14	124000	700	40	331.3	157.4	12.5	68.6	60.5	0.0	24.0
15	132000	700	70	261.4	593.8	65.2	66.5	60.0	5.0	19.0
16	144000	1000	40	395.4	302.7	17.0	81.1	73.0	0.0	24.0
17	154000	1000	10	128.8	45.7	0.3	62.1	58.7	5.0	9.0
18	166000	800	15	193.8	15.6	0.8	64.3	59.4	5.0	14.0
19	173000	600	30	313.8	0.4	5.2	65.2	57.1	0.0	24.0
20	182000	1000	30	395.4	128.2	7.6	81.1	73.0	0.0	24.0
21	188000	900	10	137.7	19.3	0.3	60.9	57.2	5.0	10.0
22	198000	1000	20	334.1	15.0	2.5	80.5	73.7	5.0	19.0
23	206000	500	35	279.9	25.5	6.6	58.6	50.5	0.0	24.0
24	212000	700	15	181.6	1.7	0.7	60.4	55.5	5.0	14.0
25	217000	800	10	130.3	9.4	0.2	57.7	54.0	5.0	10.0
26	221000	1000	20	395.4	826.3	93.7	81.1	73.0	0.0	24.0
27	231000	800	70	353.8	623.6	75.8	73.0	64.9	0.0	24.0
28	238000	900	65	375.4	645.6	66.7	77.2	69.1	0.0	24.0
29	243000	600	30	306.6	7.6	5.1	63.8	55.7	0.0	24.0
30	256000	1000	30	395.4	128.2	7.6	81.1	73.0	0.0	24.0
31	262000	800	20	269.4	9.9	2.0	71.6	65.4	5.0	18.0
32	273000	700	30	331.3	35.3	5.8	68.6	60.5	0.0	24.0
33	278000	700	40	331.3	157.4	12.5	68.6	60.5	0.0	24.0
34	285000	600	40	306.6	112.3	11.0	63.8	55.7	0.0	24.0
35	294000	800	35	353.8	134.9	9.7	73.0	64.9	0.0	24.0
36	304000	1000	15	235.1	26.7	1.0	73.1	67.9	5.0	15.0
37	313000	1000	20	334.1	15.0	2.5	80.5	73.7	4.0	20.0
38	324000	1000	15	235.1	26.7	1.0	73.1	67.9	5.0	15.0
39	333000	900	10	122.4	34.7	0.3	59.1	55.7	5.0	9.0
40	340000	900	25	375.4	17.3	4.4	77.2	69.1	0.0	24.0
41	350000	1000	10	145.0	29.6	0.3	64.0	60.3	5.0	10.0
42	356000	800	5	52.1	17.7	0.0	46.9	45.1	5.0	4.0
43	365000	900	20	302.3	11.8	2.2	76.4	69.9	5.0	19.0
44	373000	1000	60	395.4	651.8	57.3	81.1	73.0	0.0	24.0
45	380000	700	45	331.3	218.5	17.5	68.6	60.5	0.0	24.0
46	388000	800	30	353.8	65.0	6.4	73.0	64.9	0.0	24.0
47	398000	1000	10	161.9	12.7	0.3	65.9	61.9	5.0	11.0
48	405000	1200	25	432.9	90.7	5.4	88.4	80.3	0.0	24.0
49	420000	3000	15	676.2	109.2	3.0	134.1	127.7	0.0	24.0
50	434000	5000	10	598.7	274.0	1.3	134.1	134.1	0.0	20.1
51	449000	8000	15	397.3	1697.1	6.1	134.1	134.1	0.0	12.9
52	469000	10000	10	328.2	1417.1	2.3	134.1	134.1	0.0	10.4

Table 4-2. Curve Outline for Minimum Required Specifications

PI#	Station	R	I	L_s	L_c	L_l	V_{ts}	V_{sc}	B_p	B_{max}
1	9000	400	40	190.9	88.4	7.2	60.5	54	0.0	30.0
2	16000	500	20	154.5	20.1	1.2	65.9	61.1	9.0	21.0
3	22000	700	30	251.9	114.6	5.2	78.8	72.3	0.0	30.0
4	33000	1000	50	298.9	573.8	31.6	92.9	86.4	0.0	30.0
5	40000	600	90	232.2	710.2	132.4	72.9	66.4	0.0	30.0
6	54000	800	40	268.6	289.9	13.2	83.8	77.3	0.0	30.0
7	62000	600	10	103.3	1.4	0.2	62.3	59	9.0	13.7
8	72000	900	50	284.2	501.2	28.6	88.5	82	0.0	30.0
9	81000	1000	40	293.6	404.6	16.1	91.3	0	0.0	30.0
10	96000	600	20	168.8	40.6	1.4	71.8	67	9.0	21.0
11	101000	500	50	213.2	223.1	16.6	67.2	60.7	0.0	30.0
12	107000	600	85	233.2	290.4	19.6	73.2	66.7	0.0	30.0
13	117000	800	20	268.6	10.7	2.0	83.8	77.3	0.0	30.0
14	124000	700	40	251.9	236.8	11.7	78.8	72.3	0.0	30.0
15	132000	700	70	250.9	604.3	65.0	78.5	72	0.0	30.0
16	144000	1000	40	298.9	399.2	16.2	92.9	86.4	0.0	30.0
17	154000	1000	10	167.9	6.7	0.3	80.8	76.6	5.0	18.0
18	166000	800	15	192.1	16.9	0.8	78.5	73.5	0.0	30.0
19	173000	600	30	233.2	80.9	4.6	73.2	66.7	0.0	30.0
20	182000	1000	30	298.9	224.7	7.0	92.9	86.4	0.0	30.0
21	188000	900	10	149.0	8.0	0.3	75.3	71.3	5.0	22.0
22	198000	1000	20	298.9	50.2	2.3	92.9	86.4	0.0	30.0
23	206000	500	35	213.2	92.2	6.0	67.2	60.7	0.0	30.0
24	212000	700	15	180.6	2.7	0.7	73.8	68.8	5.0	22.0
25	217000	800	10	138.9	0.8	0.3	71	67	5.0	16.8
26	221000	1000	20	298.9	922.8	91.8	92.9	86.4	0.0	30.0
27	231000	800	70	268.6	708.8	74.0	83.8	77.3	0.0	30.0
28	238000	900	65	284.2	736.8	65.1	88.5	82	0.0	30.0
29	243000	600	30	233.2	80.9	4.6	73.2	66.7	0.0	30.0
30	256000	1000	30	298.9	224.7	7.0	92.9	86.4	0.0	30.0
31	262000	800	20	264.9	14.4	2.0	82.7	76.2	0.0	30.0
32	273000	700	30	251.9	114.6	5.2	78.8	72.3	0.0	30.0
33	278000	700	40	251.9	236.8	11.7	78.8	72.3	0.0	30.0
34	285000	600	40	233.2	185.6	10.2	73.2	66.7	0.0	30.0
35	294000	800	35	268.6	220.1	9.0	83.8	77.3	0.0	30.0
36	304000	1000	15	216.1	45.8	1.0	91.2	86.4	9.0	21.0
37	313000	1000	20	298.9	50.2	2.3	92.9	86.4	0.0	30.0
38	324000	1000	15	216.1	45.8	1.0	91.2	86.4	9.0	21.0
39	333000	900	10	149.3	7.8	0.3	79.1	75.3	9.0	16.0
40	340000	900	25	284.2	108.5	3.9	88.5	82	0.0	30.0
41	350000	1000	10	173.0	1.5	0.3	85.5	81.4	9.0	17.4
42	356000	800	5	69.4	0.4	0.0	62.9	60.7	9.0	7.9
43	365000	900	20	284.2	29.9	2.2	88.5	82	0.0	30.0
44	373000	1000	60	298.9	748.3	55.8	92.9	86.4	0.0	30.0
45	380000	700	45	251.9	297.9	16.5	78.8	72.3	0.0	30.0
46	388000	800	30	268.6	150.3	5.8	83.8	77.3	0.0	30.0
47	398000	1000	10	170.7	3.8	0.3	84	79.9	9.0	17.5
48	405000	1200	25	326.6	197.0	5.0	101.2	94.7	0.0	30.0
49	420000	3000	15	447.0	338.4	2.6	134.1	134.1	0.0	30.0
50	434000	5000	10	299.5	573.2	1.2	134.1	134.1	0.0	19.0
51	449000	8000	15	219.0	1875.4	6.1	134.1	134.1	0.0	13.0
52	469000	10000	10	219.0	1526.3	2.2	134.1	134.1	0.0	13.0

Table 4-3. Horizontal Detailing Example for Design Specifications

Hypothetical Maglev Route
Version 1

Accelerations (g) Limits:

Lateral	+/- .1		
Vertical	0.95 to 1.2	Roll Rate	5 deg/sec
Normal	+/- 0.16	Roll Accel	15 deg/sec^2

Station	Description Name	Target Dist.(m)	Target Radius(m)	Target Grade(%)	TrgtSpeed (MPS)
0	Terminal #1	0.0		3.50	0.0
8758	TS at PI#1	8750.5		3.50	52.9
8963	SC at PI#1	8955.6	400	3.50	46.4
9037	CS at PI#1	9029.7		3.50	46.4
9242	ST at PI#1	9234.9		3.50	78.9
15830	TS at PI#2	15814.2		-2.00	52.2
15995	SC at PI#2	15979.6	500	-2.00	47.0
16005	CS at PI#2	15988.7		-2.00	47.0
16170	ST at PI#2	16154.1		-2.00	52.2
21676	TS at PI#3	21653.7		2.50	68.3
21957	SC at PI#3	21934.9	700	2.50	61.5
22043	CS at PI#3	22020.1		2.50	61.5
22324	ST at PI#3	22301.4		2.50	68.3
32397	TS at PI#4	32337.2		1.00	80.3
32730	SC at PI#4	32670.5	1000	1.00	73.5
33270	CS at PI#4	33209.9		1.00	73.5
33603	ST at PI#4	33543.1		1.00	80.3
39623	TS at PI#5	39395.9		0.00	64.4
39932	SC at PI#5	39705.6	600	-10.00	56.3
40068	CS at PI#5	39840.6		-10.00	56.3
40377	ST at PI#5	40150.3		-10.00	64.4

An example of horizontal detailing is shown below.

Example: Horizontal detailing of PI No. 1 for design specification.

The outline of the first PI is shown below:

PI No.	Station	R	I	L_s	L_c	L_1	V_{ts}	V_{sc}	θ_p	θ_{max}
1	9000	400	40	205.2	74.1	7.3	52.9	46.4	5.0	19.0

The nominal stationing of the transition curves are calculated as follows:

Point			Station
TS	9000 - (205.2+74.1/2)	=	8758
CS	9000 - (74.1/2)	=	8963
SC	9000 + (74.1/2)	=	9037
TS	9000 + (205.2+74.1/2)	=	9242

Since there is a stationing loss of 7.3m in this point of intersection, the actual route distance is approximated as nominal stationing minus stationing loss due to curvature. The target velocity for PI No. 1 is 134.1 m/sec. The actual calculated allowable speeds are as shown above.

4.3 Vertical Curve Severity Analysis

The hypothetical route drawing was studied for severity of the vertical radii. The minimum radius in a vertical curve can be estimated by the following approach:

For vertical curves (see figure in Table 4-4),

$t = ax^2$

$d^2x/dt^2 = 2a \simeq = 1/R_{vmin}$

$(S_1 - S_2) / LVC = 2a$

$R_{vmin} = -LVC/(S_1 - S_2)$

Note $S = S\%/100$

Table 4-4. Vertical Curve Severity (by Inspection)

	PVI Station (m)	Entry Slope (S_1) %	Exit Slope (S_2) %	Length (LVC)m	$R_{vmin} = -\frac{LVC}{S_1 - S_2}$
1.	10 + 000	+3.5	-2.0	700	-12,700
2.	40+	0	-10.0	1,500	-15,000
3.	44	-10.0	0	1,500	+15,000
4.	105	-0.5	+3.5	500	+12,500
5.	205	0	+10.0	1,500	+15,000
6.	209	+10.0	0	1,500	-15,000
7.	300	+2.0	-3.0	700	-14,000
8.	366	-1.5	+2.5	500	+12,500
9.	393	+3.5	-10.0	1,600	-11,850
10.	398	-10.0	-1.0	1,100	+12,220

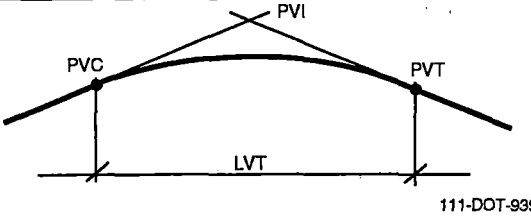

111-DOT-9399-8

The R_{vmin} sign is positive for concave landscape and negative for convex landscape. This sign convention is used in the analyses because it agrees with the g's convention. This study revealed that in general, the vertical radii for this route are very large. Table 4-4 lists the evaluated R_{vmin} for the most severe curves. It shows that vertical curves at stations 10,000, 105,000, 209,000, 366,000, and 393,000 are the most severe and need speed restrictions studies.

The acceleration, a (g's), acting on these vertical curves can be easily evaluated using the following equation:

$$a = \frac{V^2}{gR}$$

Table 4-5 shows the speed limits evaluated for the ten most severe curves. It shows that only five curves have speed limitations, all of which are due to the cresting vertical curves. There are no speed limitations due to the sags in the route.

Table 4-5. Speed Limits on Vertical Curves

Vertical Curve		Speed Limit (m/sec)		
		Design Goal	Min. Req'd.	
No.	Station	-0.05g , +0.2g	-0.1g, +0.3g	V. Radius of Curve (km)
1	10,000	78.9	111.6	-12.7
2	40,000	85.8	121.3	-15
3	44,000	>135 (172)	>>135	+15
4	105,000	>135 (157)	>>135	+12.5
5	205,000	>135 (172)	>>135	+15
6	209,000	85.8	121.3	-15
7	300,000	82.9	117.2	-14
8	366,000	>135 (157)	>>135	+12.5
9	393,000	76.2	107.8	-11.85
10	398,000	>135 (155)	>>135	+12.22

4.4 Vertical Detailing

A comparably simple vertical detailing approach has been used since the vertical radii are very large in comparison to the horizontal radii. These radii being very large, there is no significant stationing loss. No detailed spirals have been developed for vertical curves because of limited effect on the vehicle performance. Ride quality checks have been carried out in all stations noted in the above table and all zones with combined vertical and horizontal curvature. The stationing are developed by positioning point A at half length of vertical curvature (LVC) before the point of vertical intersection (PVI). Point B is positioned at PVI and Point C is at half LVC after the PVI. The loss of stationing due to horizontal easement curves are treated in the same manner as in horizontal detailing. Table 4-6 shows an example of the detailing up to PVI station 50,000.

4.5 Combining the Horizontal and Vertical Details

The horizontal and vertical details are combined and sorted to generate the characterized route. All segments are sorted according to the travel distance. Any horizontal/vertical interfering curves are re-evaluated for acceleration limit violations. Table 4-7 shows the effect of combining the horizontal and vertical detailed examples.

Table 4-6. Vertical Detailing Example for Design Specifications

Station (m)	Calculated Station (m)	Grade (%)	Calculated Speed (m/s)
			134.1
9650 A 10K	9635.3	3.50	
10000 B 10K	9985.3	-2.00	78.9
10350 C 10K	10335.3	-2.00	78.9
16700 A 17K	16682.9	-2.00	134.1
17000 B 17K	16982.9	2.50	134.1
17300 C 17K	17282.9	2.50	134.1
24700 A 25K	24672.1	2.50	134.1
25000 B 25K	24972.1	1.00	134.1
25300 C 25K	25272.1	1.00	134.1
34900 A 35K	34808.2	1.00	134.1
35000 B 35K	34908.2	0.00	134.1
35100 C 35K	35008.2	0.00	134.1
39250 A 40K	39158.0	0.00	134.1
40000 B 40K	39638.0	-10.00	85.8
40750 C 40K	40388.0	-10.00	85.8
43250 A 44K	42888.0	-10.00	134.1
44000 B 44K	43638.0	0.00	134.1
44750 C 44K	44388.0	0.00	134.1
49900 A 50K	49538.0	0.00	134.1
50000 B 50K	49638.0	-1.00	134.1

Table 4-7. An Example of Combined Horizontal and Vertical Details

Station Name	Description	Target Dist.(m)	Target Radius(m)	Target Grade(%)	SpeedLmt (MPS)
0	Terminal #1	0.0		3.50	0.0
8758	TS at PI# 1	8750.5		3.50	134.1
8963	SC at PI# 1	8955.6	400	3.50	52.9
9037	CS at PI# 1	9029.7		3.50	46.4
9242	ST at PI#	9234.9		3.50	52.9
9650	A 10K	9635.3		3.50	134.1
10000	B 10K	9985.3		-2.00	78.9
10350	C 10K	10335.3		-2.00	78.9
15830	TS at PI# 2	15814.2		-2.00	134.1
15995	SC at PI# 2	15979.6	500	-2.00	52.2
16005	CS at PI# 2	15988.7		-2.00	47.0
16170	ST at PI# 2	16154.1		-2.00	52.2
16700	A 17K	16682.9		-2.00	134.1
17000	B 17K	16982.9		2.50	134.1
17300	C 17K	17282.9		2.50	134.1
21676	TS at PI# 3	21653.7		2.50	134.1
21957	SC at PI# 3	21934.9	700	2.50	68.3
22043	CS at PI# 3	22020.1		2.50	61.5
22324	ST at PI# 3	22301.4		2.50	68.3
24700	A 25K	24672.1		2.50	134.1
25000	B 25K	24972.1		1.00	134.1
25300	C 25K	25272.1		1.00	134.1
32397	TS at PI# 4	32337.2		1.00	134.1
32730	SC at PI# 4	32670.5	1000	1.00	80.3
33270	CS at PI# 4	33209.9		1.00	73.5
33603	ST at PI# 4	33543.1		1.00	80.3
34900	A 35K	34808.2		1.00	134.1
35000	B 35K	34908.2		0.00	134.1
35100	C 35K	35008.2		0.00	134.1
39250	A 40K	39158.2		0.00	134.1
39623	TS at PI# 5	39395.9		0.00	134.1
40000	B 40K	39638.0		-10.00	64.4
39932	SC at PI# 5	39705.6	600	-10.00	58.1
40068	CS at PI# 5	39840.6		-10.00	56.3
40377	ST at PI# 5	40150.3		-10.00	64.4
40750	C 40K	40388.0		-10.00	134.1
43250	A 44K	42888.0		-10.00	134.1
44000	B 44K	43638.0		0.00	134.1
44750	C 44K	44388.0		0.00	134.1
49900	A 50K	49538.0		0.00	134.1
50000	B 50K	49638.0		-1.00	134.1

4.6 Curved Guideway Lengths in SST

The curved portion of the SST guideway requires a different approach in designing, analyzing, constructing, and cost estimating. The effort required depends on the severity of the curvature. A distribution of the curved guideway in the complete SST was performed. Figure 4-1 shows a bar graph of the curved lengths at various radii. It was used to estimate the cost and also gives a summary of the geometry of the complete SST route.

4.7 Characterized Routes for Two Sets of Ride Quality Parameters

Using the above procedure, a complete characterized route geometry has been developed for the Design Goal ride quality. This data is presented in detail in Table 17 in Appendix A. The same procedure was repeated to develop the characterized route geometry for the Minimum Required ride quality. The completed data is presented in detail in Table 18 in Appendix A. Tables 17 and 18 in Appendix A are presented in readable format to permit debugging and closer inspection.

4.8 Summary

- The route characterization procedure used in this analysis has been detailed.
- Using the above procedure, two horizontal curve outlines, one for the Design Goal ride quality and another for the Minimum Required ride quality have been tabulated.
- Speed limits for vertical curves have been tabulated in Table 4-5.
- The individual data are combined to form the characterized route. Stationing loss due to curve development has been considered. Detailed acceleration studies have been carried out where horizontal/vertical curves coexist.

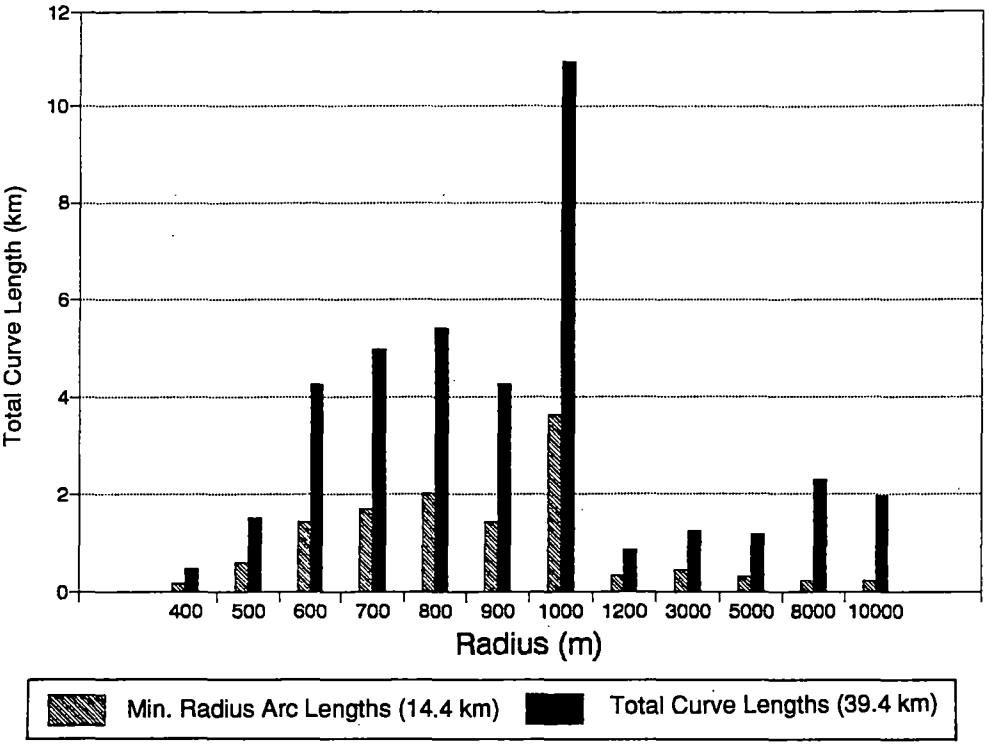

Figure 4-1. Summation of all Curved Guideway Lengths in SST

5. TRAIN PERFORMANCE CALCULATOR PROGRAM (TPC) OVERVIEW

The train performance calculator (TPC) is a computer model that simulates the electrical and mechanical performance of the vehicle along a route. The TPC used is derived from the Parsons De Leuw Chopper Simulation Program. The program was developed by Parsons De Leuw, Inc. (PDI) for performance simulation of electrically powered transit vehicles with solid-state "chopper" controllers for acceleration control (as opposed to, for example, cam-controllers). It has been extensively used to simulate and design traction power systems for numerous transit agencies, including the following recent examples:

- Design of Washington Metro System (extensions ongoing).
- Design of Singapore Metro System (1988).
- Design of Shanghai Metro System (1990).
- Study and concept design for Houston and Honolulu monorail systems (1991).
- Extension Service Plan for BART, San Francisco (ongoing).

5.1 Simulation Program Validation

The simulation program output was validated in 1984 under an UMTA program using chopper-controlled vehicles and a steel-wheel on-rail system. The computed results were compared to field measurements from an instrumented test-train run on the San Francisco BART system and found to be very close to the predicted performance. This, along with the other various transit systems performance modeling results, indicates the high reliability of the program. An enhanced version of the program has been used to simulate the performance of Foster-Miller, Inc. maglev vehicles. The modifications are summarized in subsection 5.3.

5.2 Simulation Program Description

The TPC program is the first part of the four-part PDI software system for designing transit power distribution systems. The TPC helps to predict train performance and energy consumption for an electrically powered vehicle operating along a given alignment. In a typical transit system analysis, the output from the train simulation is subsequently used by the other three programs (RMS program, Train Scenario Selector Program and Voltage Drop Program). These programs help to determine optimum substation capacity, location and component sizes based on thermal loading and voltage criteria, for a given passenger level. For the SST project, only the first part, the TPC program, has been used to simulate vehicle performances in the Design Goal (SSTLEFT) and Minimum Required (SSTMID) routes discussed earlier.

Analytical Technique

The TPC program utilizes consecutive small time interval approximations to simulate train performance and energy consumption. A numerical scheme has been implemented in which the acceleration is calculated at discrete time intervals controlled by the normal jerk limit. This acceleration is used to update the current speed and the vehicle location.

Maglev Vehicle Performance

For a Maglev vehicle, the propulsion system is modeled to provide constant tractive effort based on g-limits of ride comfort up to a speed defined by the system power. Between this speed and the maximum speed (134.1 m/sec), the vehicle acceleration is increasingly limited by the decreasing difference between constant power available and increasing power required as discussed in (5-1). The vehicle performance curve is reproduced in Figure 5-1.

Maglev Tractive Power

The tractive power for the Maglev vehicle is calculated based on the power required to overcome the following resistances:

- The rolling resistance of the rubber tires when the vehicle is not levitated
- Magnetic drag as a function of vehicle speed.
- Aerodynamic drag as a function of the square of the vehicle speed.
- Grade force (resistance/assistance) as a function of percent grade and the vehicle weight.
- Curve resistance as a function of the curve radius.
- Inertial force (a function of desired acceleration or deceleration).

Thus the tractive power can be calculated by combining above components of resistances/ assistances. These forces can be simplified as the force equation shown below:

$$F = A_D + B_D V + C_D V^2 + (W + R_o) \bullet \frac{A}{g} + \frac{W \bullet 5730 \bullet .8}{R_C \bullet 2000} + \frac{W \bullet G_R}{100}$$

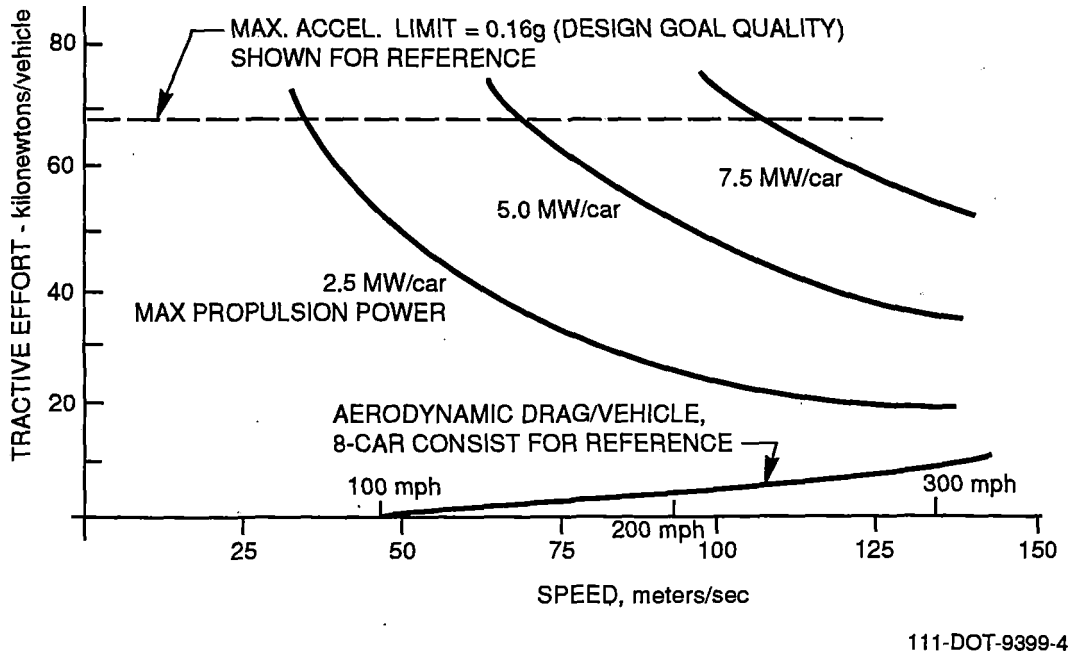

Figure 5-1. Maglev Vehicle Performance Curve

where

AD, BD, C_D: TPC coefficients (Davis Terms)
V: Speed, mph
W: Vehicle weight, pounds
R_o: Train equivalent rotary inertia, pounds
A: Acceleration, mphps
g: Acceleration due to gravity (21.95 mphps)
RC: Curve radius in feet
G_R: Grade in percent
F: Force in pounds.

The coefficients AD, B_D, and C_D are standard TPC coefficients, the values of which are already established for conventional transit vehicles. For the purposes of Maglev simulations PDI has distributed the various drag terms as equivalent of these coefficients. For example, the constant resistance term has been approximated as 1010 kg based on the experience with Monorail systems. The predominant resistance is due to the aerodynamic drag which constitutes the C term.

The force equation is then converted to the tractive power as follows:

$$P = F \bullet V \bullet K/\varepsilon$$

where
P: Power in Watts
ε: Propulsion system efficiency
K: Unit conversion constant

Impact of Horizontal Curves

In a conventional vehicle (steel wheel-on-rail), two things are considered when the train negotiates a curve. The speed is usually restricted to reduce the outward radial force and a small amount of power consumption is added to overcome the curve resistance between the wheel and the rail given by the fifth term in the force equation. For the Maglev vehicle, the latter effect should be minimal due to the absence of the physical contact between the guideway and the vehicle beyond levitation speed. A relationship has not yet been established. PDI opted to retain the original empirical relation in the program, which may be somewhat conservative. However, the overall impact is insignificant for this study, since the energy consumed in going through the curves was found to be typically 0.2 percent of the total.

5.3 Program Modification/Enhancement

Several modifications were incorporated to make the program compatible with Maglev train operation:

- Conversion of input/output data to desired metric units.
- Accepting empirical relationship for levitation and aero-drags as the design progressed.
- Increasing array sizes and data format to accept up to 400 data points for a given segment (such as grade or speed changes).
- Included output data for power consumption in various drags, braking energy available for regeneration.

- Composite graphical output capability for most parameters.
- Consideration for ride quality by restricting incremental changes in accel/decel rates within the specified longitudinal jerk limit.
- Algorithm was modified to simulate the mid-point of a train rather than the front end for enhanced accuracy.

5.4 TPC Input File

The velocity-independent data were developed into a data file. This data file has two sets of data. The first set consists of parameters which are independent of route geometry, such as: the vehicle mass; length; maximum power capacity; allowed accelerations/jerk limits; voltage level (distribution); drag coefficients; dwell time; and calculation iteration limits. These are formatted as independent variables in the master data segment of the TPC input file.

The second set consists of data dependent on the characterized route geometry. This set is formatted as station dependent data. Table 5-1 is an example of the data for the first 30 km distance of SSTMID route.

The actual TPC input file combines all categories of the Maglev simulation data. Table 5-2 shows the actual TPC input data in the ASCII form and other required simulation control parameters.

5.5 TPC Output

The TPC output consists of detailed numerical tabular data, including distance, time, total power, average accelerations, energy consumptions in various drags/curves, and summary of the performance data. The summary provides the breakdown of run length, power consumption (kWh) and run time between all stations and gives the specific power consumption rate and average speed over the route including total travel distance and the average speed of the vehicle. Several such summary outputs are presented in the next section.

Table 5-3 shows a sample output for the input file shown in Table 5-2. The TPC output is processed to develop the speed, power, and acceleration profiles for the complete route. These profiles are presented in Section 6.

Output Check

The TPC output was studied in detail and debugged by TPC experts at PDI. Additional checks have been carried out by Foster-Miller by comparing the outputs to theoretical estimates of drag and power consumption, and time to reach rated speed using various acceleration and power levels. Figure 5-2 illustrates the various components of the resistances and accelerations at different speeds in a trial run. These curves refer to runs carried out on the Foster-Miller trial route, before the completion of the SSTLEFT and SSTMID routes characterization. The TPC output was compared with the parameters shown in the Figure 5-2 and agreement was found at different speeds.

Figure 5-3 shows the acceleration curves generated using the above procedure for various power levels. These studies clarified the characteristics of the expected maglev speed curves and helped decide the choice of power levels required for the TPC simulations used in the next section.

Table 5-1. Data for Minimum Required Ride Quality (SSTMID)

Speed m/s	Location m	Grade %	Radius m	Description
0	0.0	3.5		Terminal #1
134.1	8757.8	3.5		TS PI #1
60.5	8948.7	3.5	400	SC PI #1
54.0	9037.0	3.5		CS PI #1
60.5	9227.9	3.5		ST PI #1
134.1	9635.7	3.5		A 10K
111.6	9985.7	-2.0		B 10 K
111.6	10335.7	-2.0		C 10K
134.1	15820.0	-2.0		TS PI #2
65.9	15974.5	-2.0	500	SC PI #2
61.1	15994.5	-2.0		CS PI #2
65.9	16149.0	-2.0		ST PI #2
134.1	16683.3	-2.0		A 17K
134.1	16983.3	2.5		B 17K
134.1	17283.3	2.5		C 17K
134.1	21668.9	2.5		TS PI #3
78.8	21920.8	2.5	700	SC PI #3
72.3	22035.4	2.5		CS PI #3
78.8	22287.3	2.5		ST PI #3
134.1	24672.9	2.5		A 25K
134.1	24972.9	1.0		B 25K
134.1	25272.9	1.0		C 25K
134.1	32355.6	1.0		TS PI #4

5.6 Summary

The train performance calculator (TPC) program has its origin in performance simulation of electrically powered transit vehicles with solid-state controller for acceleration control. The program was enhanced for maglev simulations as described in subsection 5.3. Examples of the actual input and output files are presented for the first 30 km distance. The complete output for the first 30 km distance cited in this section is presented in Appendix A. The procedure used to validate for maglev simulations have also been described. Additional details of the complete set of final runs studied for this report are presented in the next section, and the data on all additional test runs exists at Foster-Miller and PDI.

References

5-1. *Maglev System Concept Definition Final Report,* Foster-Miller, Inc., DOT/FRA/ORD-92/01, October 1992.

Table 5-2. An Example of TPC Input

```
1          DCCO CHOPPER SIMULATION PROGRAM        PAGE NO.    1

           INPUT FILE: sstmid.inp
           START PROGRAM RUN- DATE:  6/30/1992    TIME: 13: 9


RUN NO.SSTMID(rev 6/29/92)8CAR TRAIN, 134 M/S MAX SPEED, DWELL=0 SEC
ROUTE ALIGNMENT: S-800km  MAX POWER= 40 MW; 0.2 g; aero drag= 5.1 V3 W

MAX. ACCEL.= 2.000   M/S2    MAX. DECEL.= 2.000   M/S2
TRAIN WEIGHT OF  210686. KG  WITH EQUIVALENT ROTATIONAL WEIGHT OF      0. KG
MAX PROPULSION MECHANICAL KW OF 40000. TO 134.  M/S  , THEN DECAY AT   0. KW PER  M/S
ABSOLUTE SPEED LIMITS- MIN. SAFETY BLOCK OF   210. METERS
AUXILIARY POWER OF  3200.0 KW
PROPULSION SYSTEM EFFICIENCY OF  .950
DWELL TIME OF    0. SECONDS
JERK LIMIT:   .70   M/S2    PER SEC.
DAVIS TERMS- 1010.0 KG      .000 KG  PER  M/S       .5150 KG  PER  M/S  SQUARED
MODIFIED A & B DAVIS TERMS:
B PRIME TERM AFFORDS INVERSE DECAY VS. SPEED:

        ABOVE SPEED      A TERM IS      B TERM IS      B PRIME IS
            M/S              KG          KG / M/S           KG

            40.0          3535.0            .000           .0

           DISC/DISKETTE TRANSFER FILE OUTPUT: x1
           NOMINAL TRAIN VOLTAGE OF 2100.
1          DCCO CHOPPER SIMULATION PROGRAM        PAGE NO.    2


           STATION TO STATION RUN NO.    1

           INPUT FILE: sstmid.inp
           START PROGRAM RUN- DATE:  6/30/1992    TIME: 13: 9

           DEPARTURE STATION-- TERM STA 1          AT LOCATION          0.
           ARRIVAL STATION--   TERM STA 2          AT LOCATION     398250.
```

Table 5-2. An Example of TPC Input (Continued)

CIVIL INPUT DATA:

SPEED	LOCATION	GRADE (%)	CURVE R	MODIFIED C DAVIS TERM
	.0			
134.00		3.50	.00	
	8757.8			
60.50		3.50	40.00	
	8948.7			
54.00		3.50	.00	
	9037.0			
60.50		3.50	.00	
	9227.9			
134.00		3.50	.00	
	9635.7			
111.60		-2.00	.00	
	9985.7			
111.60		-2.00	.00	
	10335.7			
134.00		-2.00	.00	
	15820.0			
65.90		-2.00	50.00	
	15974.5			
61.10		-2.00	.00	
	15994.5			
65.90		-2.00	.00	
	16149.0			
134.00		-2.00	.00	
	16683.3			
134.00		2.50	.00	
	16983.3			
134.00		2.50	.00	
	17283.3			
134.00		2.50	.00	
	21668.9			
78.80		2.50	70.00	
	21920.8			
72.30		2.50	.00	
	22035.4			
78.80		2.50	.00	
	22287.3			
134.00		2.50	.00	
	24672.9			
134.00		1.00	.00	
	24972.9			
134.00		1.00	.00	
	25272.9			
134.00		1.00	.00	
	32355.6			
92.90		1.00	100.00	
	32654.5			

Table 5-3. An Example of TPC Output File

DCCO Chopper Simulation Program Page No. 3
Station to Station Run No. 1
Input File: sstmid.inp
Start program run - Date: 6/30/1992 Time: 13:9

Actual Location	Time (sec)	Speed m/s	Avg kW	kW-sec x1000	Avg. Accel. m/s^2	Curve kW-sec x1000	A.Davis kW-sec x1000	B/B'Davis kW-sec x1000	C. Davis kW-sec x1000
			3363.		0.73				
1.	2.0	1.5		6.73		0.0	0.0	0.0	0.0
			4887.		1.89				
8.	4.0	5.2		16.50		0.0	0.1	0.0	0.0
			7041.		2.00				
22.	6.0	9.2		30.58		0.0	0.2	0.0	0.0
			9167.		2.00				
45.	8.0	13.2		48.92		0.0	0.4	0.0	0.0
			11299		2.00				

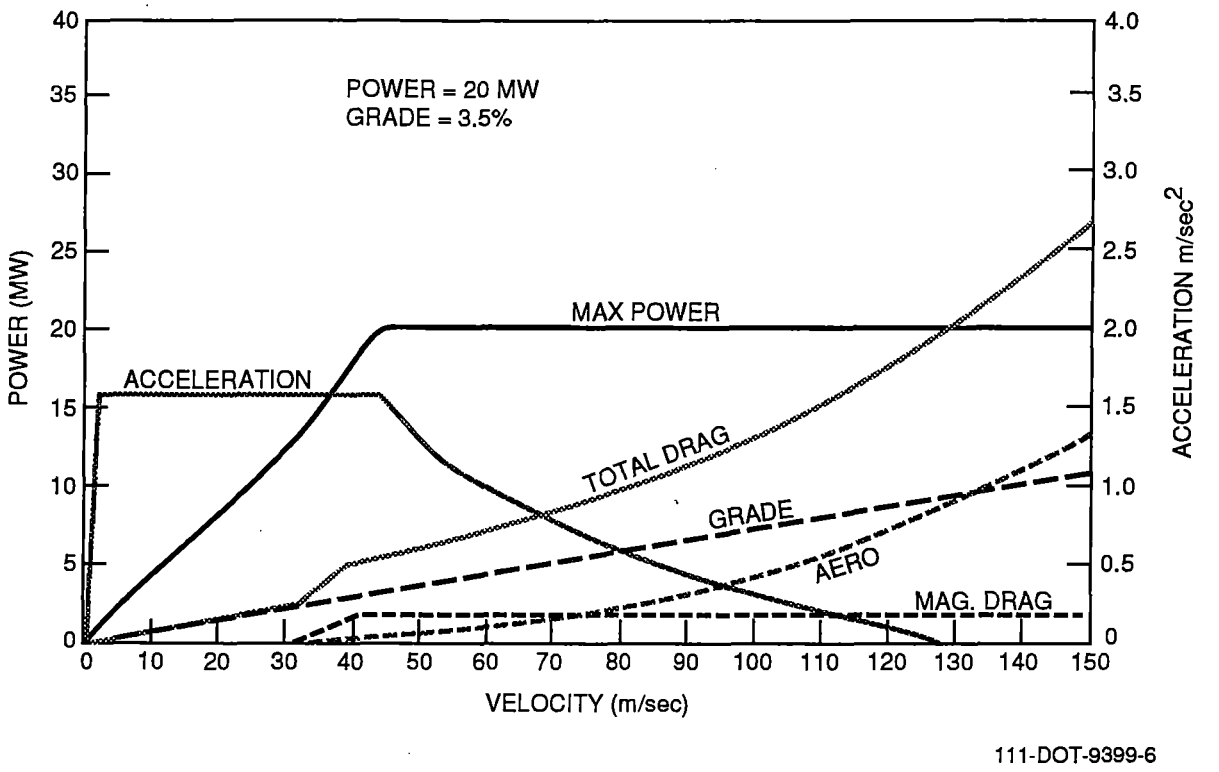

Figure 5-2. Resistances, Accelerations and Power Curves at Various Speeds

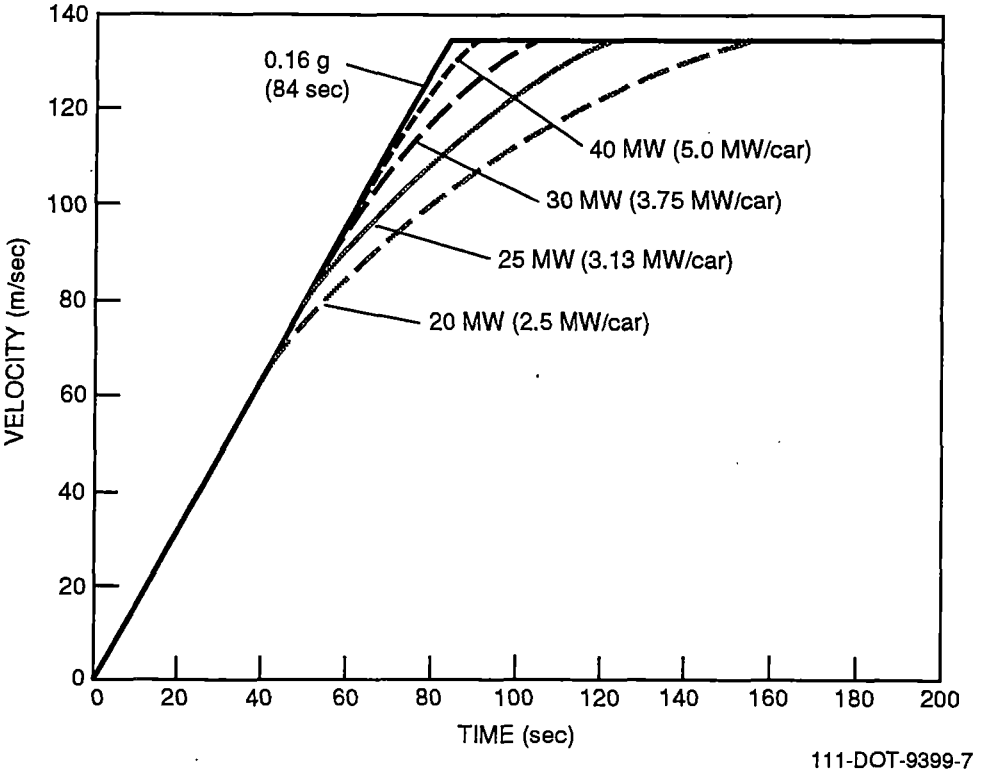

Figure 5-3. Theoretical Estimates of the Velocity Profiles of Foster-Miller Maglev Vehicle at Various Power Ratings

6. SST SIMULATION

The TPC simulation involves several runs with varying car consists, power levels, accelerations, and ride qualities. In this section, a typical set of plots are presented, relating distance versus speed, distance versus total power consumed, and distance versus acceleration, using Minimum Required ride quality. The summary of the results from the runs are provided though the detailed output results are too voluminous to be printed in this report.

6.1 Parameter Selection Criteria

The mechanical, aerodynamic, magnetic, and operational parameters chosen for simulating the vehicle performance are described below.

Car Consists

Most runs were carried out with an eight-car consist. This represented the longest consist foreseen to achieve capacity with reasonably short waiting time between trains (3 min 45 sec between trains). Also, the substation size required for the upper end of the accel range was still reasonable, supplying 40 MW net propulsive power. One-car vehicle simulation was also done for performance comparison.

Power Levels

Power level is defined as the maximum propulsive power used by the vehicle. For an eight-car consist, (a range of 20 to 40) MW was used for the maximum propulsive power. Thirty MW per train or 3.75 MW per car is considered as the design power for the vehicle. This power level will allow a sustained maximum speed in a 3.5 percent positive grade in a tangent track. Twenty MW per train or 2.5 MW per car power was used to evaluate the effectiveness of the lower rated system, and any negative side effects in terms of vehicle performance. Forty MW per vehicle or 5 MW per car was used to see the advantage of faster accelerations at higher speeds. For a single car vehicle the 7.5 MW power was considered to be the design maximum propulsive power. Several runs were also carried out using 5 MW per car power. In addition to the propulsive power the substation would supply additional power due to the power delivery system efficiency of 95 percent, and auxiliary ("hotel") onboard power consumption of 400 kW per car.

Normal Accelerations

Normal acceleration limits are dictated by the ride quality specifications. For Design Goal ride quality 0.16g has been used as the maximum normal acceleration/deceleration. For Minimum Required ride quality 0.2g has been used as maximum normal acceleration/deceleration limit. Some cases have been run at 0.16g maximum normal acceleration/deceleration to compare the effect of decreasing the normal acceleration on the vehicle performance.

Jerk Rates

Jerk rates specified in Table 2-1 have been used during the TPC simulation. For both Design Goal ride quality and Minimum Required ride quality, 0.07g/sec longitudinal jerk rates have been used. For Minimum Required ride quality, additional simulations with 0.25g/sec, which was considered too high for simulating 0.2g accelerations, have been carried out. TPC runs were also carried out without using jerk rate limits to check the cumulative effect of jerk rates on vehicle performance.

Aerodynamic Drag

Aerodynamic drag power estimates used in the SST analysis are shown below for a single car and eight-car consists:

No. of Cars	Aerodynamic Drag Power
1	$1.88V^3$ Watts
8	$5.10V^3$ Watts
	where V = speed in m/sec

Magnetic Drag

The estimated magnetic drag power used for the Severe Segment Test is summarized below:

No. of Cars	Magnetic Drag Power	
	MW	MW
	V<40 m/sec	V>40 m/sec
1	0.0	0.32
8	0.0	1.4

6.2 TPC Results

Tables 6-1 through 6-10 summarize the input for the TPC runs.

6.3 Maglev Performance Profiles

The Maglev performance in the Severe Segment Tests can be studied in greater detail by generating profiles of speed, power consumption, and acceleration over the complete route. These three profiles are presented below; they represent the Case 9 run described earlier, where an eight-car consist was limited to 30 MW power and accelerated at 0.2g within 0.25 g/sec jerk limit. The Minimum

Table 6-1. TPC Runs Carried Out

Case No.	Specs.	No. of Cars	Power (MW)	Accel/Decel	Jerk
1	Design	1	7.5	0.16g	0.07 g/sec
2	Design	8	20	0.16	0.07
3	Design	8	30	0.16	0.07
4	Design	8	40	0.16	0.07
5	Min Req	1	7.5	0.20	0.07
6	Min Req	8	20	0.20	0.07
7	Min Req	8	30	0.20	0.07
8	Min Req	8	40	0.20	0.07
9	Min Req	8	30	0.20	0.25

Table 6-2. Result for Case 1

VARIABLES:

ROUTE DATA FILE	SSTLEFT	
RIDE QUALITY	DESIGN	
#OF CARS	1	
POWER(MW)	7.5	
TRAIN WEIGHT OF	36915	kg
MAX. SPEED	134	M/S
MAX. ACCEL.	1.600	m/s^2
MAX. DECEL.	1.600	m/s^2
JERK RATE	0.07	G/sec
AERODYNAMIC DRAG	$1.88V^3$ W	(where V-velocity in m/s)
MAGNETIC DRAG	0.32 MW	(if V>40 m/s) else 0.0MW

AUXILIARY POWER/CAR	400.0 KW
PROPULSION SYSTEM EFFICIENCY	95%
DWELL TIME	0 SECONDS

OUTPUT SUMMARY DATA:

DEPARTURE STATION	ARRIVAL STATION	RUN LNG(M)	POWER (KWH)	TIME (SEC)
0.0	398250	398249.7	5090.9	4273.5
398250	468213	69963.7	911.8	621.4
468214	798213	330000.0	4251.8	2553.5

KWH PER TRAIN KM:	12.85
TOTAL TRAVEL DISTANCE (KM):	798.213
TOTAL TRAVEL TIME (SECONDS):	7448.4
AVERAGE SPEED (KM PER HOUR):	385.80

THE MAXIMUM AVAILABLE REDUCTION IN KWH PER MILE OR PER KM DUE TO REGENERATION, ASSUMING FULLY RECEPTIVE LINE IS 14.5 PERCENT.

Table 6-3. Result for Case 2

VARIABLES:

ROUTE DATA FILE	SSTLEFT	
RIDE QUALITY	DESIGN	
#OF CARS	8	
POWER(MW)	20	
TRAIN WEIGHT OF	210686	kg
MAX. SPEED	134	M/S
MAX. ACCEL.	1.600	m/s^2
MAX. DECEL.	1.600	m/s^2
JERK RATE	0.07	G/sec
AERODYNAMIC DRAG	$5.10V^3$ W	(where V-velocity in m/s)
MAGNETIC DRAG	1.4 MW	(if V>40 m/s) else 0.0MW

AUXILIARY POWER/CAR	400.0 KW
PROPULSION SYSTEM EFFICIENCY	95%
DWELL TIME	0 SECONDS

OUTPUT SUMMARY DATA:

DEPARTURE STATION	ARRIVAL STATION	RUN LNG(M)	POWER (KWH)	TIME (SEC)
0.0	398250	398249.7	21856.2 ~~25896.7~~	4684.7
398250	468213	69963.7	3352.6 ~~3493.2~~	638.9
468214	798213	330000.0	14541.0 ~~14601.9~~	2570.8

KWH PER TRAIN KM:	49.80	300 J/seat·m
TOTAL TRAVEL DISTANCE (KM):	798.213	
TOTAL TRAVEL TIME (SECONDS):	7894.4	
AVERAGE SPEED (KM PER HOUR):	364.00	

THE MAXIMUM AVAILABLE REDUCTION IN KWH PER MILE OR PER KM DUE TO REGENERATION, ASSUMING FULLY RECEPTIVE LINE IS 22.3 PERCENT.

Table 6-4. Result for Case 3

VARIABLES:

ROUTE DATA FILE	SSTLEFT	
RIDE QUALITY	DESIGN	
#OF CARS	8	
POWER(MW)	30	
TRAIN WEIGHT OF	210686 kg	
MAX. SPEED	134 M/S	
MAX. ACCEL.	1.600 m/s^2	
MAX. DECEL.	1.600 m/s^2	
JERK RATE	0.07 G/sec	
AERODYNAMIC DRAG	$5.10V^3$ W	(where V-velocity in m/s)
MAGNETIC DRAG	1.4 MW	(if V>40 m/s) else 0.0MW

AUXILIARY POWER/CAR	400.0 KW
PROPULSION SYSTEM EFFICIENCY	95%
DWELL TIME	0 SECONDS

OUTPUT SUMMARY DATA:

DEPARTURE STATION	ARRIVAL STATION	RUN LNG(M)	POWER (KWH)	TIME (SEC)
0.0	398250	398249.7	24625.6	4421.9
398250	468213	69963.7	3470.5	625.0
468214	798213	330000.0	14603.6	2554.2

KWH PER TRAIN KM:	53.49
TOTAL TRAVEL DISTANCE (KM):	798.213
TOTAL TRAVEL TIME (SECONDS):	7601.1
AVERAGE SPEED (KM PER HOUR):	378.05

THE MAXIMUM AVAILABLE REDUCTION IN KWH PER MILE OR PER KM DUE TO REGENERATION, ASSUMING FULLY RECEPTIVE LINE IS 25.6 PERCENT.

Table 6-5. Result for Case 4

VARIABLES:

ROUTE DATA FILE	SSTLEFT	
RIDE QUALITY	DESIGN	
#OF CARS	8	
POWER(MW)	40	
TRAIN WEIGHT OF	210686	kg
MAX. SPEED	134	M/S
MAX. ACCEL.	1.600	m/s^2
MAX. DECEL.	1.600	m/s^2
JERK RATE	0.07	G/sec
AERODYNAMIC DRAG	$5.10V^3$ W	(where V-velocity in m/s)
MAGNETIC DRAG	1.4 MW	(if V>40 m/s) else 0.0MW

AUXILIARY POWER/CAR	400.0	KW
PROPULSION SYSTEM EFFICIENCY	95%	
DWELL TIME	0	SECONDS

OUTPUT SUMMARY DATA:

DEPARTURE STATION	ARRIVAL STATION	RUN LNG(M)	POWER (KWH)	TIME (SEC)
0.0	398250	398249.7	25896.7	4306.1
398250	468213	69963.7	3493.2	620.4
468214	798213	330000.0	14601.9	2553.1

KWH PER TRAIN KM:	55.11
TOTAL TRAVEL DISTANCE (KM):	798.213
TOTAL TRAVEL TIME (SECONDS):	7479.6
AVERAGE SPEED (KM PER HOUR):	384.19

THE MAXIMUM AVAILABLE REDUCTION IN KWH PER MILE OR PER KM DUE TO REGENERATION, ASSUMING FULLY RECEPTIVE LINE IS 26.9 PERCENT.

Table 6-6. Result for Case 5

VARIABLES:

ROUTE DATA FILE	SSTMID	
RIDE QUALITY	MIN.REQD.	
#OF CARS	1	
POWER(MW)	7.5	
TRAIN WEIGHT OF	36915	kg
MAX. SPEED	134	M/S
MAX. ACCEL.	2 ~~1.600~~	m/s^2
MAX. DECEL.	2 ~~1.600~~	m/s^2
JERK RATE	0.07	G/sec
AERODYNAMIC DRAG	$1.88V^3$ W	(where V-velocity in m/s)
MAGNETIC DRAG	0.32 MW	(if V>40 m/s) else 0.0MW

AUXILIARY POWER/CAR	400.0 KW
PROPULSION SYSTEM EFFICIENCY	95%
DWELL TIME	0 SECONDS

OUTPUT SUMMARY DATA:

DEPARTURE STATION	ARRIVAL STATION	RUN LNG(M)	POWER (KWH)	TIME (SEC)
0.0	398480	398479.9	5515.5	3850.0
398480	468446	69966.0	934.9	604.0
468446	798446	330000.0	4267.2	2538.4

KWH PER TRAIN KM:	13.42
TOTAL TRAVEL DISTANCE (KM):	798.446
TOTAL TRAVEL TIME (SECONDS):	6992.4
AVERAGE SPEED (KM PER HOUR):	411.07

THE MAXIMUM AVAILABLE REDUCTION IN KWH PER MILE OR PER KM DUE TO REGENERATION, ASSUMING FULLY RECEPTIVE LINE IS 14.6 PERCENT.

Table 6-7. Result for Case 6

VARIABLES:

ROUTE DATA FILE	SSTMID	
RIDE QUALITY	MIN.REQD.	
#OF CARS	8	
POWER(MW)	20	
TRAIN WEIGHT OF	210686	kg
MAX. SPEED	134	M/S
MAX. ACCEL.	2.0	m/s^2
MAX. DECEL.	2.0	m/s^2
JERK RATE	0.07	G/sec
AERODYNAMIC DRAG	$5.10V^3$ W	(where V-velocity in m/s)
MAGNETIC DRAG	1.4 MW	(if V>40 m/s) else 0.0MW

AUXILIARY POWER/CAR	400.0 KW
PROPULSION SYSTEM EFFICIENCY	95%
DWELL TIME	0 SECONDS

OUTPUT SUMMARY DATA:

DEPARTURE STATION	ARRIVAL STATION	RUN LNG(M)	POWER (KWH)	TIME (SEC)
0.0	398480	398479.9	21899.0	4254.7
398480	468446	69966.0	3387.5	621.1
468446	798446	330000.0	14574.3	2558.0

KWH PER TRAIN KM:	49.92
TOTAL TRAVEL DISTANCE (KM):	798.446
TOTAL TRAVEL TIME (SECONDS):	7433.8
AVERAGE SPEED (KM PER HOUR):	386.66

THE MAXIMUM AVAILABLE REDUCTION IN KWH PER MILE OR PER KM DUE TO REGENERATION, ASSUMING FULLY RECEPTIVE LINE IS 21.4 PERCENT.

Table 6-8. Result for Case 7

VARIABLES:

ROUTE DATA FILE	SSTMID	
RIDE QUALITY	MIN.REQD.	
#OF CARS	8	
POWER(MW)	30	
TRAIN WEIGHT OF	210686	kg
MAX. SPEED	134	M/S
MAX. ACCEL.	2.0	m/s^2
MAX. DECEL.	2.0	m/s^2
JERK RATE	0.07	G/sec
AERODYNAMIC DRAG	$5.10V^3$ W	(where V-velocity in m/s)
MAGNETIC DRAG	1.4 MW	(if V>40 m/s) else 0.0MW

AUXILIARY POWER/CAR	400.0 KW
PROPULSION SYSTEM EFFICIENCY	95%
DWELL TIME	0 SECONDS

OUTPUT SUMMARY DATA:

DEPARTURE STATION	ARRIVAL STATION	RUN LNG(M)	POWER (KWH)	TIME (SEC)
0.0	398480	398479.9	25288.4 ~~21899.0~~	3977.4
398480	468446	69966.0	2494.1 ~~3387.5~~	606.8
468446	798446	330000.0	14640.4 ~~14574.3~~	2540.5

KWH PER TRAIN KM:	54.31
TOTAL TRAVEL DISTANCE (KM):	798.446
TOTAL TRAVEL TIME (SECONDS):	7124.8
AVERAGE SPEED (KM PER HOUR):	403.44

THE MAXIMUM AVAILABLE REDUCTION IN KWH PER MILE OR PER KM DUE TO REGENERATION, ASSUMING FULLY RECEPTIVE LINE IS 25.2 PERCENT.

Table 6-9. Result for Case 8

VARIABLES:

ROUTE DATA FILE	SSTMID	
RIDE QUALITY	MIN.REQD.	
#OF CARS	8	
POWER(MW)	40	
TRAIN WEIGHT OF	210686	kg
MAX. SPEED	134	M/S
MAX. ACCEL.	2.0	m/s^2
MAX. DECEL.	2.0	m/s^2
JERK RATE	0.07	G/sec
AERODYNAMIC DRAG	$5.10V^3$ W	(where V-velocity in m/s)
MAGNETIC DRAG	1.4 MW	(if V>40 m/s) else 0.0MW

AUXILIARY POWER/CAR	400.0 KW
PROPULSION SYSTEM EFFICIENCY	95%
DWELL TIME	0 SECONDS

OUTPUT SUMMARY DATA:

DEPARTURE STATION	ARRIVAL STATION	RUN LNG(M)	POWER (KWH)	TIME (SEC)
0.0	398480	398479.9	2709.1 ~~21899.0~~	3841.0
398480	468446	69966.0	2536.8 ~~3387.5~~	603.3
468446	798446	330000.0	14691.0 ~~14574.3~~	2538.7

KWH PER TRAIN KM:	56.69
TOTAL TRAVEL DISTANCE (KM):	798.446
TOTAL TRAVEL TIME (SECONDS):	6983.0
AVERAGE SPEED (KM PER HOUR):	411.63

THE MAXIMUM AVAILABLE REDUCTION IN KWH PER MILE OR PER KM DUE TO REGENERATION, ASSUMING FULLY RECEPTIVE LINE IS 27.0 PERCENT.

Table 6-10. Result for Case 9

VARIABLES:

ROUTE DATA FILE	SSTMID	
RIDE QUALITY	MIN.REQD.	
#OF CARS	8	
POWER(MW)	30	
TRAIN WEIGHT OF	210686	kg
MAX. SPEED	134	M/S
MAX. ACCEL.	2.0	m/s^2
MAX. DECEL.	2.0	m/s^2
JERK RATE	0.25	G/sec
AERODYNAMIC DRAG	$5.10V^3$ W	(where V-velocity in m/s)
MAGNETIC DRAG	1.4 MW	(if V>40 m/s) else 0.0MW

AUXILIARY POWER/CAR	400.0 KW
PROPULSION SYSTEM EFFICIENCY	95%
DWELL TIME	0 SECONDS

OUTPUT SUMMARY DATA:

DEPARTURE STATION	ARRIVAL STATION	RUN LNG(M)	POWER (KWH)	TIME (SEC)
0.0	398480	398479.9	25408.8 ~~21899.0~~	3967.3
398480	468446	69966.0	3483.6 ~~3387.5~~	603.8
468446	798446	330000.0	14627.6 ~~14574.3~~	2539.5

KWH PER TRAIN KM:	54.51
TOTAL TRAVEL DISTANCE (KM):	798.446
TOTAL TRAVEL TIME (SECONDS):	7110.6
AVERAGE SPEED (KM PER HOUR):	404.24

THE MAXIMUM AVAILABLE REDUCTION IN KWH PER MILE OR PER KM DUE TO REGENERATION, ASSUMING FULLY RECEPTIVE LINE IS 25.5 PERCENT.

Required ride quality SST route was used for this simulation. In this run the average speed was 112.3 m/sec. The total Terminal 1 to Terminal 4 run time for this simulation is 118.5 min. Though these numbers are clearly shown in the earlier tables, the profiles provide a clearer picture of the vehicle performance. Since for all practical purposes all these profiles look very similar for the nine runs described earlier, only one set of these profiles have been printed here.

Speed Profile

The speed profile for the Minimum Required ride quality SST route is shown in Figure 6-1. The vehicle attained and sustained the designed maximum vehicle speed over eight times during the run. The four terminals where the vehicle has zero speeds are clearly marked. Such plots describe the route characteristics as well. The three segments of varying degrees of severities, described in Section 1, can be clearly seen from the figure.

Power Profile

The power profile for the 30 MW-rated vehicle is plotted in Figure 6-2. The maximum power consumption rate near 35 MW accounts for the tractive effort, auxiliary power of 3200 kW, and a system efficiency of 95 percent. The power profile in Segment 1 shows the availability of high regenerative braking possibilities. The estimated maximum available reduction in kWh or per km due to regeneration, assuming fully receptive line is 25.5 percent for the entire route. In Segment 2 and Segment 3 the duration of maximum power consumption is very short. There is only one instance of the power consumption reaching near 35 MW. In Segment 2 there are only two additional short instances of power consumption near 24 MW. Segment 3 is devoid of any power requirements above 21 MW for a sustained time interval. This indicates that for non-severe segments the substation power requirements are about 40 percent lower than that required for very severe segments (assuming non regenerative systems). For mildly severe segments, the possible reduction in required substation power is approximately 30 percent.

Acceleration Profile

Figure 6-3 shows the acceleration profile for the Case 9 run. The accelerations reflect the 0.2g limits used in this case. As expected, the accelerations are most severe in the first segment, due to the large number of small radius turns.

6.4 Dynamic Ride Quality Studies

The dynamic analysis of the effects on actual ride quality using the ride quality specifications will be described in Section 8. As opposed to the static analysis described in Section 2, this study used the dynamic program MAGSIM and considered all vehicle and guideway parameters contributing to the jerk/jolt limits. More detailed ride quality studies may be needed in some very severe segments as will be addressed by Dr. Blader in Part II of this report.

The net effect on the route characterization for such very severe segments is the improvement on the easement curves design. From the point of view of the TPC simulations, the minor adjustments in the curve parameters and speed profiles in the route have a very minor effect on the vehicle performance, as evidenced by several trial studies. The estimated change for the run time of about 120 min, due to these small adjustments in the spiral design to further improve the ride quality, is less than 1 percent. Therefore, although the ride quality specification used has a very significant influence on vehicle performance in SST, these minor secondary adjustments have almost an unnoticeable influence when studied in relation to the complete route.

PARSONS DE LEUW, INC. Maglev 8-car, 30MW, 0.2g accel, 0.25g/s jerk rate, Route SSTMID

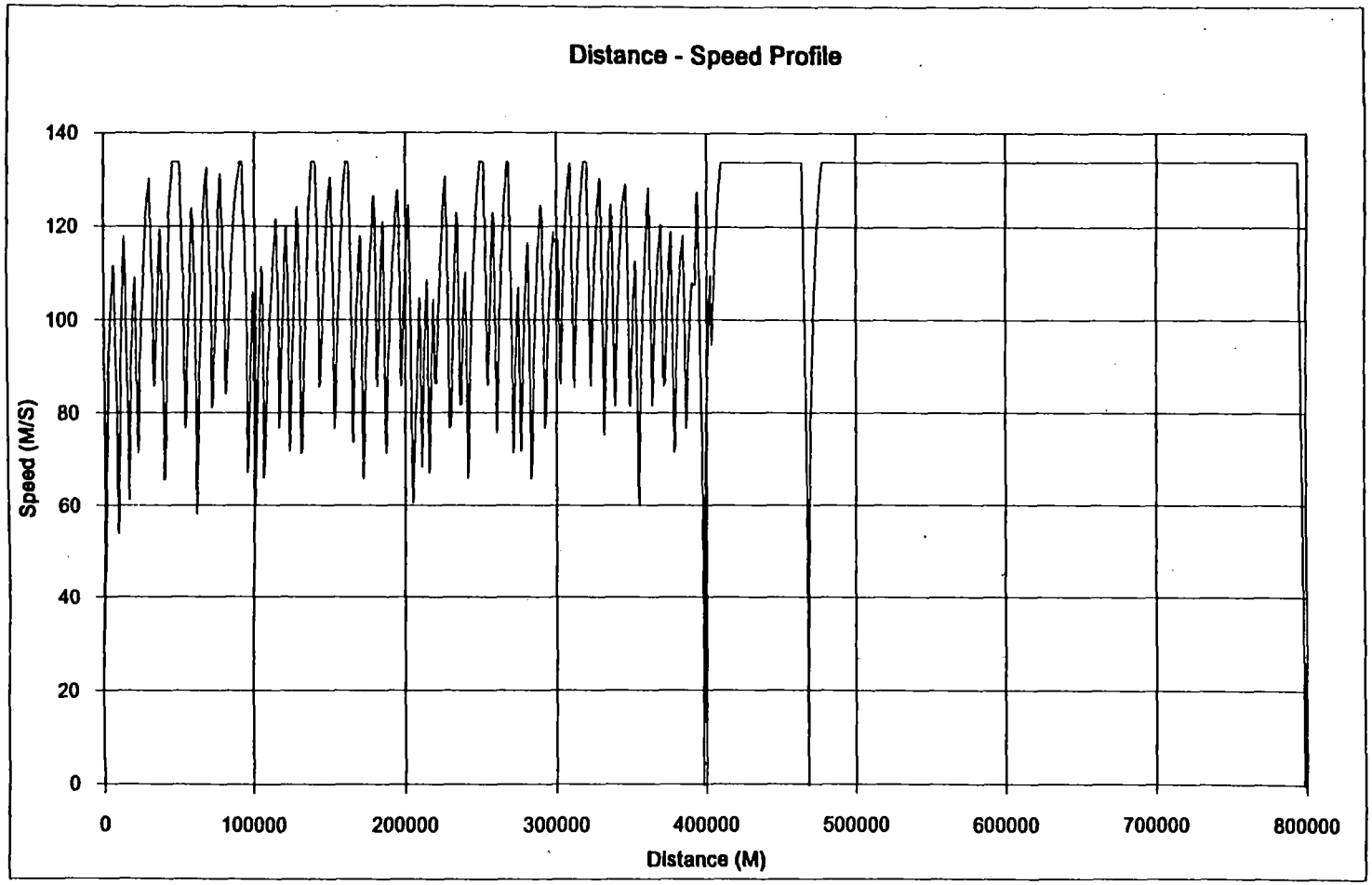

8C30MWDS.XLC 7/7/92

Figure 6-1. Maglev Speed Profile Generated from a TPC RUN

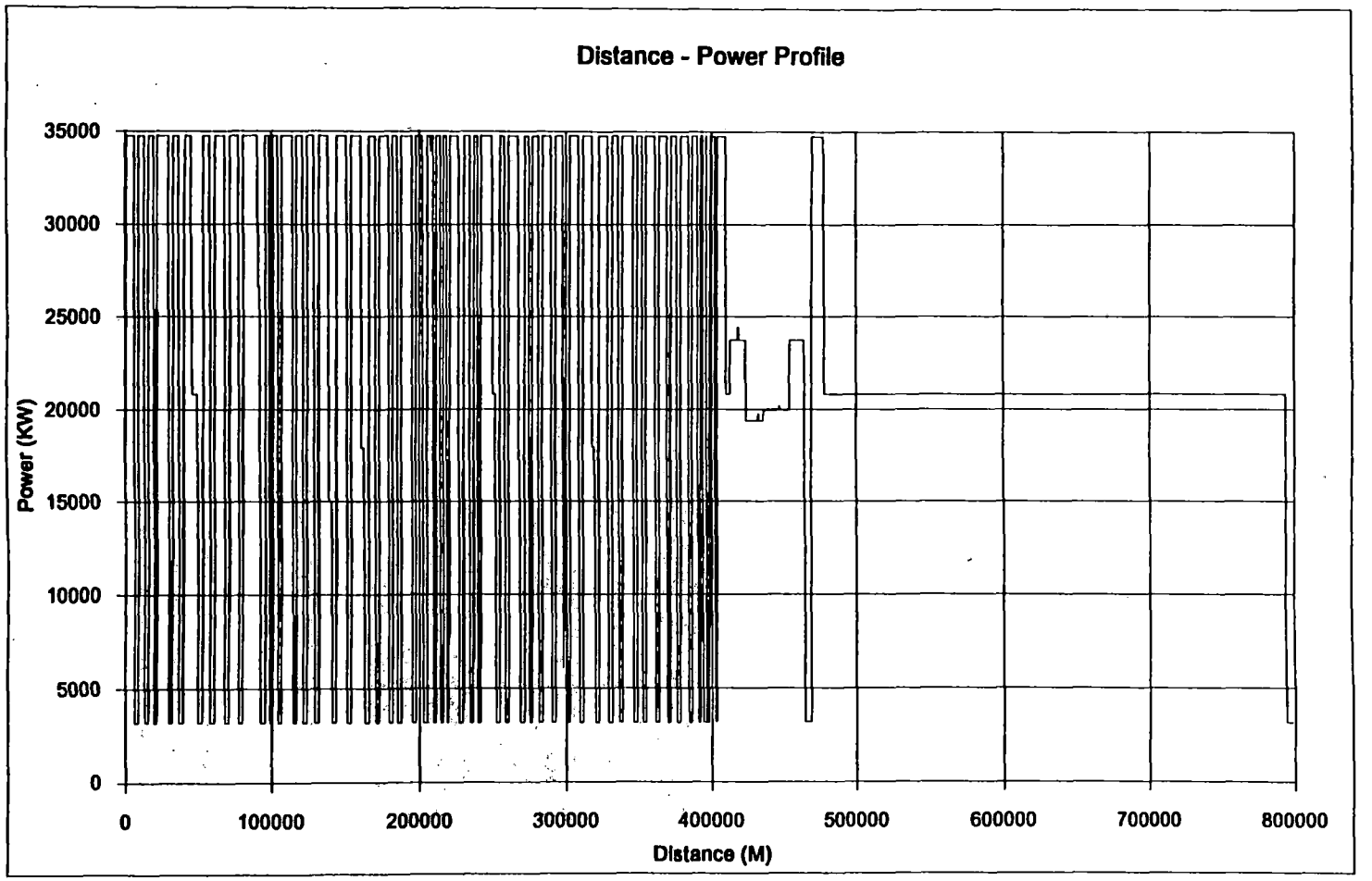

8C30MWDP.XLC 7/7/92

Figure 6-2. Maglev Power Profile Generated from a TPC Run

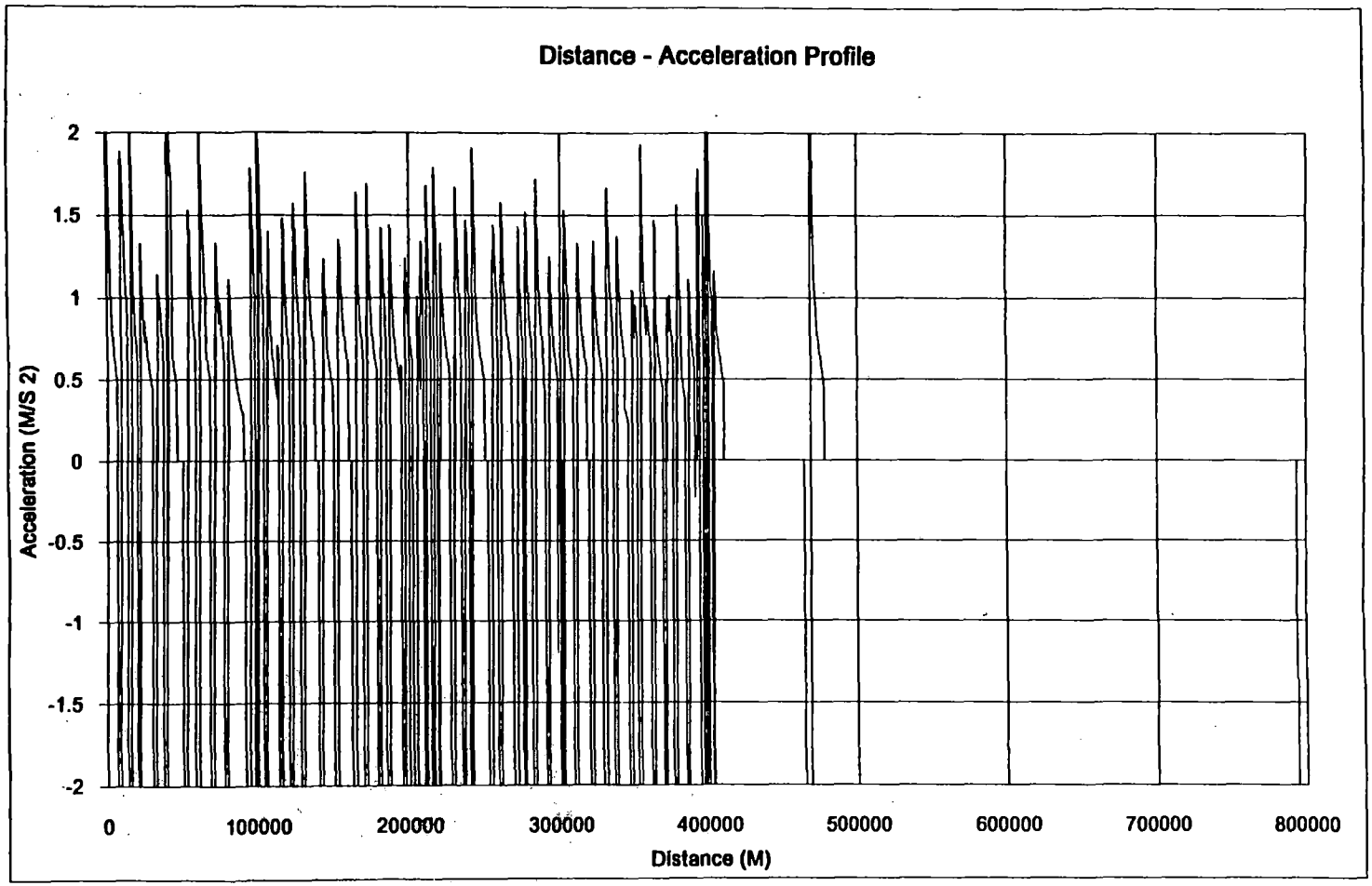

8C30MWDA.XLC 7/7/92

Figure 6-3. Maglev Accel Profile Generated from a TPC Run

6.5 Headway Studies

The vehicle headway studies were carried out for 9,600 passenger/hr utilization. Using the velocity and profiles from the TPC simulations, the consist separation along the complete route with vehicle spaced at 225 sec headway was continuously calculated. Figure 6-4 for an eight-car consist shows the separation profile for one such study. It showed that the minimum separation encountered on the whole route is 15.7 km. Similarly a four-car consist for the same passenger/hr utilization will require a headway of 112 sec which will result in a minimum separation of 7.9 km.

6.6 In-Tunnel Operations

The chief issues involved with in-tunnel Maglev operation are mostly those concerned with the complex aerodynamic interaction between the high-speed Maglev consists and the tunnel passage, including not only the tunnel proper itself, but also entries, exits and subsidiary shafts. The civil construction details of the tunnel itself are outside the scope of this report, but the important design features needed for effective high speed Maglev operation will be described after an explanation of the technical tradeoffs involved.

Our goal is to design the 5 km tunnel in the SST for maximum cruise speed operation of 134 m/sec (300 mph). This can be accomplished if the tunnel design is such that these pressure transients and drag increases associated with high-speed travel in-tunnel can be accommodated. Therefore, we will address these two areas in this section.

Our analysis shows that the behavior of a typical vehicle consist in a tunnel can be characterized by a pressure profile such as that shown in Figure 6-5. It is the management of these pressure transients and drags that are of primary concern in designing high-speed tunnels so as to control both

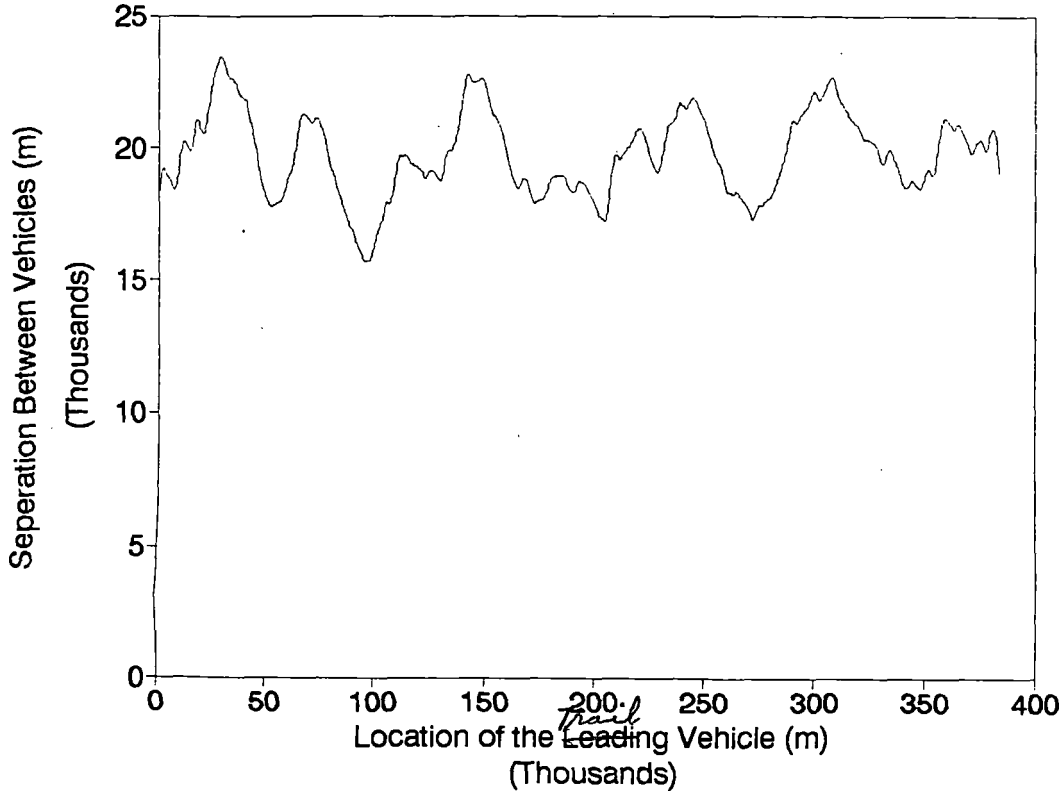

Figure 6-4. Maglev Headway Profile for an Eight-Car Consist Generated by Processing a TPC Output

Our analysis shows that the behavior of a typical vehicle consist in a tunnel can be characterized by a pressure profile such as that shown in Figure 6-5. It is the management of these pressure transients and drags that are of primary concern in designing high-speed tunnels so as to control both the sharpness and magnitude of these pressures, and overall train drag.

The initial pressure transient at a flush faced tunnel entry is shown in Figure 6-6. This is characterized by a rapid pressure rise due to the nose entry, followed by a continuing rise at a much lower rate due to the following part of the vehicle body. The slope of the initial rise is on the order of 1,000 N/m^2/sec (1 kPa/sec or 0.15 psi/sec) up to a value which is strongly dependent on the ratio of train cross section to the total cross section of the tunnel, also referred to as the "blockage ratio." The pressure rise rate is dependent primarily on V^3, while the magnitude of the rise is proportional to V^2.

As far as the magnitude of the pressure rise is concerned, the design of the skin structure of the vehicle could be unduly affected by inward pressures much greater than the 3 kPa (1/2 psi) range, and also would be uncomfortable for occupants if doors and gaps were not sealed well. In order to achieve this level with some design margin, say 2.5 kPa (1/3 psi), the blockage ratio for the tunnel must be in the 1:6 or 1:7 range or less for full speed operation, meaning a generous tunnel cross section would be required for high speed travel. Foster-Miller estimates suggest that this also would restrict overall train drag increases to about 50 to 60 percent over free-stream conditions, which could still be easily manageable by the Maglev propulsion and power delivery systems, as will be discussed later in this report.

One important conclusion here for a two-way system is that due to the high expense of tunneling, the only reasonable solution to the need for a tunnel which is 6 or 7 times the vehicle cross section

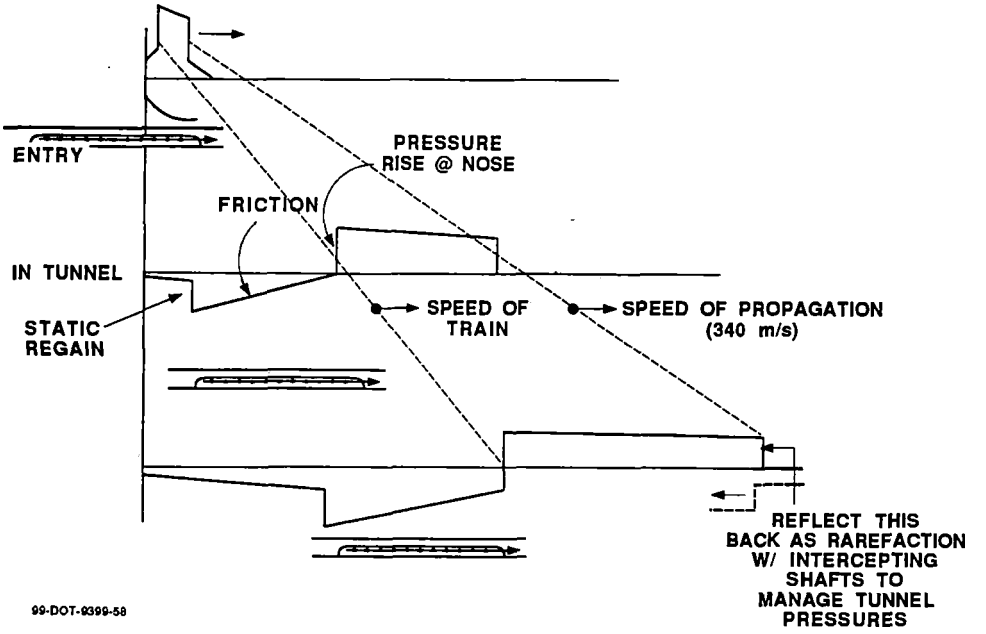

Figure 6-5. Typical Pressure Profile in High Speed Tunnel

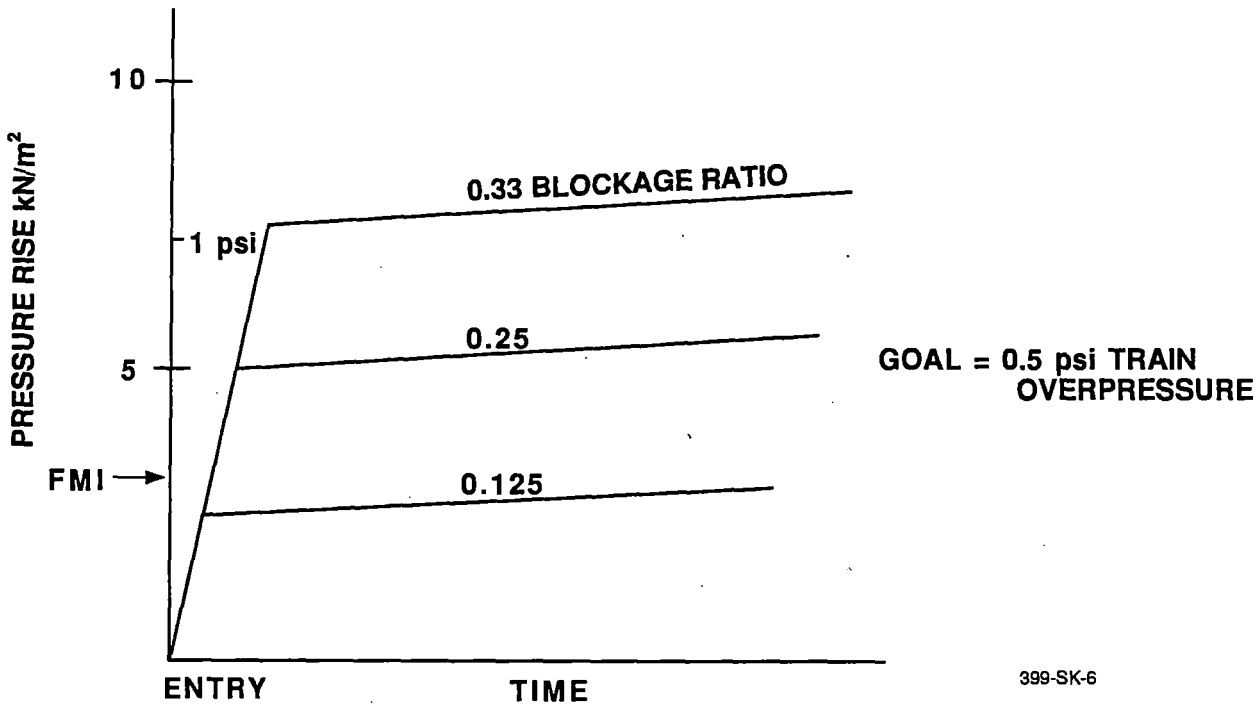

Figure 6-6. Tunnel Pressure Rise at Tunnel Entry

is to provide one tunnel for two-way travel, containing two at-grade guideways but only permitting one consist in the tunnel at any one time.* This policy would result not only in tunnel cross-sectional area in the range of 60 m^2, but also eliminate the need for wide separation of the guideways in tunnel which would otherwise be needed to protect against gusts from opposing trains.

Such a tunnel cross section is shown in Figure 6-7. Here, two at-grade guideways are shown supported on a transverse concrete floor slab, with utility passages below. The most efficient shape would be a "TV" shape with large top, bottom and side radii and small corner radii, with the tunnel structure being determined by site conditions.

An analysis of the average drag increase in this tunnel for a single consist shows that the drag increase will be on the order of 50 to 60 percent, as mentioned previously. This means that the propulsion power for a multi-car consist of several cars will increase by 0.8 to 1.0 MW per car for the 38 sec spend in the 5 km tunnel. An energy analysis shows that the total energy consumed over the SST route will increase by less than 0.2 percent, which has practically an unmeasureable effect on specific energy consumption. Since the substation design has adequate short-term rating to supply this even at the upper end of the propulsion power range being considered in the SST route analysis, the tunnel design approach for full speed operation will be adopted. The remainder of this discussion will then focus on the design details needed to minimize pressure transients during entry and exit of the tunnel.

*The projected Japanese commercial Maglev design for the 500 km inland route between Tokyo and Osaka uses a tunnel cross section nearly eight times that of the vehicle.

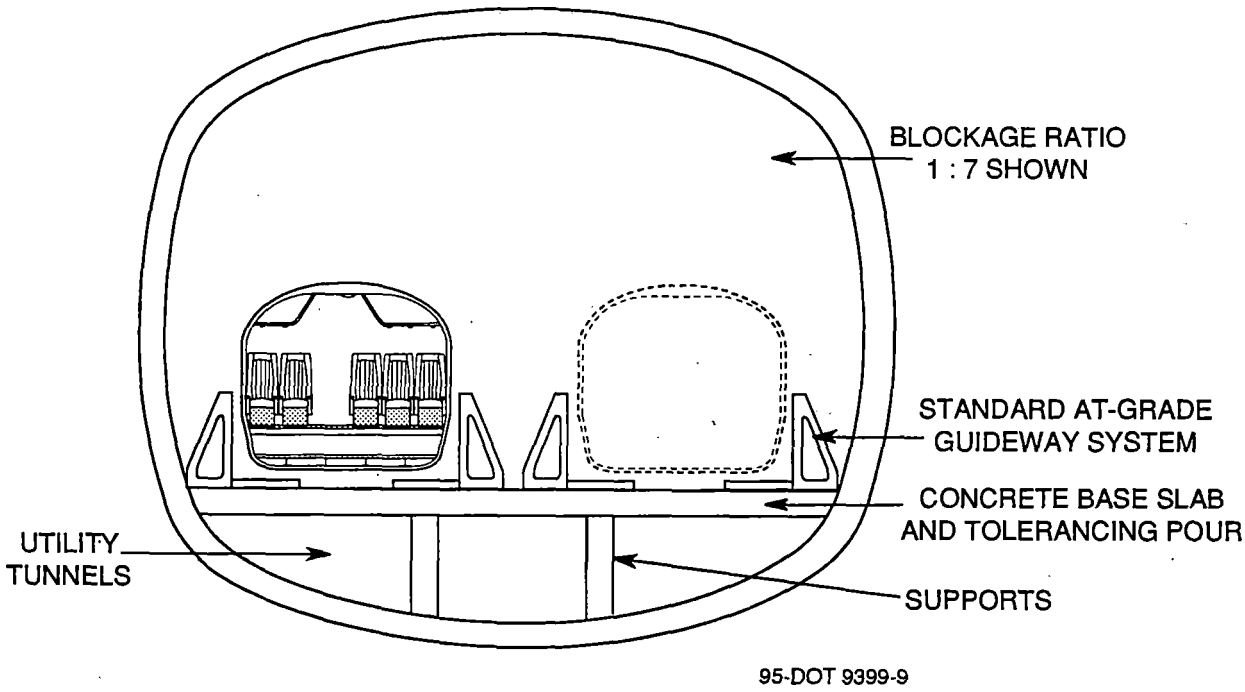

Figure 6-7. Tunnel Cross Section

Control of the rate of pressure rise is equally important, both from the point of view of passenger comfort and for the disconcerting "impact" sound of tunnel entry. One proven method of reducing the rate of rise is with entry and exit flares, which must be engineered to be as economical as possible and still achieve design targets. These flares should be three-dimensional for best effect. The BART system, English-French "Chunnel" and the German ICE all use or will use flares, although the first two are characterized by lower speeds and tighter tunnels. To size these flares for high-speed Maglev applications, we can refer to Figure 6-8, which shows how various length flares reduce the slope of pressure rise. Note that these flares do not significantly reduce the ultimate magnitude of the pressure rise, but greatly delay the onset (rate) of this pressure. Figure 6-8 uses an entry area that is twice the final tunnel area, in the interest of practicality, although similar relationships could be shown for other "initial" blockage ratios.

As a typical guide, German standards call for rise rates of 200 Pa/sec (0.03 psi/sec) which is thought to be quite conservative in light of using sealed cars. Using a somewhat greater value of 300 Pa/sec and looking at Figure 6-8, we can see that a flare on the order of 150m or so (500 ft) could be used. These rise rates could easily be tolerated even with leaky car seals.

Further attention to pressure rises within the tunnel itself can be made if we refer again to Figure 6-5. Note that the advancing "entry" pressure front can be reflected back from any substantial change in tunnel area. The important ones to consider are the sudden openings represented by the other end of the tunnel and by any intercepting shafts. These will reflect the advancing pressure wave back as a rarefaction, which will in turn combine with both the advancing front and other disturbances. This affords the opportunity to further moderate pressure effects in the tunnel by judicious combination of these pressure waves using both the tunnel ends and intermediate shafts. While detailed study of these interactions over various speed ranges has not yet been done, initial estimates suggest that use of two auxiliary vent shafts in, say, a 5 to 10 km tunnel might produce some benefit. (Additionally,

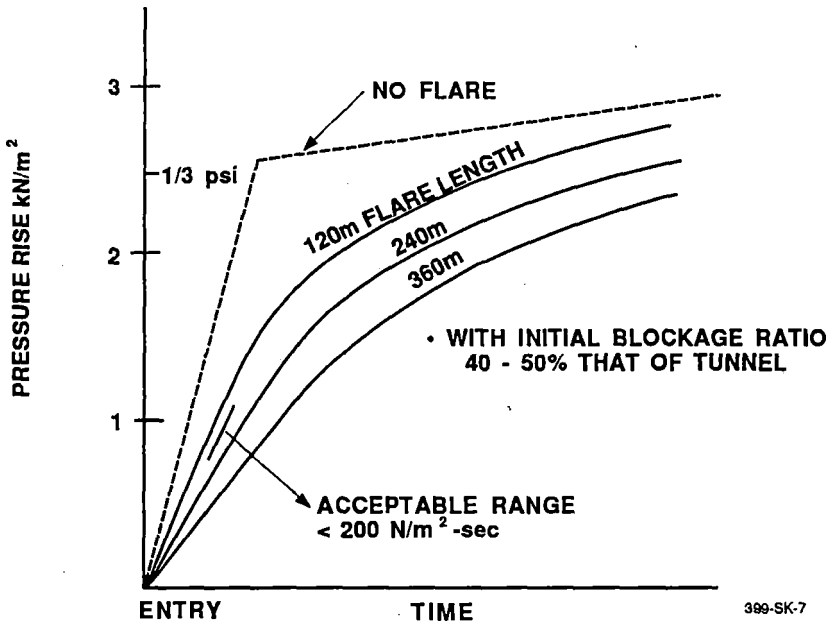

Figure 6-8. Pressure Rise Reduction with Flared Entry

these shafts might contain "leaky" filters or diffusers to further damp pressure transients.) These shafts could be placed within 1 km from each end, or a shorter distance for significantly shorter tunnels. Further work would be needed to justify these preliminary concepts, however.

A proper tunnel and flare design for full speed two-way Maglev operation, therefore, could consist of a typical tunnel cross section of about 60 m^2, with entry and exit flares 200m long and 120 m^2 in initial area, assuming a 10 m^2 vehicle cross section and only one train allowed in the tunnel at any one time. Two additional cross shafts could be used to further mitigate pressure transients. These features are shown together in Figure 6-9, using the cross section seen in Figure 6-7.

6.7 Summary

In this section results for nine final runs of the SST simulations have been presented. Many more runs were carried out to streamline and debug the TPC simulations of the SST, including runs on an earlier 351 km trial route developed by Foster-Miller, plus short route runs to check compatibility between the spiral designs and TPC simulation algorithms. These included full graphical presentation of speed, power and acceleration profiles.

The results show that the total travel time for the 800 km route is approximately 2 hr for each of the nine cases. Using the more aggressive Minimum Required ride quality levels, thus does not greatly reduce the total travel time.

In addition, the chief issues involved with in-tunnel Maglev operation were addressed in this section. Proper tunnel and flare design will allow for full speed in-tunnel operation with essentially a negligible increase in total energy consumption.

A more detailed analysis of the simulation output will be presented in the following sections. The dynamic modeling ride quality analysis is then presented in Part II.

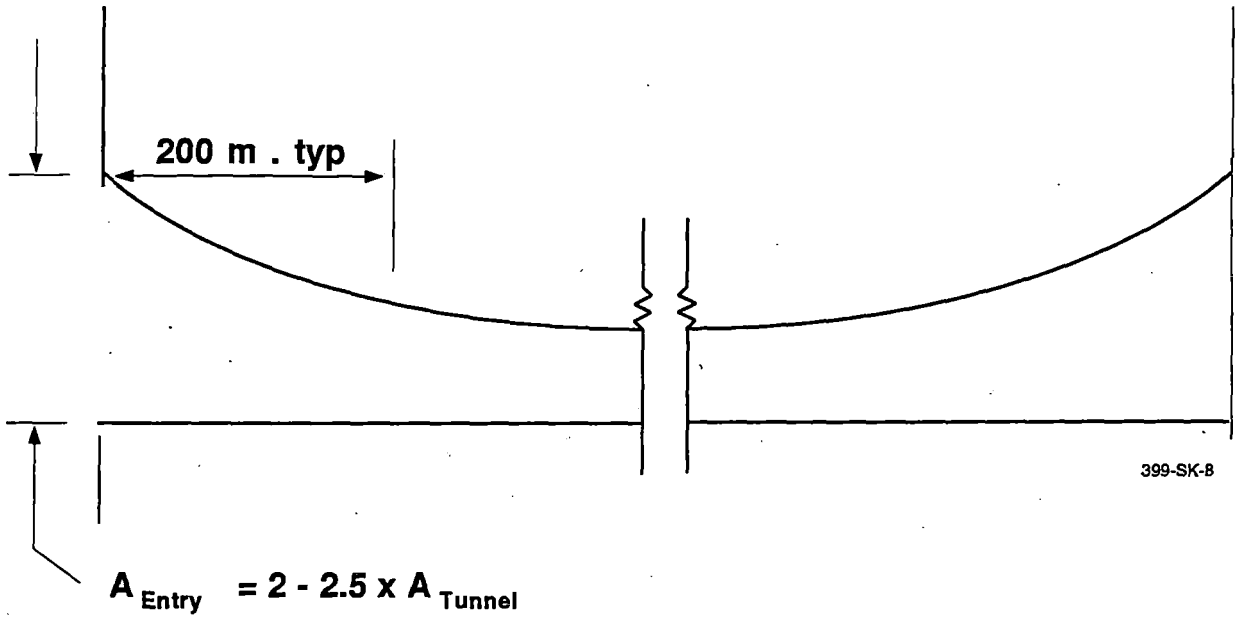

Figure 6-9. Tunnel Flares at Entry Exit

7. SUMMARY OF RESULTS

7.1 Performance Characteristics

This section summarizes the evaluation of performance characteristics over the SST route. A final set of the TPC results were summarized in Section 6. The complete TPC output is too voluminous to be printed here, but a small section is presented in Appendix B. Output files are available at both Foster-Miller, Inc., Waltham, MA and Parsons DeLeuw Inc., Washington, DC.

A summary and tradeoff analyses of the above simulations are presented here which consist of:

- Complete speed and power consumption profiles over the route for the two sets of optimized curve layouts and ride qualities: Design Goal and Minimum Required (SSTLEFT and SSTMID respectively).
- Study of the effect of ride quality parameters on average vehicle speed.
- Study of the effect of car power ratings on trip time.
- Study of the effect of ride quality parameters on trip time.
- Study of the effects of power ratings and ride quality parameters on specific power consumption.

7.2 Speed and Power Profiles for the Complete SST Route

Both speed and power profiles for Design Goal ride quality and Minimum Required ride quality specifications are plotted in Figures 7-1 and 7-2 respectively. Speed and power profiles shown in Figure 7-1 correspond to vehicle consist using a power rating of 3.75 MW/car and Design Goal ride quality. (This run is described under Case 3 in Section 6.) For this case, the average speed for the entire route is 105.0 m/sec and the specific power consumption is 6.7 kWhr/car-km.

Figure 7-2 corresponds to the Minimum Required ride quality specifications using the same vehicle parameters as in Figure 7-1. (This run is described in detail under Case 7 previously.) The average speed for the entire route in this case is 112.1 m/sec and the specific power consumption is 6.8 kWhr/car-km.

Two important clarifications should be reiterated here. First, each curve design throughout the route was optimized twice: once for Design Goal and again for the Minimum Required ride qualities. Therefore, there are actually slightly different route geometries, speed limits, etc. associated with negotiation for the SST route for each of these two ride qualities, each of which maximized the "envelope" of ride quality conditions. Secondly, the "maximum car power" referred to is the actual propulsive power delivered to each car, whereas the total power seen in the plots includes allowance for the "hotel" power plus a 5 percent transmission loss along the ROW.

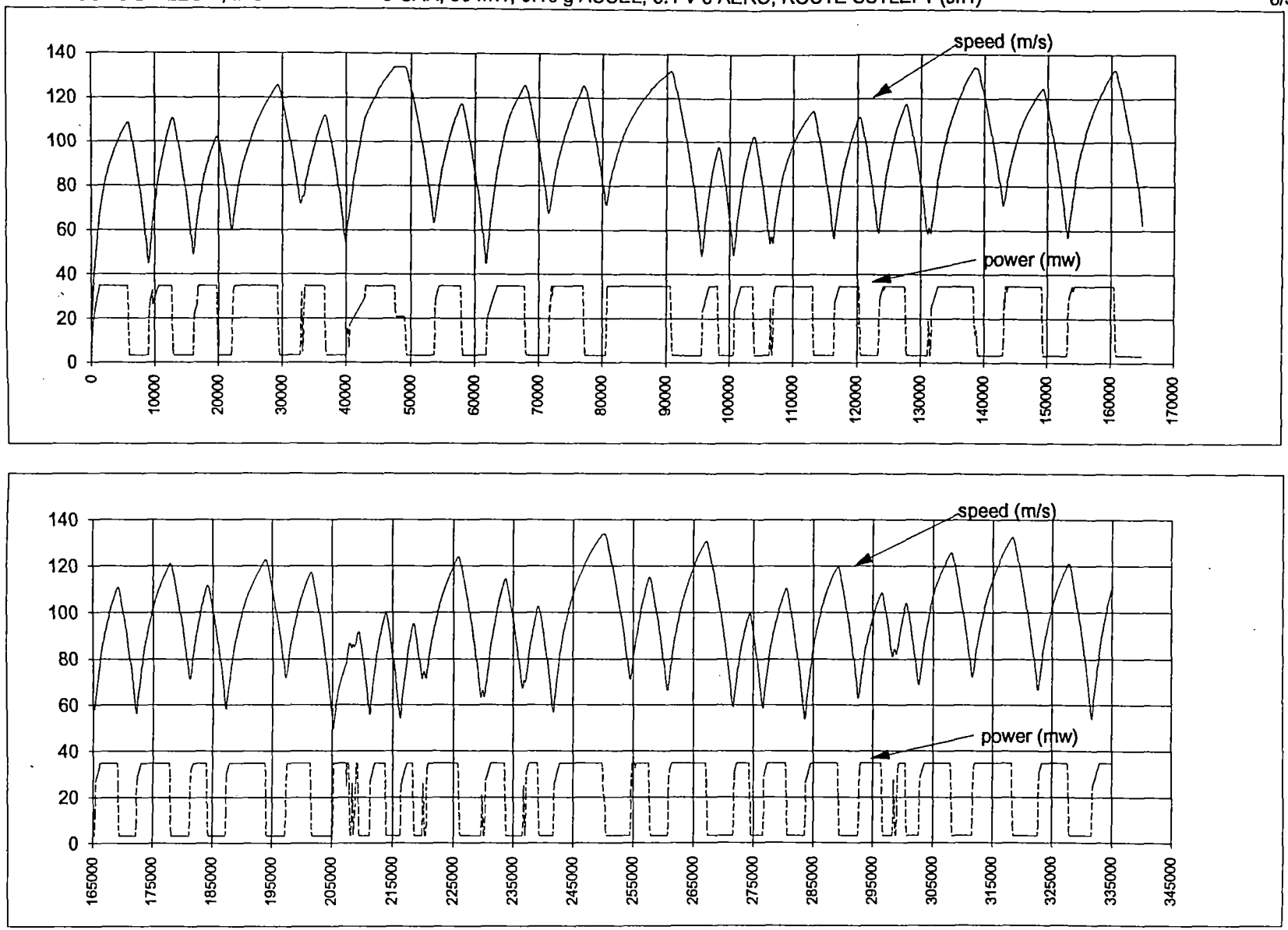

Figure 7-1. Speed and Power Profile for Design Goal Ride Quality

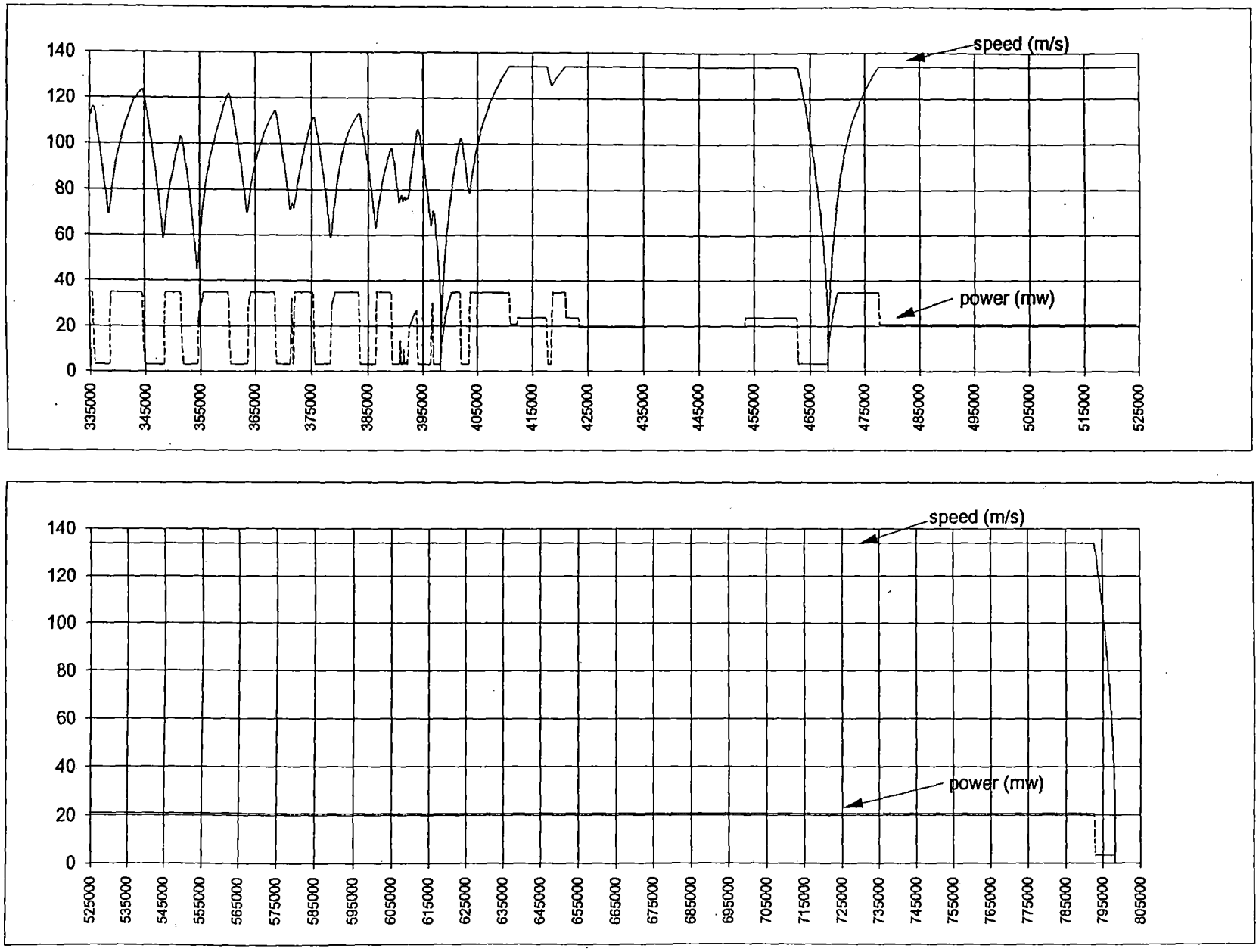

Figure 7-1. Speed and Power Profile for Design Goal Ride Quality (Continued)

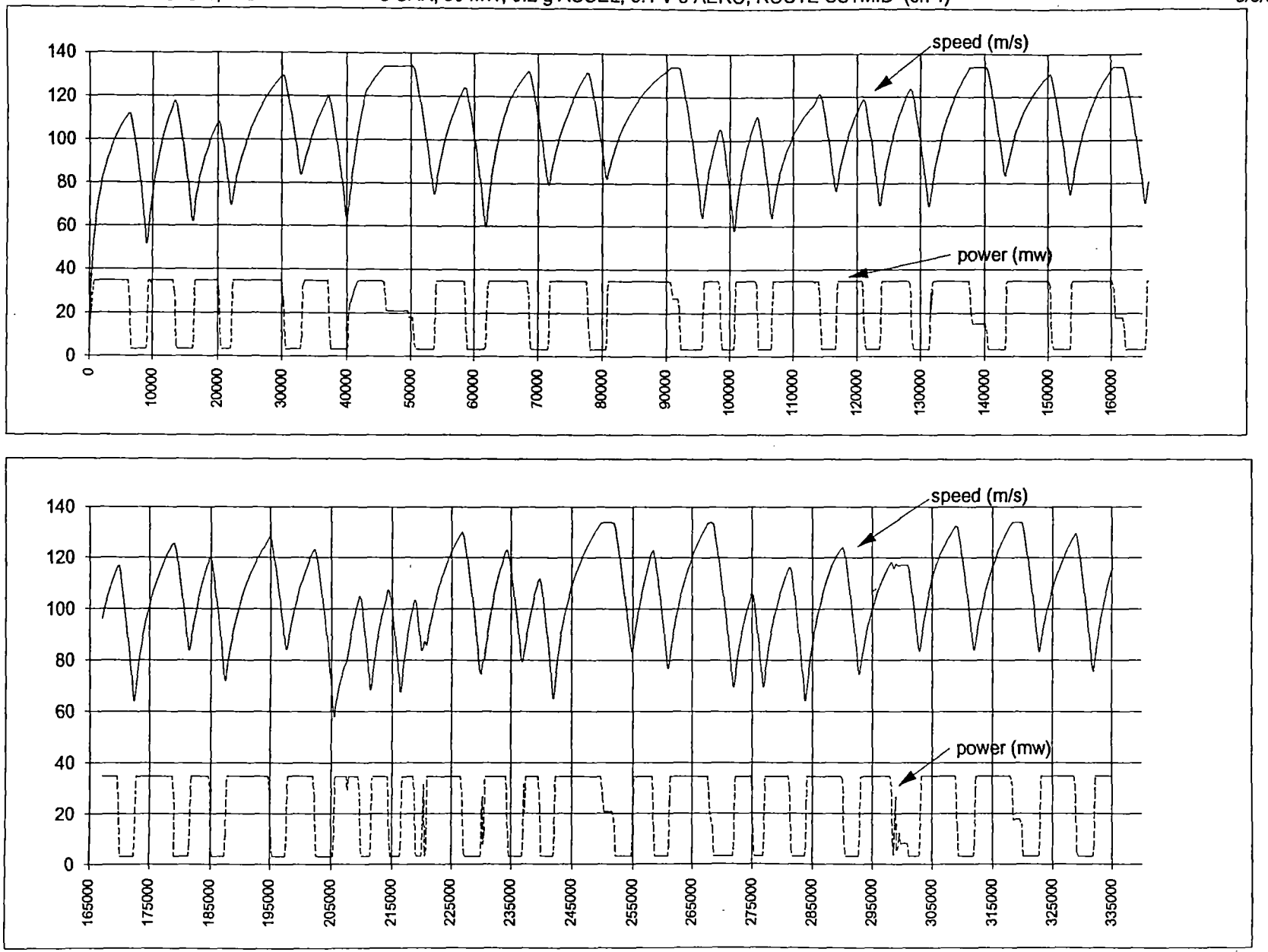

Figure 7-2. Speed and Power Profile for Minimum Required Ride Quality

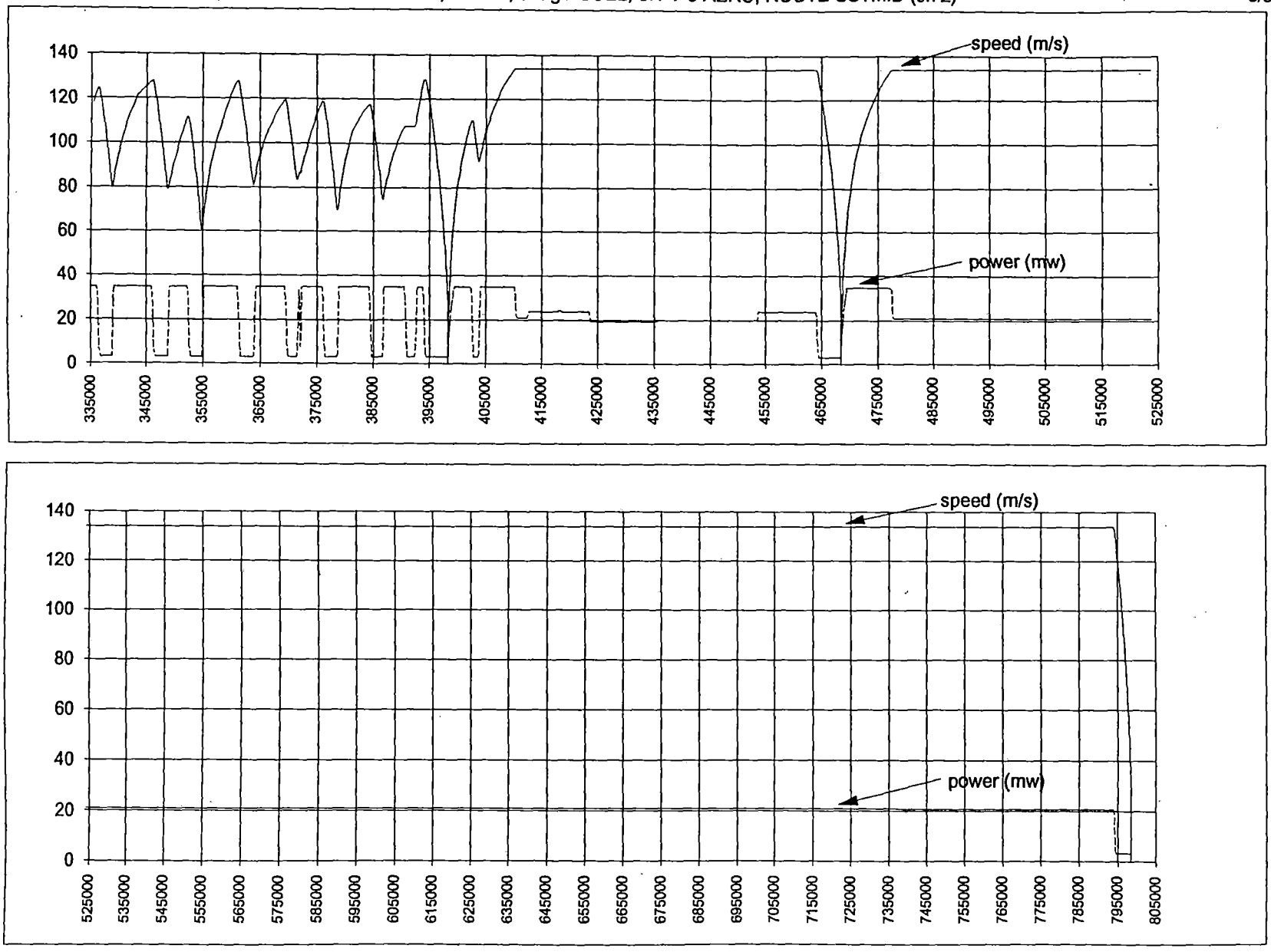

Figure 7-2. Speed and Power Profile for Minimum Required Ride Quality (Continued)

The vehicle design specification dictates the tractive power of around 30 MW for an eight-car consist and therefore the speed and power profiles are presented for the 30 MW vehicle power (3.75 MW/car). To obtain the effects of various maximum power ratings of the system, the TPC simulations were carried out for 20 MW, 30 MW, and 40 MW system maximum power. This corresponds to 2.5 MW, 3.75 MW and 5 MW per car. The detailed speed profiles using these power levels are compared for the first four PIs of the route in Figure 7-3. This shows the effect of available traction power on the speed profiles over short severe segments.

7.3 Effect of Maximum Power Rating on Average Speed Over the Route

The maximum propulsion available to the car has a small influence on the vehicle average speed over the range of 2.5 to 5.0 MW/car. Table 7-1 shows the average speed of the vehicles with various maximum power ratings and car consists. Average speed has been evaluated for each of the three segments of the SST route and also for the complete route. The first four cases (1 to 4) refer to the Design Goal ride quality simulations and the next five refer to Minimum Required ride quality simulations. A jerk rate of 0.07 g's/sec was used in all the eight cases except for the Case No. 9 where a 0.25 g's/sec was used. The case numbers referred in this table refer to the same case numbers used in Section 6. More details on the specifications and results can be studied in Section 6, if required.

To simplify the results, the above data are represented in the graphical form. Figure 7-4 shows a bar graph for 2.5, 3.75, and 5 MW per car maximum power, using Design Goal ride quality specifications and curve design (Case No. 2, 3 and 4 in Table 7-1). The effect of maximum car power on average speed, in very severe segments such as the Segment 1, is more pronounced. There is a 9 percent change in average speed for a 2.5 MW (100 percent) maximum power increase. The maximum car power has less influence on the average speeds in less severe segments, as seen in Segment 2. The average speed goes up by 3 percent in this segment on increasing power rating by the same 2.5 MW. In non-severe segments such as the Segment 3, the effect of increasing car power ratings is almost negligible, since even 2.5 MW per car is sufficient to cruise at maximum velocity

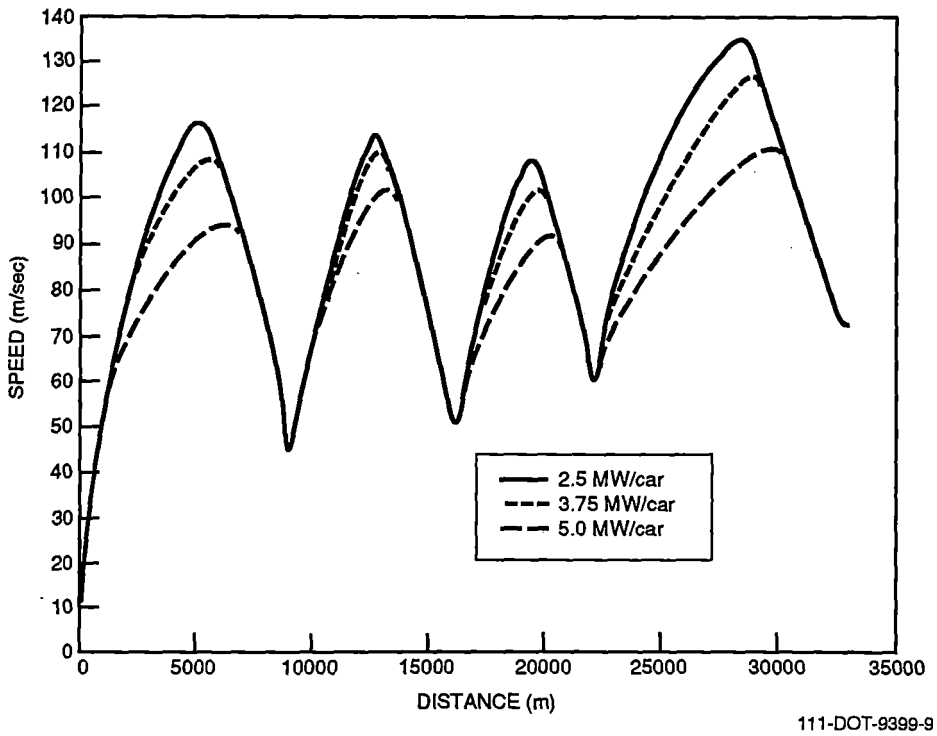

Figure 7-3. Speed Profiles at Various Power Ratings between the First Four PIs

Table 7-1. Average Speed in Various Segments of SST (m/sec)

Case No.	No. Cars in Consist	Ride Quality	Maximum Propulsion Power Per Car (MW)	Average Speed (m/sec)			
				Segment 1	Segment 2	Segment 3	Route Average
1	1	Design goal	7.5	93.2	112.6	129.2	107.2
2	8	Design goal	2.5	85.0	109.5	128.4	101.1
3	8	Design goal	3.75	90.1	111.9	129.2	105.0
4	8	Design goal	5.0	92.5	112.8	129.3	106.7
5	1	Min reqd	7.5	103.4	115.8	130.0	114.2
6	8	Min reqd	2.5	93.6	112.6	129.0	107.4
7	8	Min reqd	3.75	100.1	115.3	129.9	112.1
8	8	Min reqd	5.0	103.7	116.0	130.0	114.3
9	8	Min reqd*	3.75	100.4	115.9	129.9	112.3

*Test case for 0.25g accel limit

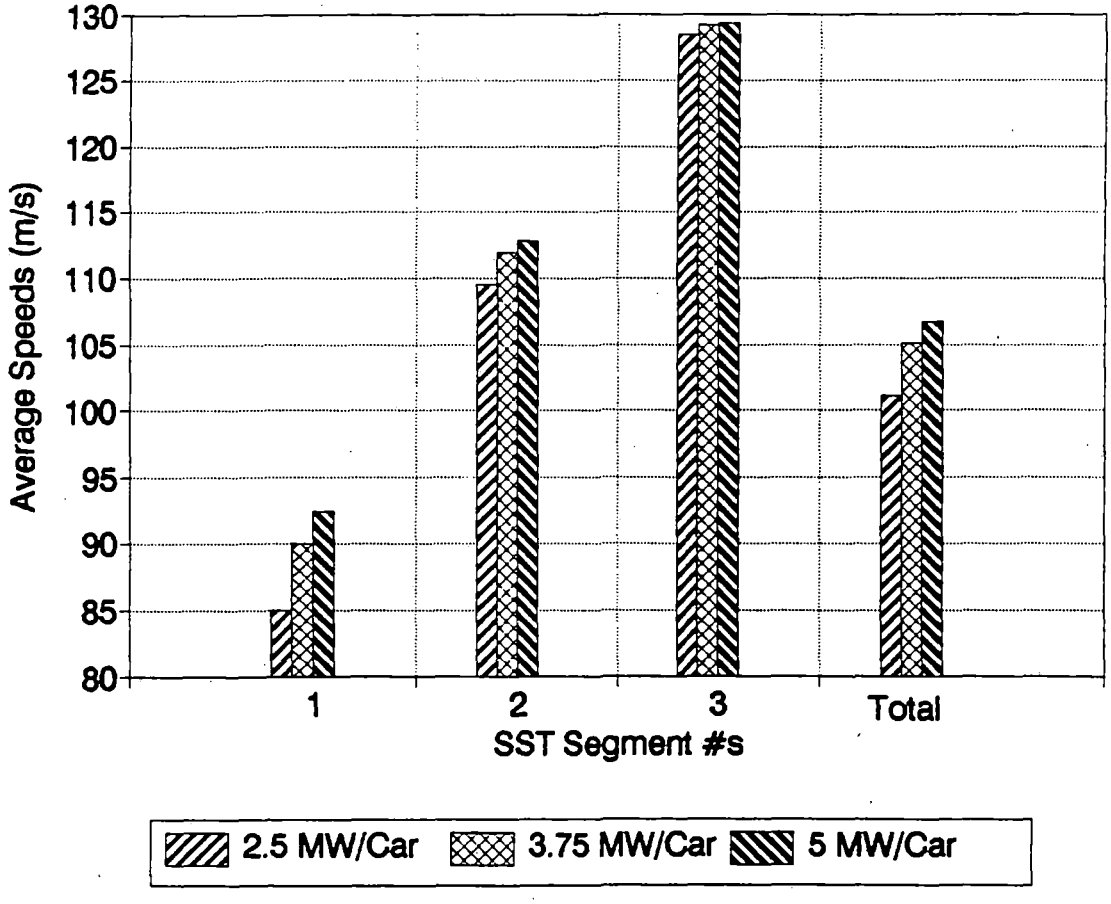

Figure 7-4. Effect of Car Power Ratings on Average Vehicle Speed (Design Goal Ride Quality and Curve Design)

for multicar consists. Here, there is only a 0.7 percent increase in average speed for the 100 percent increase in car power rating.

Figure 7-5 shows a bar graph for 2.5, 3.75, and 5 MW maximum power per car, using Minimum Required ride quality specifications and curve design (Case No. 6, 7 and 8 in Table 7-1). The effects of power variations are slightly more pronounced, with an 11 percent rise in Segment 1. In less severe segments, the influence of power ratings is same as in the case of Design Goal ride quality studies (3 percent in Segment 2 and 0.8 percent in Segment 3). For the complete route (Total) of 800 km, an average speed variation of up to 6 percent was caused by changing the car power ratings over the 2.5 to 5.0 MW/car range.

7.4 Effect of Ride Quality on Average Vehicle Speed

The ride quality has a more consistent effect on the average vehicle speed at all power levels. Recall that curve designs over the entire route were optimized for both the Design Goal and Minimum Required ride quality cases. The average speeds for Design Goal ride quality (Cases 2 to 4) and Minimum Required ride quality specifications (Cases 6 to 8), are seen in Table 7-1. In each case, there is 6.2 percent, 6.7 percent and 7.1 percent increase in the average speed at a 2.5, 3.75, and 5 MW per car maximum power rating respectively. Figure 7-6 shows the influence graphically.

7.5 Total Trip Time

The total trip time has also been evaluated for the individual route segments for all cases. Total trip times are for the complete 800 km* of the SST route exclusive of station dwell time. The

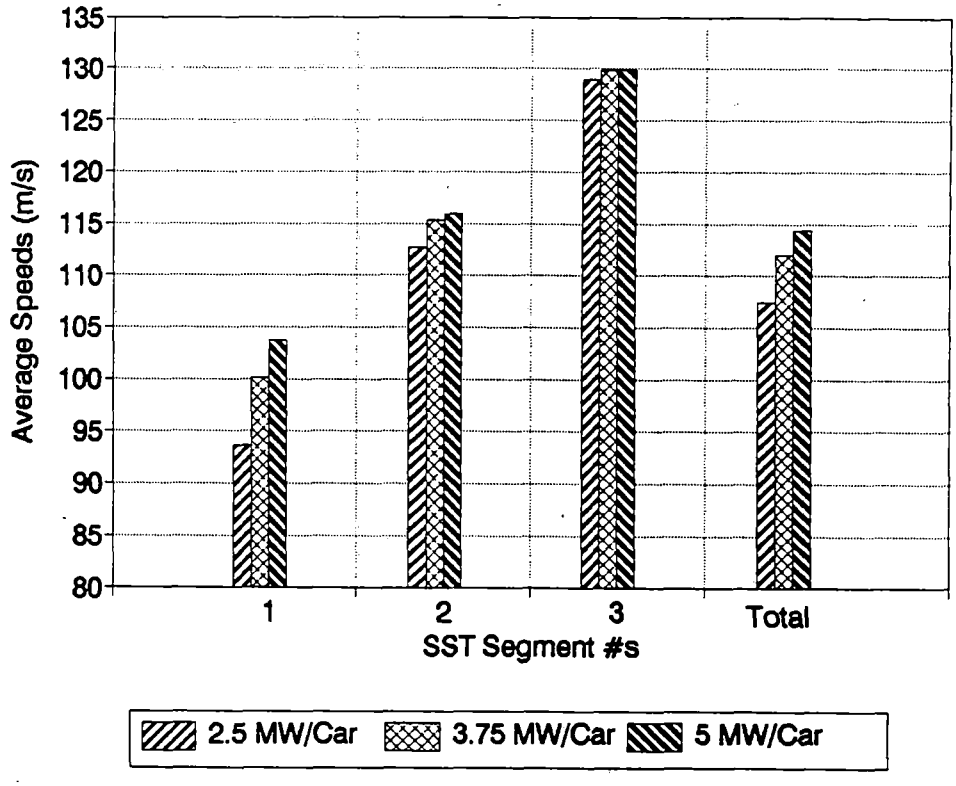

Figure 7.5. Effect of Car Power Ratings on Average Vehicle Speed (Minimum Required Ride Quality and Curve Design)

*Reference distance before incorporating detailed arc length calculations which result in 1.4 to 1.6 km reduction (0.2 percent).

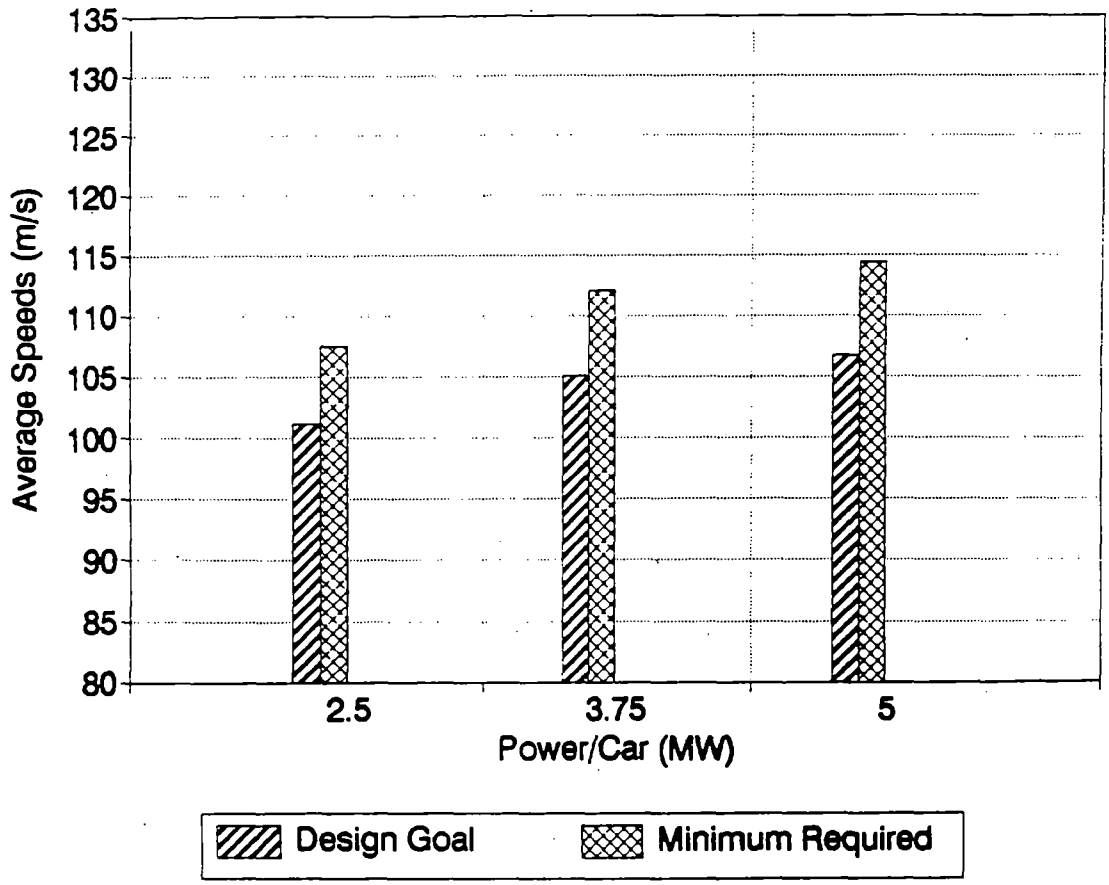

Figure 7-6. Effect of Ride Quality on Average Vehicle Speed

calculated trip time for an eight-car vehicle using Design Goal ride quality is 127 min (with a power rating per car of 3.75 MW). Table 7-2 shows all trip times for all nine cases.

The table also shows the trip times for the individual SST route segments. It is seen that the trip times are almost constant for Segments 2 and 3, which are not severe in nature. The trip time is quite sensitive to varying parameters in the most severe of the segments, Segment 1. The effects of varying parameters on trip time for the complete SST routes is examined next.

Effect of Vehicle Power on Trip Time

The trip time for the complete route is only slightly affected by the vehicle maximum propulsion power. For example, using Design Goal ride quality specifications, a trip time saving of 5 min (4 percent) was achieved by increasing the maximum power by 50 percent (from 2.5 MW per car to 3.75 MW per car). Also, a further 33 percent increase in maximum power (from 3.75 MW per car to 5 MW per car) saved an additional 2 min (1.6 percent) in trip time.

Figure 7-7 shows a comparison between the effects of power changes both in severe segments (Segment 1 of the route; see upper graph) and in less severe segments (Segment 3 of the route; see lower graph), for Design Goal ride quality. In severe segments the 100 percent increase in maximum power resulted in an 8 percent improvement in trip time, but in less severe segments the effect is almost unmeasurable (less than 0.5 percent).

Table 7-2. Trip Times (in minutes)

Case No.	No. of Cars	Ride Quality	Power/Car (MW)	Jerk (g/sec)	Trip Time (min) Segment 1	Segment 2	Segment 3	Total
1	1	Design goal	7.5	0.07	71.2	10.4	42.6	124.1
2	8	Design goal	2.5	0.07	78.1	10.6	42.8	131.6
3	8	Design goal	3.75	0.07	73.7	10.4	42.6	126.7
4	8	Design goal	5	0.07	71.8	10.3	42.6	124.7
5	1	Min reqd	7.5	0.07	64.2	10.1	42.3	116.5
6	8	Min reqd	2.5	0.07	70.9	10.4	42.6	123.9
7	8	Min reqd	3.75	0.07	66.3	10.1	42.3	118.7
8	8	Min reqd	5	0.07	64.0	10.1	42.3	116.4
9	8	Min Reqd*	3.75	0.25	66.1	10.1	42.3	118.5

*(0.25 g accel limit)

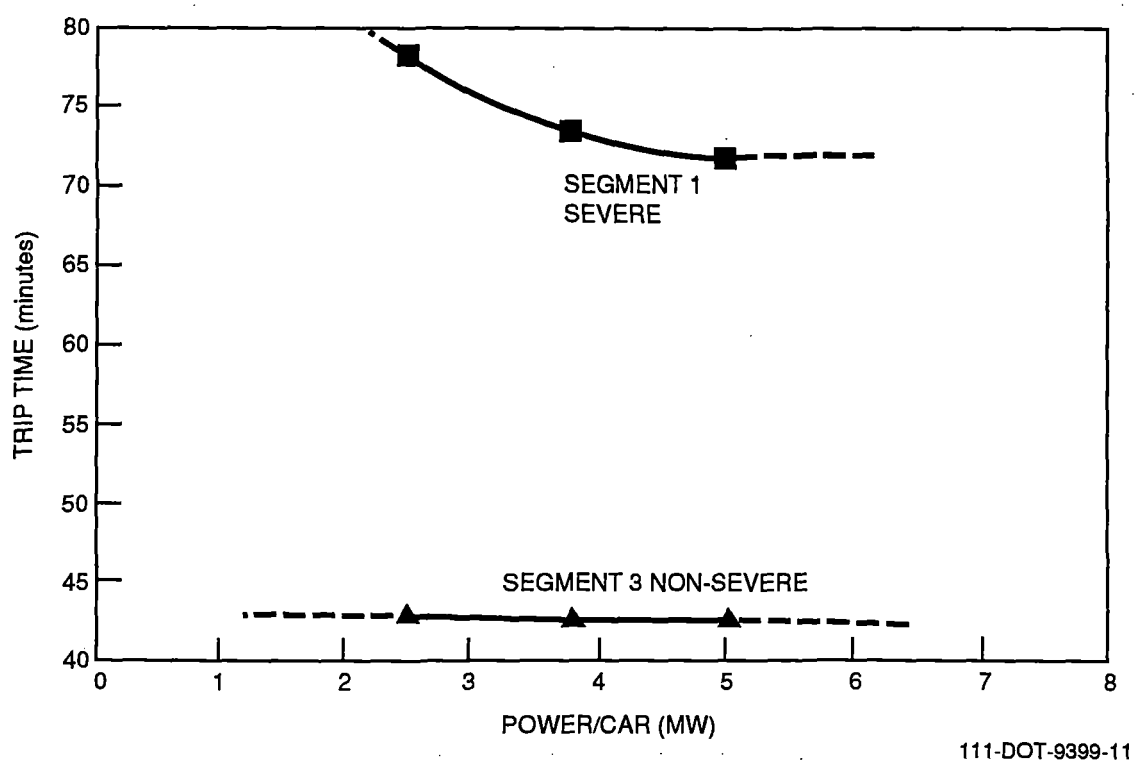

Figure 7-7. Effect of Ride Quality on Vehicle Trip Time in Severe and Less Severe Segments

Effect of Ride Quality on Trip Time

Ride quality levels and associated curve design has a significant effect on the trip time in severe segments. This is primarily due to the higher speed and g-loads used in turns for the Minimum Required ride quality case. This resulted in shorter spirals for curve entries and exits, and longer minimum radius sections in the optimized curve geometry. A secondary effect is due to the higher maximum accel rate allowed. Figure 7-8 shows the graphical representation of the trip time variations due to ride quality selection. The upper curve represents trip times for Design Goal ride quality where as the lower curve represents trip times for Minimum Required ride quality. Over the range of car maximum power ratings, the trip times for Minimum Required ride quality is about 8 min shorter than that for Design Goal ride quality (a 6 percent difference).

Figure 7-9 shows the overall effect of varying both ride quality and maximum car power on the trip time. Increase in both car power ratings and ride quality severity gives an overall saving of up to 15.2 min in travel time, an 11.5 percent improvement.

7.6 Specific Power Consumption

In this report, the power consumption unit of kWh per car per km is termed the specific power consumption. There is a potential for about 25 percent reduction in specific power consumption, particularly in Segment 1, if regenerative braking with a fully receptive line is considered. The regenerative braking potential is not included in the reported specific power consumptions. Table 7-3 lists the specific power consumptions for the first eight cases discussed in Section 6. The specific power consumptions for one-car consist cases are higher than eight-car consist cases due to the design

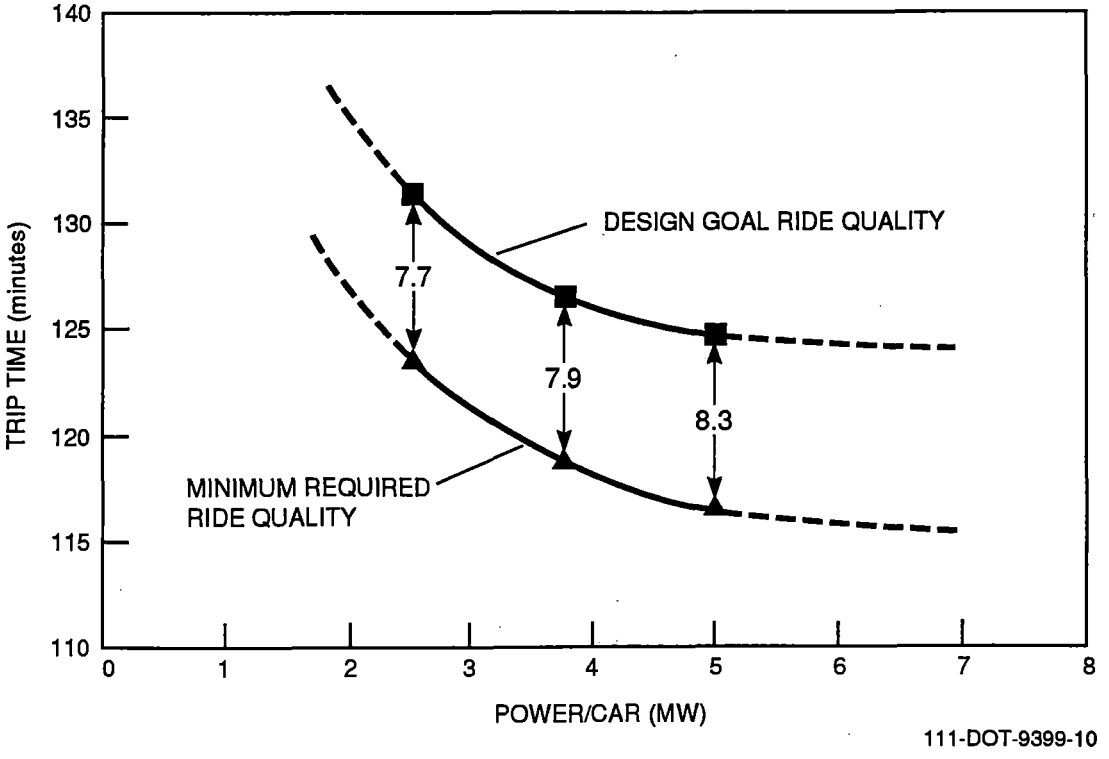

Figure 7-8. Effect of Ride Quality on Vehicle Trip Time

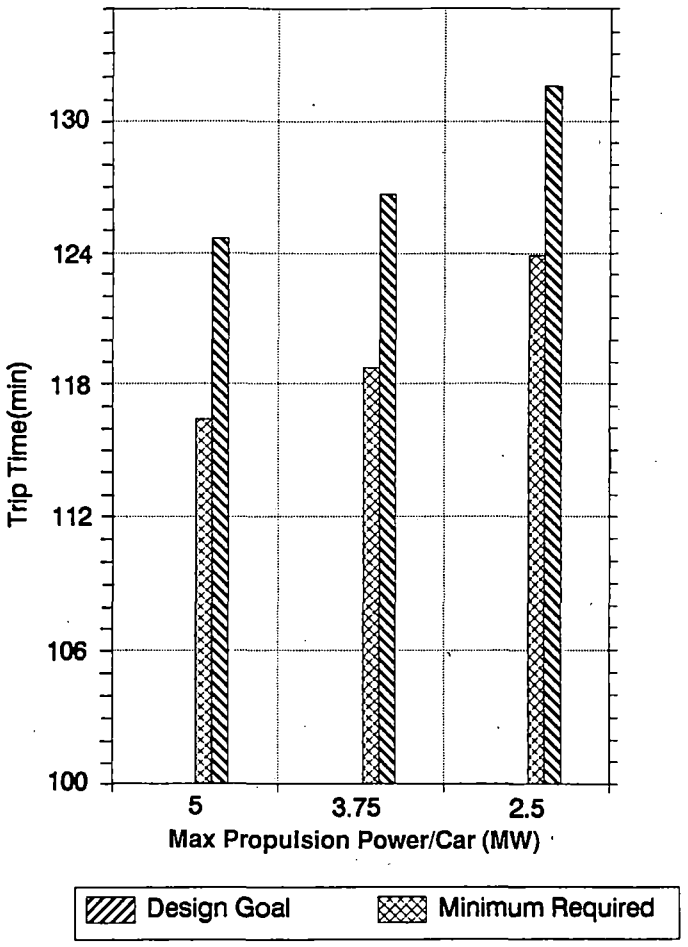

Figure 7-9. Combined Effect of Ride Quality and Car Power Ratings on Vehicle Trip Time

and aerodynamic factors. For the complete range of eight-car consist runs, the specific power consumption changes only by 14.5 percent from the minimum of 6.2 kWh/car-km at 2.5 MW maximum car power using Design Goal ride quality to the maximum of 7.1 kWh/car-km at 5 MW maximum car power using Minimum Required ride quality. Note again that "car power" is pure propulsive power, with "hotel" power and 5 percent line losses added for "total" power consumption.

Figure 7-10 shows the specific power consumption for all maximum car power ratings and both the ride qualities. The graph shows that increasing maximum car power ratings result in about a 3 percent change in the specific power consumption, while at lower maximum car power ratings, the variation is less.

A last comparison can be made of the specific energy consumption over the different route segments. While data for all the cases are available at Foster-Miller, an example (see Table 7-4) using the mid-range value of 3.75 MW propulsion power per car will demonstrate the effect.

Table 7-4 shows the expected higher specific energy consumption required in the sections containing frequent curves and grades such as Segment 1. The frequent accels, decels and grades consume energy at a rate 25 to 30 percent greater than the gentler Segment 2 or the flat and straight Segment 3, even though average speeds are lower.

Table 7-3. Specific Power Consumption

Case No.	Number of Cars in Consists	Ride Quality	Maximum Propulsuion Power/Car (MW)	Power Consumption	
				kWh/car-km	kWh/consist-km
1	1	Design goal	7.5	12.9	12.85
2	8	Design goal	2.5	6.2	49.8
3	8	Design goal	3.75	6.7	53.49
4	8	Design goal	5.0	6.9	55.11
5	1	Min reqd	7.5	13.4	13.42
6	8	Min reqd	2.5	6.2	49.92
7	8	Min reqd	3.75	6.8	54.31
8	8	Min reqd	5.0	7.1	56.69

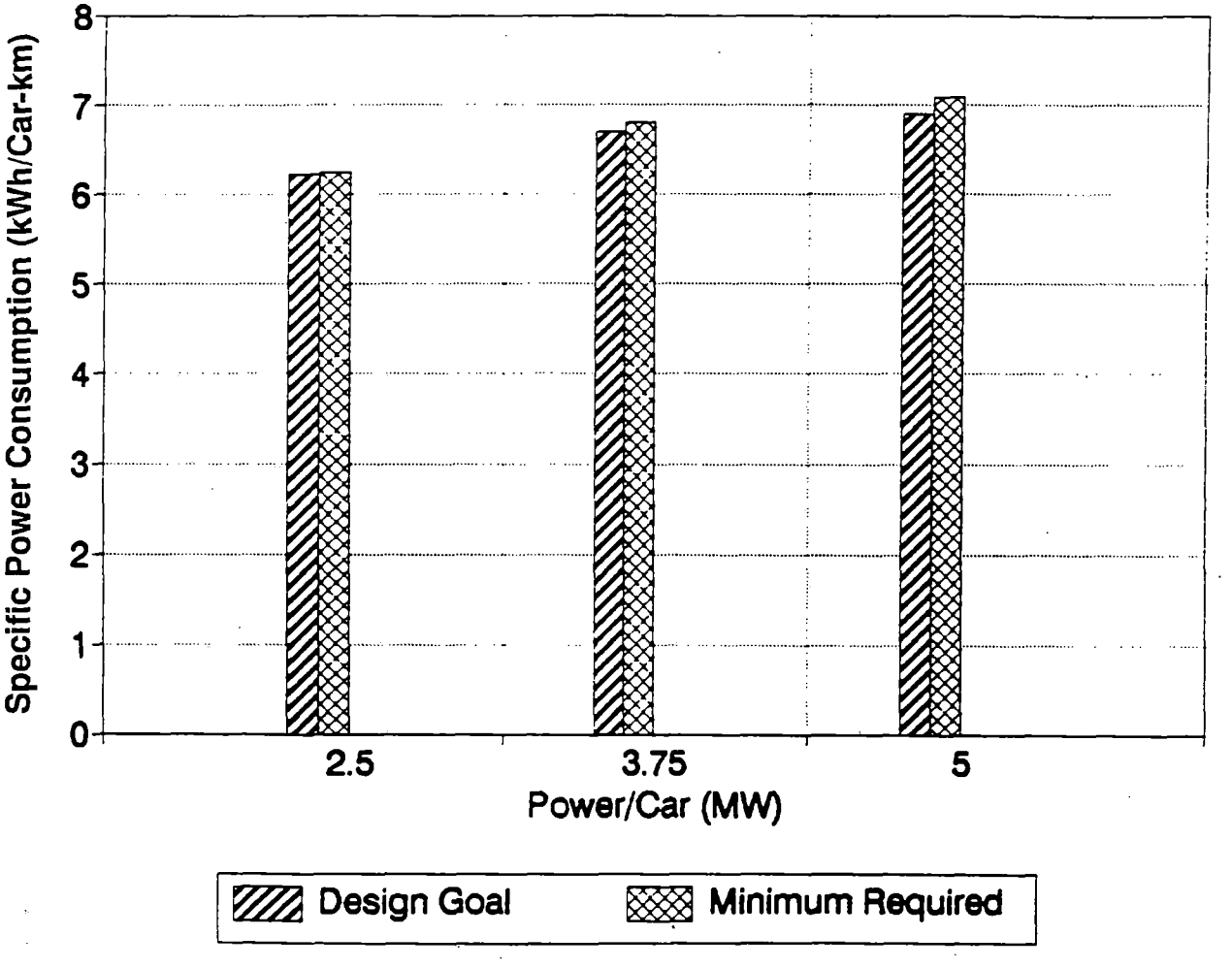

Figure 7-10. Combined Effect of Ride Quality and Car Power Ratings on Vehicle Specific Power Consumption

Table 7-4. Specific Power Consumption for Different SST Route Segments

		Total Specific Energy Consumption (Watt-hr per Passenger-km)			
Case No.	Ride Quality	Segment 1 (398 km)	Segment 2 (70 km)	Segment 3 (330 km)	Route Average
3	Design goal	103	82.5	74	89.1
7	Min reg	106	83	74	90.6
Note: 3.75 MW maximum propulsion power/car, 8-car consist, 75 pax/car.					

8. CONCLUSIONS & RECOMMENDATIONS

8.1 Conclusions

The tasks carried out in this project and the conclusions that have been reached to date can be summarized as follows:

- A semi-automated route characterization method based on the ride qualities has been developed. Two characterized routes, SSTLEFT and SSTMID have been developed using this method.

- Both the characterized routes (SSTLEFT and SSTMID) conform to the government ride quality specifications, including jerk rates, as evidenced by an analysis using state-of-the-art dynamic simulation program MAGSIM, discussed in Part II.

- The PDI-TPC program was enhanced to carry out Maglev simulations. The enhanced TPC results were checked using Foster-Miller trial route. The SST simulations were carried out after finding the results satisfactory.

- The complete performance evaluation simulations of the Maglev vehicle over the SST routes (SSTLEFT and SSTMID) have been carried out using the PDI-TPC program, and the results are presented in this report. Several runs have been documented to facilitate tradeoff analysis.

- The average run time of the Maglev vehicle over the 800 km SST route is approximately 2 hr. The minimum run time achieved using "Minimum Required" ride quality is 116 min and the maximum run time with more comfortable "Design Goal" ride quality is 132 min.

- For the more severe segments, maximum car power ratings in excess of 5 MW per car have little effect on the trip time. In less severe segments maximum car power ratings above 2.5 MW per car have little effect on the trip time. The recommended rating for full route use is 3.5 to 4.0 MW per car.

- The specific power consumption is between 6.2 to 7.1 kWh per car-km or only 82 to 95 watt-hr per psgr-km, without regenerative braking. This is significantly lower than many other high speed transportation systems, including some existing Maglevs. This can be attributed to high levitation and LSM efficiencies, regeneration capability, and aero drag control.

- Headway required between consists over the SST route to achieve 9600 psgr/hr in each direction has been evaluated. For eight-car (600-seat) consists with 225-sec headway, the minimum consist separation encountered along the route is 15.7 km, and is considered well within safety guidelines. For four-car consists at 112-sec headway, the minimum consist separation over the route would be about 7.9 km. This condition still permits safe braking of the consist under a worst case degraded mode condition.

If desired, the performance and curve design studies for the "Seat/Belt" ride quality parameters could also be carried out using the same procedure used for the Design Goal and Minimum Required ride quality studies. The trip time for such a severe route with this very aggressive ride quality is estimated to be 110 min.

8.2 Secondary Applications of SST Route Definition

The work performed at Foster-Miller using the Severe Segment Test route characteristics utilized this valuable source of data during the study phases of power systems, vehicle design, and guideway design. The trial route study data had previously been used in understanding the vehicle power requirements, the regenerative braking viability studies, and cost estimation of the guideway for single track versus two-track designs.

8.3 Foster-Miller Recommendations

The trip time of 120 min over the SST route, using both an economically sized propulsion system for 3.5 MW peak propulsion power and lightweight titling body vehicles is certainly satisfactory, especially considering that the minimum possible trip time for an 800 km straight route using a cruise speed of 134 m/sec is still 101 min (allowing for accel and decl). However, this used the Minimum Required ride quality parameters (including optimized curves) which if adopted, might be too severe for passenger acceptance. By the same token, use of the Design Goal ride quality results in about 8 min longer trip time than for the Minimum Required quality for the range of powers considered, about a 6 percent increase.

Using the Foster-Miller analysis tools now developed, further reductions from the Design Goal trip times could be made by selectively relaxing some of the parameters in conjunction with the government to see the maximum payoff for the least effect on passenger comfort. These might include (1) the bank angle limitation of 24 deg; (2) Negative vertical g-limit of -.05g (actually +0.95g); and judicious experimentation with roll rate and roll accel. Since the analysis methods include power consumption data, these could be traded off against incremental energy savings. Studies could be confined to a portion of the route, probably using the first segment.

Another worthwhile area to address would be the streamlining of the Foster-Miller/PDI curve design/TPC analysis itself. While we believe the methodology itself is direct, sound and reasonably efficient, the current approach uses multiple algorithms and programs requiring human intervention at many points. Though this produces proper results, it requires checking for data errors and also some duplication of information along the way, which is magnified when producing the large data sets required for detailed route geometry and speed information. We recommend that this procedure be more fully automated in order to take advantage of the capability for more efficient study of multiple routes, and to do tradeoffs over these routes to highlight, for example, particular geometry changes which might have large payoffs in speed and trip time.

In the longer term, some of the more detailed operational characteristics of an actual Maglev system in commercial passenger service will have to be considered in terms of how they affect both capital and operating costs. Foster-Miller's System Concept Design Study touches on several of these in Chapter 6, including both realistic dwell time requirements and station designs, and the potential for single-track operation in typical U.S. intercity markets. Foster-Miller's work on this study could be easily extended into a parametric study of these issues, using the curve design, TPC, and operating cost methodologies employed for this report in conjunction with both PDI's single-track analysis techniques and demand estimates already completed for various public agencies for specific intercity corridors. Use of a passenger demand estimate from an actual corridor would also greatly facilitate intermodal cost comparisons, for reasons discussed in subsection 10.7.

PART II

VEHICLE DYNAMIC RIDE ANALYSIS

9. DETAILED DYNAMIC RIDE ANALYSIS

9.1 Introduction

The consideration of ride quality through specific sections of the SST route is separated into two parts. First, the dynamic response to guideway irregularities is considered, using the specification and comfort limits by the International Standards Organization (ISO) and a number devised by Peplar et alia. Secondly, the effect of curve design is assessed in terms of the parameters specified. The manner of determining the response of the system in each case is through a multibody system simulation, given the name MAGSIM. For the assessment of ride quality using the ISO standard, the results are further processed into one-third octave bands using the programs DADiSP to transform to the frequency domain and Lotus 1-2-3 for final calculation and plotting. MAGSIM includes a coupled two-dimensional model of each magnet-to-guideway connection. The vehicle model used to find the ride quality includes three bodies and two bogies with the ends of the extreme bodies and remote suspensions forced to follow the guideway.

The approach to suspension design has been to separate the body and bogie modal frequencies and to optimize the damping between them. Damping is provided across the secondary suspension and has been chosen to be sufficient to reduce the bogie mode amplitudes, while being small enough not to transfer energy at the lower body mode frequencies. Roll control is undertaken using an antiroll bar and damping. An additional set of dampers was used between bodies to improve the ride quality and reduce pitching of the bogie and bodies. The ride quality requirements have thus been satisfied with a passive system.

The Severe Segment Test, previously called the hypothetical route, contains a range of geometries, including tight horizontal curves. The requirement for stops and switching leads to vertical movements having a similar effect in the vertical plane. To satisfy all conditions of speed and curvature, a combination of guideway and vehicle tilting has been chosen and its effect is included in the results given.

The four particular zones studied will be referred to as zones 1, 2, 3 and 4 are:

1. 2 km on either side of PI17.
2. From PI25 to PI26.
3. From station 391 + 000 to 395 + 000.
4. From station 445 + 000 to 449 + 000.

9.2 Particulars of the Vehicle and Guideway Design Over All Zones

The interaction between the vehicle and guideway perturbations depends predominantly on coupling caused at appropriate speeds by the near coincidence of a guideway wavelength with a wavelength of the vehicle natural response. Simulations using MAGSIM have been carried out to identify the most likely vehicle behavior for continuous guideway perturbations assessed to be the most severe possible from the worst case stackup of static and dynamic beam deflections. The results are therefore worst case results and will only be seen under a combination of adverse effects.

In the vehicle design, reported previously and labeled "Maglevj," studies had shown the benefit of moving the secondary suspension to the ends of the bogie to control the pitch and yaw modes of the bogie. The resulting body modal frequencies were also reduced by decreasing the airbag stiffness. Several runs were made and reported in the general report to identify satisfactory passive linear damping values. In the design used in the results reported here, additional dampers have been attached vertically between adjacent body corners to control pitch and the design is labeled "Maglevk."

The guideway design consists of support beams containing all the reacting coils, one beam for each side. Each beam with its guidance coils are a source of dynamic events and control the direction of the vehicle, as well as responding to the forces generated. In the MAGSIM analysis reported, they are treated as a source to the vehicle and its suspensions. The effect of particular deviations from smooth vertical and lateral guideway surfaces is a consequence of their amplitude, shape and wavelength. The shape is associated with the beam as a dynamic structure and is shown in Figure 9-1.

The principal wavelength of the guideway, even with a 54m beam length, is that between supports or 27m. The amplitude of the frequency component of the shape at this wavelength is reduced by the continuity of the beam as the span center. The beam length wave has a much smaller amplitude and others exist at higher multiples which are generally not a ride quality issue in the speed range. Amplitudes of 10 mm vertically and 4 mm laterally were used for the simultaneous excitation from the continuous beam shape. These values were chosen from a study of the beam deflections and tolerance stackup. This represents a conservative approach, since the guideway tolerance and deflection stackup is assumed to be taken in the worst (maximum) combination. The beam length is 54m over two spans with supports at its center and at the junctions with adjacent beams at each end, forming the "alternating continuous" 27m span arrangement that is the baseline design.

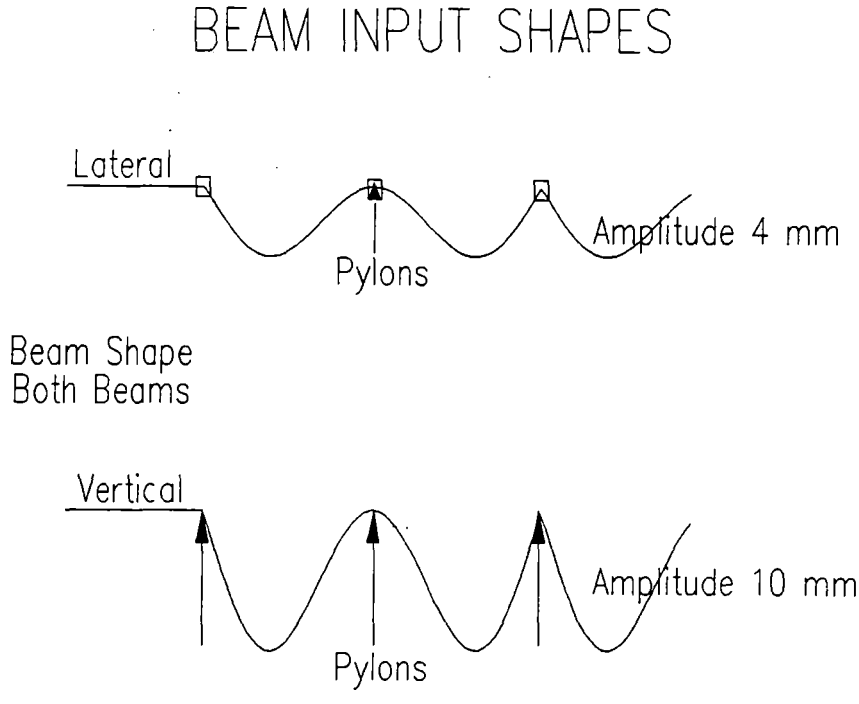

Figure 9-1. Guideway Shape Used to Investigate Ride Quality

9.3 Simulation Results for the ISO and Peplar Numbers Over the Four Zones

Ride qualities were examined for lateral and vertical comfort at the center and leading end of the body, representing the extreme case. (There are no seats that far forward and the values quoted for the leading end are not used in assessing the adherence to the specification but rather to give an extreme upper tolerance value to the results). A range of speeds was investigated from 200 km/hr to 500 km/hr and the results given in Figures 9-2 to 9-9 are for 200, 250, 300, 450 and 500 km/hr. The project speeds in the zones are 211, 263, 274 and 483 km/hr, respectively, and are intepolated from the table given. The speed varies in the energy and exit spirals, although the MAGSIM simulation is carried out at constant speed.

Table 9-1 shows a summary of the ISO results as times to discomfort. Only at the highest speed in the vertical direction is the specified ISO standard not well satisfied, better than 8 hr being usual. The 1 hr to reduced comfort required in the specification is not good enough for most other existing modes of competing transportation and a high value is desirable if not essential for passenger acceptability.

In order to calculate the number suggested by Peplar et alia., it is necessary to know the vertical and lateral acceleration and the roll rate as rms values. They are shown in Table 9-2, for the same variables as the ISO analysis above.

The conclusions for the four zones are shown in Table 9-3.

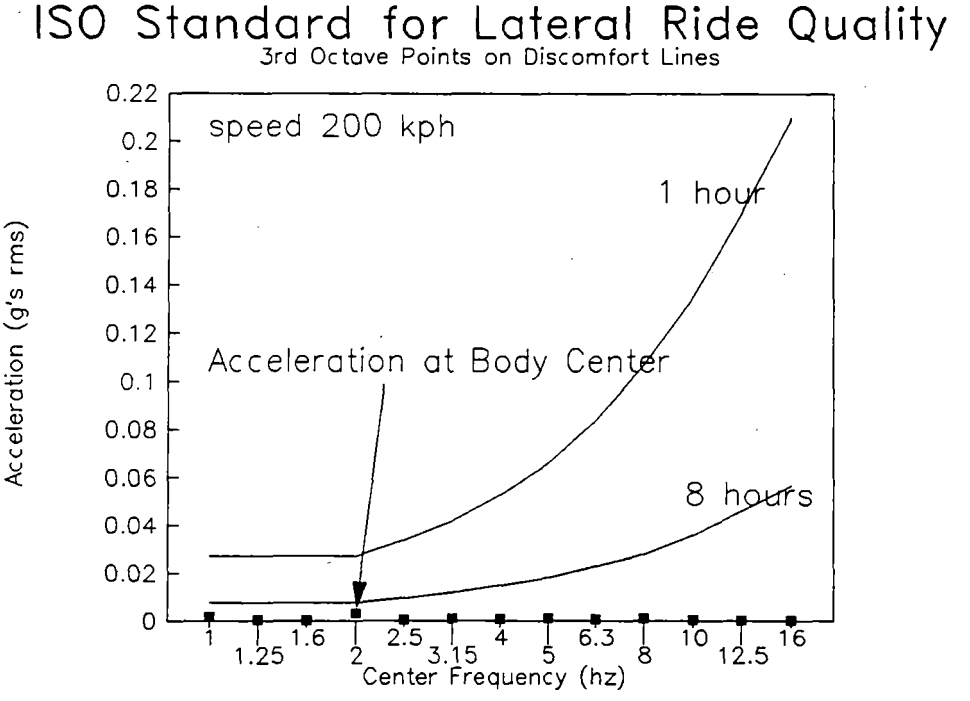

Figure 9-2. ISO 3rd Octave Band RMS Lateral Acceleration at 200 km/hr Vehicle Body Center - Continuous Beam Shape

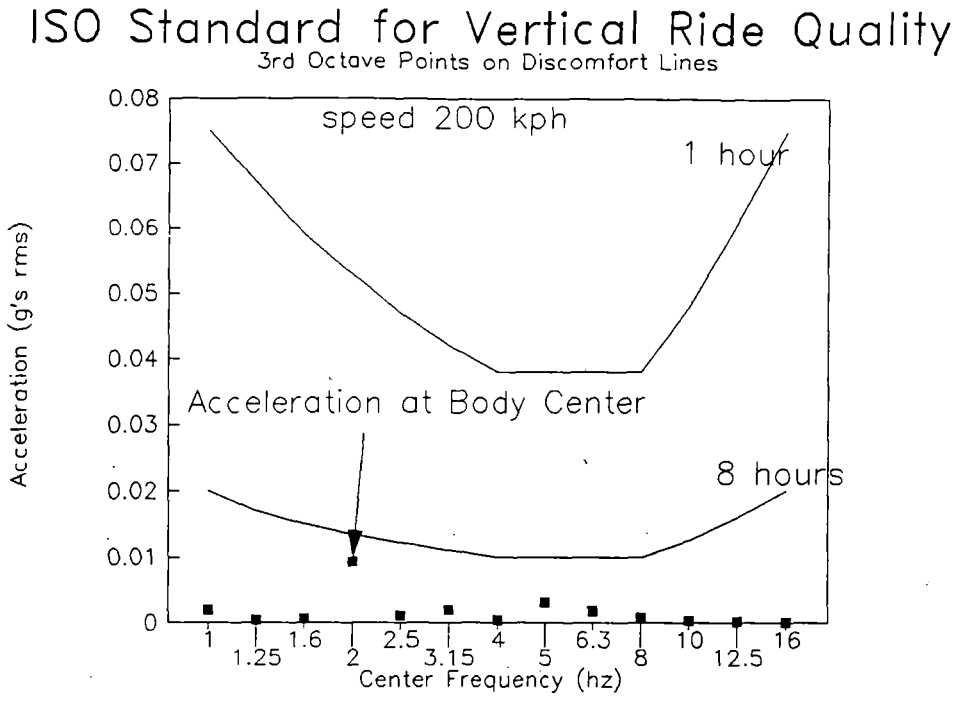

Figure 9-3. ISO 3rd Octave Band RMS Vertical Acceleration at 200 km/hr Vehicle Body Center - Continuous Beam Shape

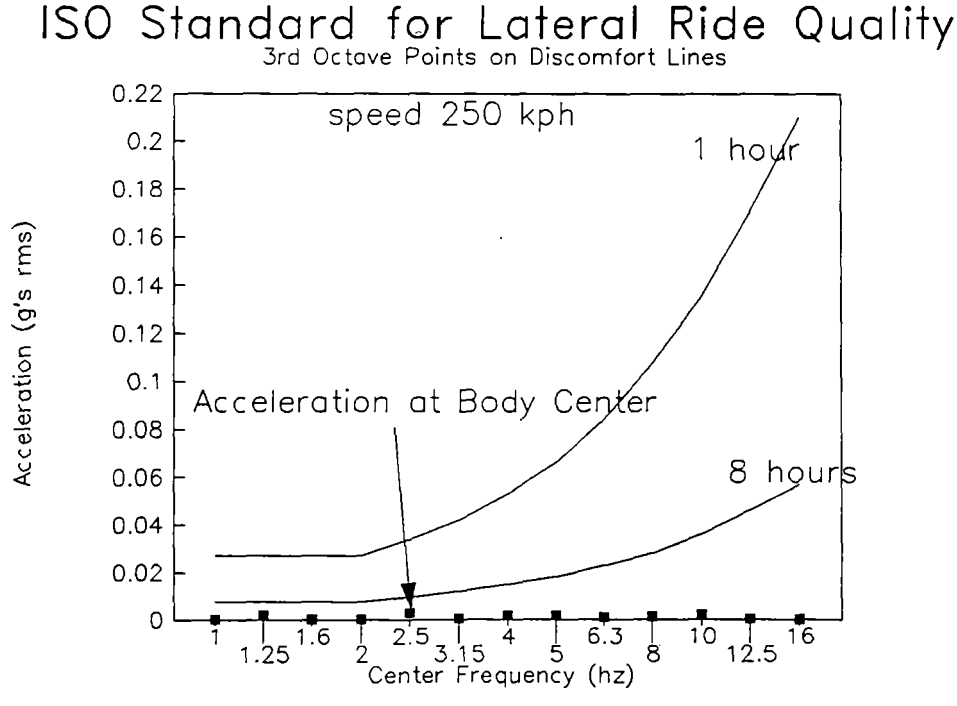

Figure 9-4. ISO 3rd Octave Band RMS Lateral Acceleration at 250 km/hr Vehicle Body Center - Continuous Beam Shape

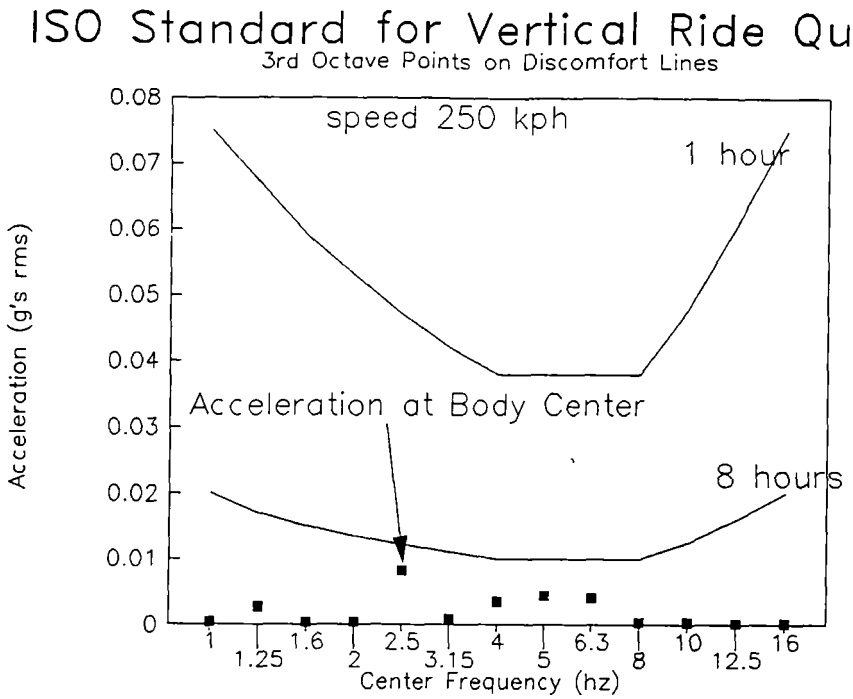

Figure 9-5. ISO 3rd Octave Band RMS Vertical Acceleration at 250 km/hr Vehicle Body Center - Continuous Beam Shape

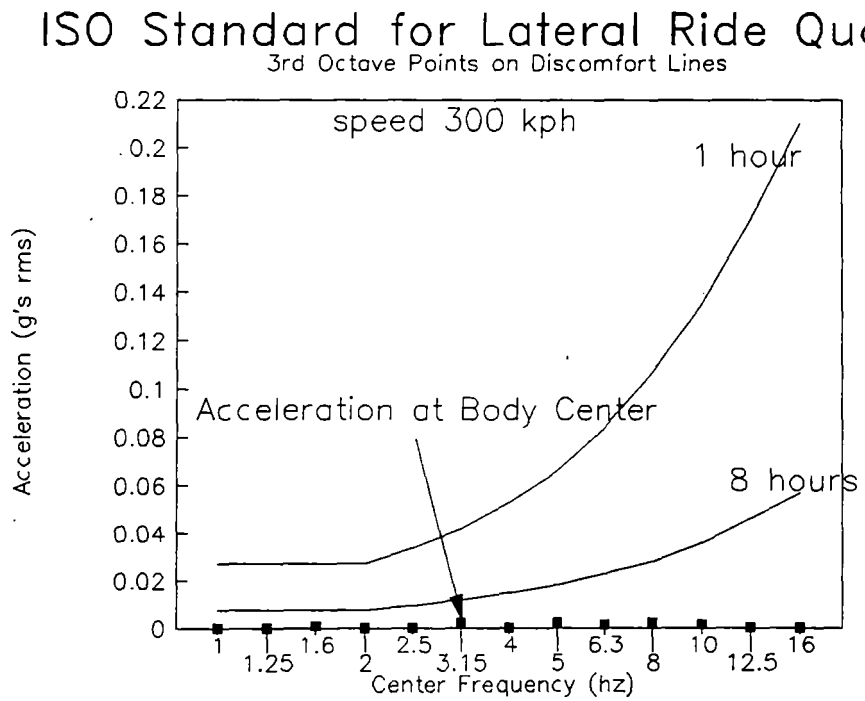

Figure 9-6. ISO 3rd Octave Band RMS Lateral Acceleration at 300 km/hr Vehicle Body Center - Continuous Beam Shape

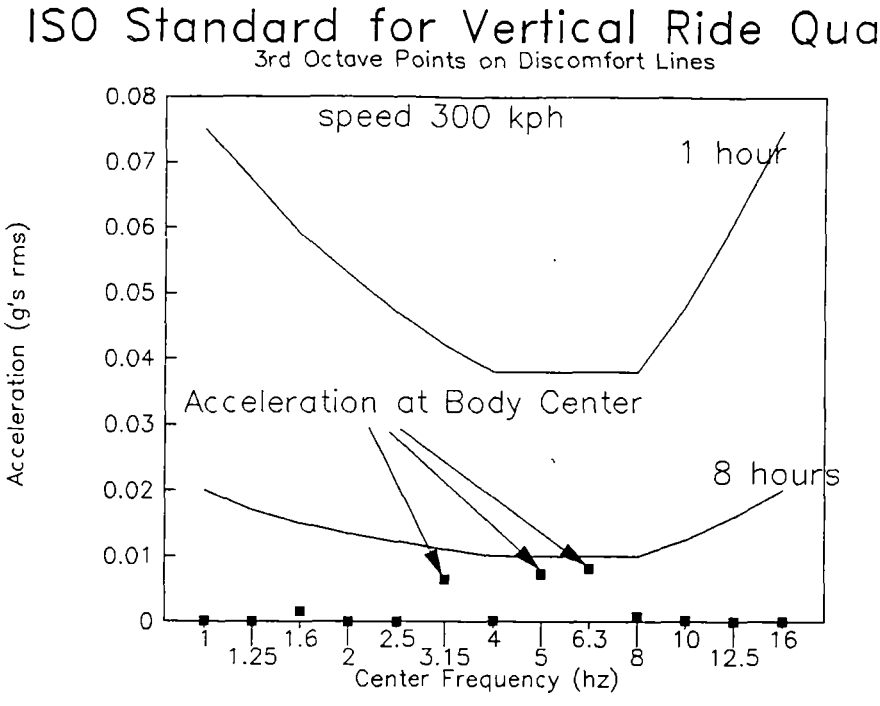

Figure 9-7. ISO 3rd Octave Band RMS Vertical Acceleration at 300 km/hr Vehicle Body Center - Continuous Beam Shape

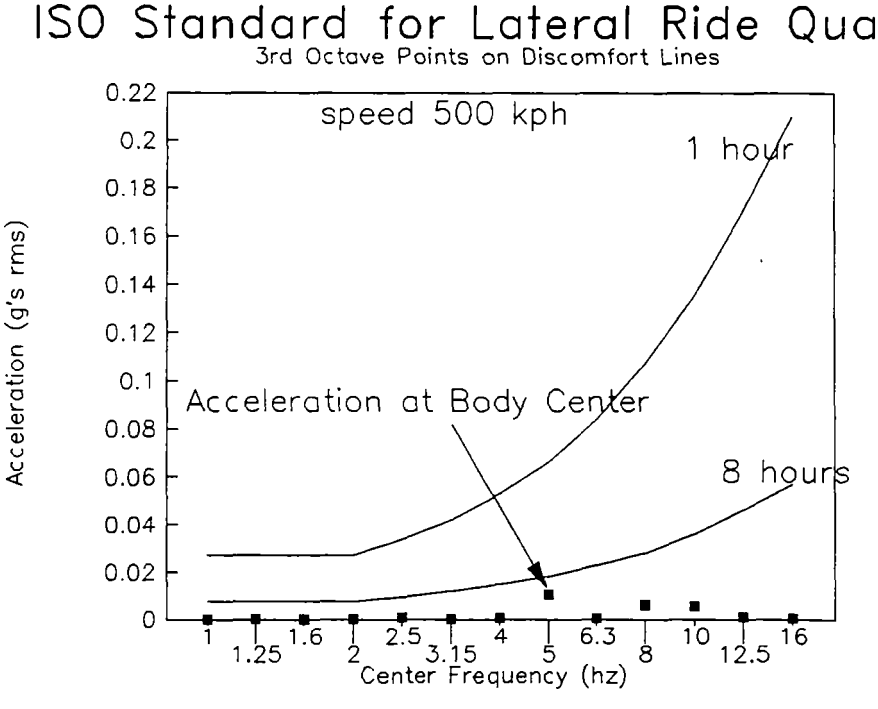

Figure 9-8. ISO 3rd Octave Band RMS Lateral Acceleration at 500 km/hr Vehicle Body Center - Continuous Beam Shape

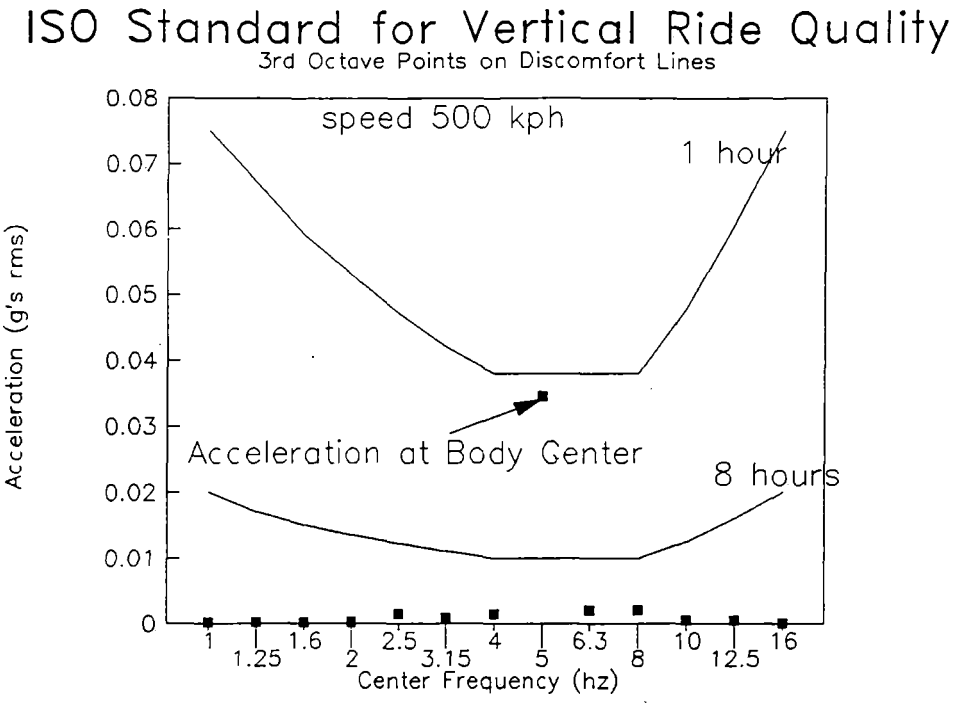

Figure 9-9. ISO 3rd Octave Band RMS Vertical Acceleration at 500 km/hr Vehicle Body Center - Continuous Beam Shape

Table 9-1. ISO Ratings for the Speeds and Locations Given

Speed km/hr	Center Lat hr	Center Ver hr	Front Lat hr	Front Ver hr
200	8+	8+	6	6
250	8+	8	8+	7
300	8+	8+	8	8
450	8+	6	8+	4
500	8+	1.5*	8+	3*

*It should be noted that the 1.5 hr simulated at 500 km/hr is a consequence of the estimated severest continuous input and the deterioration with speed occurs very suddenly at the top end of the speed range. Further small adjustments to the secondary suspension may be desirable to drive the region of poor response slightly higher. It is also recommended that a more detailed examination be made of the effect of a varying input amplitude for the beam shape at each beam.

Table 9-2. RMS Values for the Speeds and Locations Given

Speed km/hr	Center Lat g rms	Center Ver g rms	Front Lat g rms	Front Ver g rms	Roll Rate deg/sec rms
200	0.014	0.036	0.048	0.076	0.070
250	0.017	0.039	0.040	0.068	0.055
300	0.020	0.056	0.054	0.070	0.047
450	0.039	0.071	0.076	0.127	0.065
500	0.048	0.115*	0.089	0.100*	0.102

*It is worth noting that the ISO and Peplar ratings are consistent although in the analysis carried out, the response frequency band widened due to modal coupling and showed a much greater increase in the ISO time to discomfort than suggested by the reduction in the Peplar number.

Table 9-3. ISO and Peplar Summary for the Four Test Zones

Zone No.	Worst ISO (hr)	Direction	Peplar No.
1	8+	Both	2.517
2	8+	Both	2.664
3	8+	Both	2.748
4	2	Vert	4.111*

*It is worth noting that the ISO and Peplar ratings are consistent although in the analysis carried out, the response frequency band widened due to modal coupling and showed a much greater increase in the ISO time to discomfort than suggested by the reduction in the Peplar number.

9.4 Ride Quality Assessment in Response to Unperturbed Guideway Design

In addition to the perturbations giving the ride quality above, the path of the guideway consists of curves, transitions and straight sections. As an example, the first ride quality zone of the Severe Segment Test, requires a speed of 211 km/hr in a curve of 1 km radius and a total tilt of the car body of 14 deg to provide a mean unbalanced lateral acceleration no greater than 0.1g. The resulting increase in weight is about 6 percent. The unbalance of 0.1g is specified as the design target with values to 0.2g in extreme cases discussed later. The results of studies of the vehicle response in the

four zones are given below. The third zone is dominated by a 13.5 percent change in gradient. The other three zones all have significant horizontal curves. The vehicle suspension, in Maglevk, has been improved in the curves through the addition of lateral interbody dampers.

The second zone includes the exit of an 800m curve and the entrance to a 100m curve. Since they are both significant, for analytic convenience they have been treated separately and are labeled 2a and 2b. The acceleration histories in curve 2a are used as an example and given in Figures 9-10 and 9-11. A summary of the results of all the simulations is given in Table 9-4.

As a comparison with the "ride quality design goal specification" guideway, a single simulation was carried out for the guideway designed for the "minimum required condition" specification, the most severe permitted without the use of seatbelts. The first curve, 2a, in zone 2 is simulated. The speed identified for this curve in the redesigned condition is 245 km/hr and the acceleration histories are given in Figures 9-12 and 9-13.

The complete results show a dynamic roll acceleration approaching 40 deg/sec^2, a mean lateral acceleration in the curve of 0.2g, a mean vertical acceleration overload of 0.16g and a lateral jolt of 0.18g in 1 sec. The severity of this ride quality supports its use only under the extreme conditions specified.

9.5 Conclusions

The current vehicle concept, with additional improvements labeled Maglevk, is shown to provide the "design" ride quality specified with a marginally greater jolt at a single location in the very short curve at the beginning of the second test zone. Further small improvements could be made with further development, without resorting to active suspensions (other than banking). Higher speeds

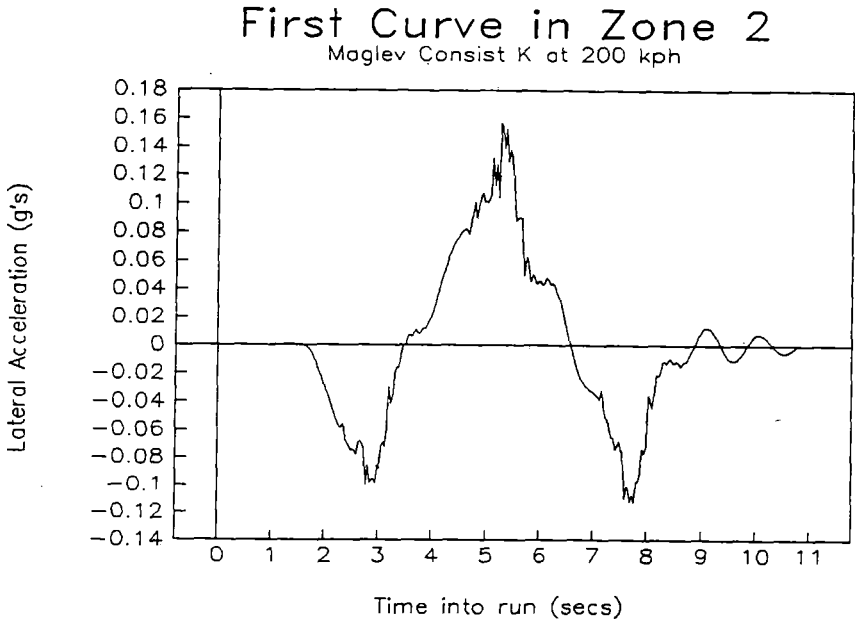

Figure 9-10. Body Lateral Acceleration during the Curve 2a from Zone 2 of the Severe Segment Test

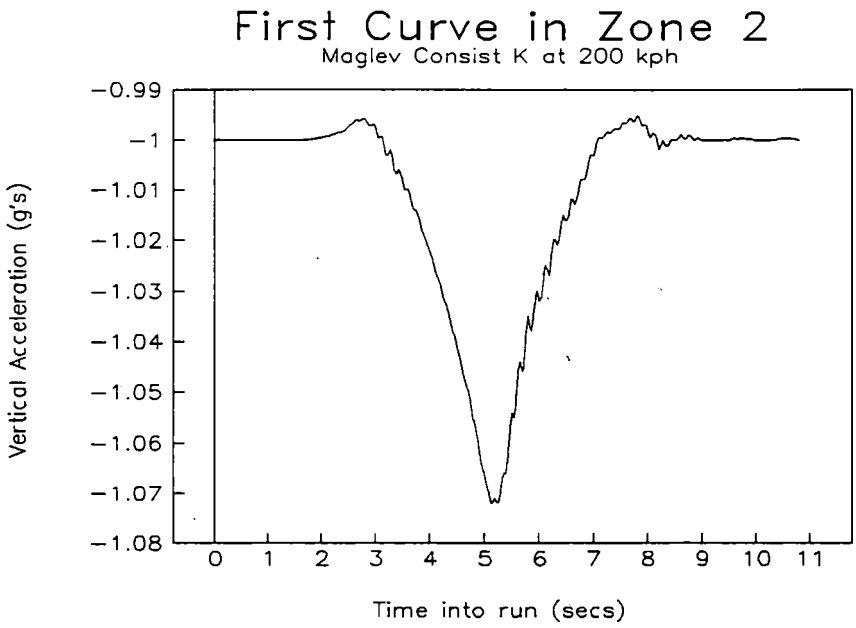

Figure 9-11. Body Vertical Acceleration during the Curve 2a from Zone 2 of the Severe Segment Test

Table 9-4. Summary of Ride Quality Data from Simulations through the Zones for Design Specified Ride Quality Guideway Design

Variable	Zone 1 210 km/hr	Zone 2a 200 km/hr	Zone 2b 260 km/hr	Zone 3 275 km/hr	Zone 4 500 km/hr
Roll acc deg/sec^2	12	15	11	-	7
Lateral acc g's	0.1	0.1	0.1	-	0.06
Vertical acc g's	0.06	0.07	0.13	0.05	0.02
Lateral jolt g/sec	0.07	0.09*	0.02	-	0.04
Vertical jolt g/sec	0.04	0.04	0.05	0.05	0.02

*This value is marginally greater than the jolt limit in the specification.

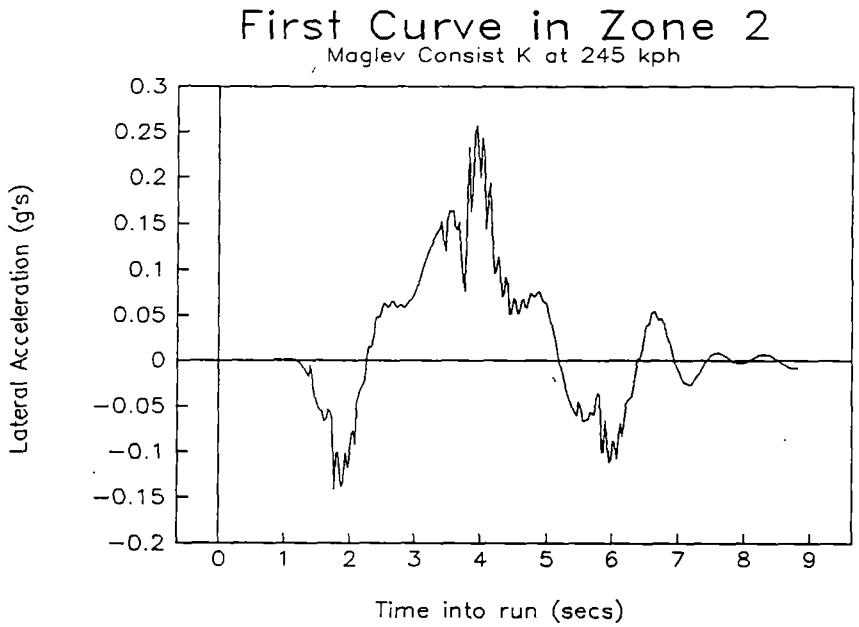

Figure 9-12. Body Lateral Acceleration during the Curve 2a from Zone 2 of the Very Severe Segment Test

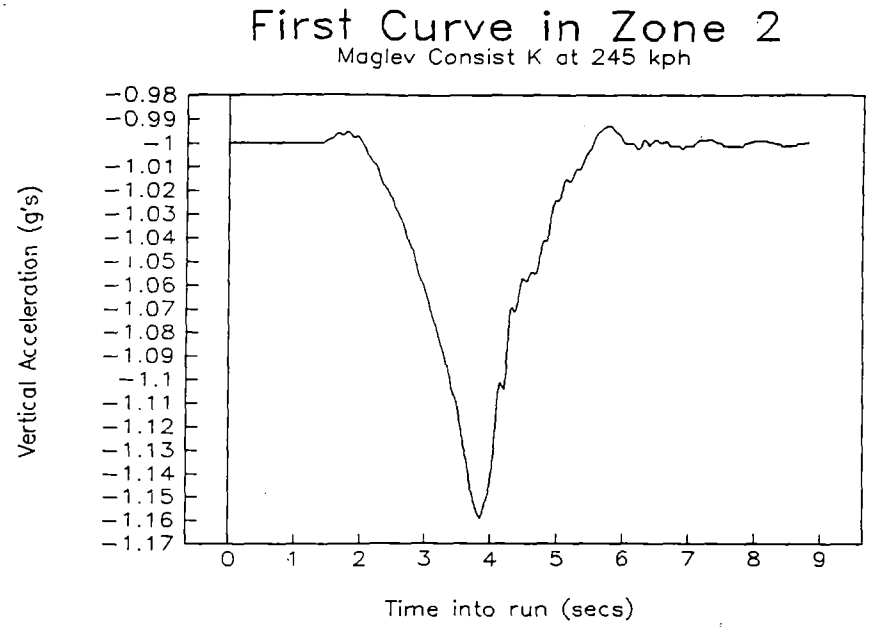

Figure 9-13. Body Vertical Acceleration during the Curve 2a from Zone 2 of the Very Severe Segment Test

than those consistent with the "design" ride specification, as expected, result in reduced ride comfort. Further consideration and analyses are desirable on the effect of randomly varying beam deflection between spans, modified shapes to the transitions and the coupling between guideway and vehicle frequencies.

The secondary suspension choice is dependent on the characteristics of the magnets and the MAGSIM coupled two-dimensional model for these is working well. The simulation program MAGSIM has the proven capability of allowing design parameters to be investigated for ride quality assessment as is indicated in the study undertaken.

PART III

SYSTEM CAPITAL AND OPERATING COSTS

REVISIONS				
ZONE	REV	DESCRIPTION	DATE	SIG

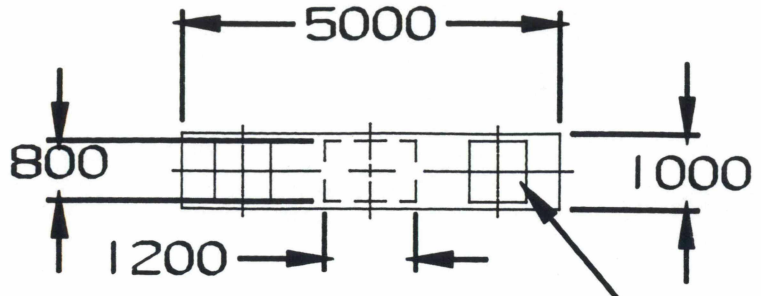

PYLON TOP
(TYPICAL)

SEAT PADS

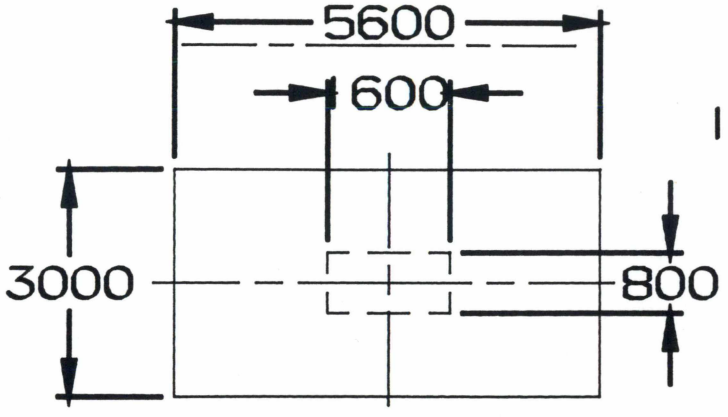

@ SIMPLE SUPPORT

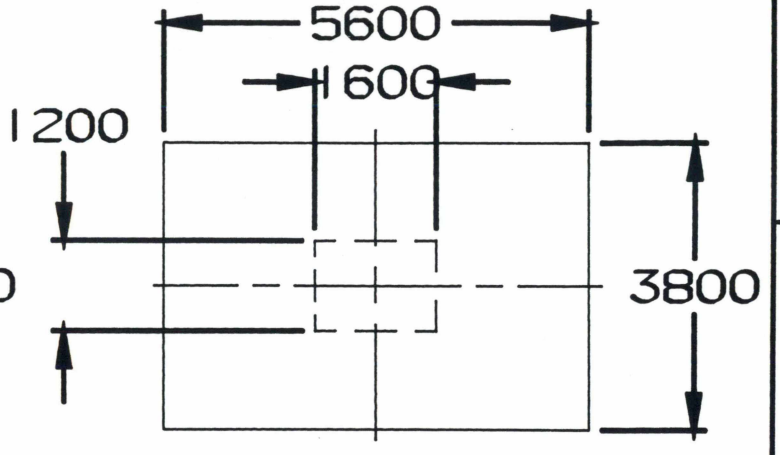

@ CONT. SUPPORT

FOOTING DETAILS
(TYPICAL)

UNLESS OTHERWISE SPECIFIED	DRAWN	FOSTER-MILLER, INC. 350 SECOND AVENUE WALTHAM, MA 02254
BREAK CORNERS .005-.015	CHECKED	
FRACT. ± / .X ± / .XX ± / .XXX ±	APPROVED	ELEVATED GUIDEWAY DETAILS
ANGLES ± / MACH. SURF. ✓ MAX.	APPLICATION	
MATERIAL	NEXT ASSY	SIZE A / FSCM 30233 / 9399104 / REV
HEAT TREATMENT	FINAL ASSY	
FINISH	MACHINE	SCALE 1/100 / WEIGHT / SHEET 1 OF 1
	PROJECT NO	

REVISIONS				
ZONE	REV	DESCRIPTION	DATE	SIG

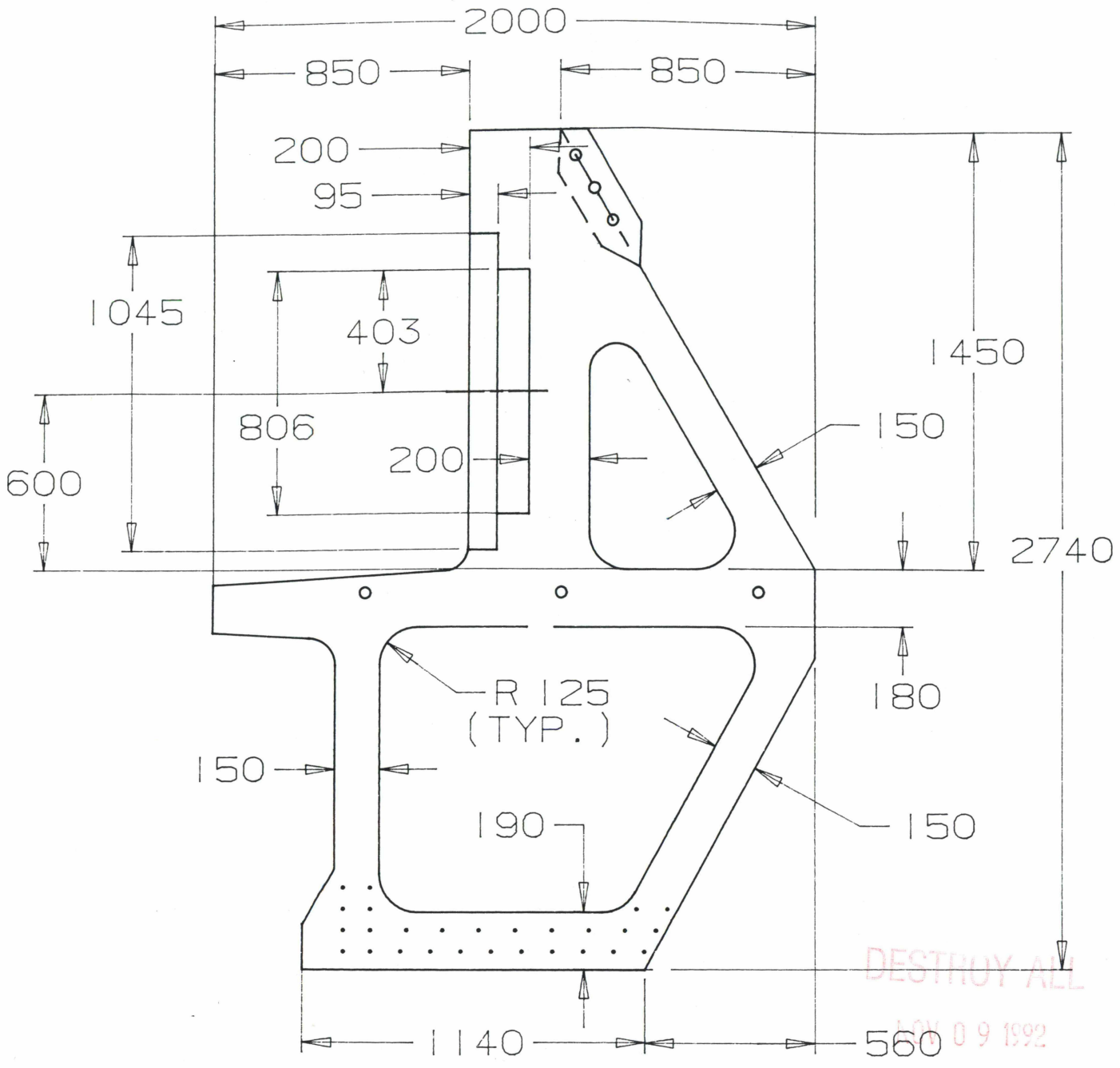

UNLESS OTHERWISE SPECIFIED	DRAWN	
BREAK CORNERS .005-.015	CHECKED	
FRACT. ± / .X ± / .XX ± / .XXX ±	APPROVED	
ANGLES ± / MACH. SURF. ✓ MAX.	APPLICATION	
MATERIAL	NEXT ASSY	
HEAT TREATMENT	FINAL ASSY	
FINISH	MACHINE	
	PROJECT NO	

FOSTER-MILLER, INC.
350 SECOND AVENUE WALTHAM, MA 02254

ELEVATED GUIDEWAY SIDE BEAM SECTION

SIZE	FSCM		REV
A	30233	9399105	
SCALE 1/20	WEIGHT	SHEET 1 OF 1	

REVISIONS				
ZONE	REV	DESCRIPTION	DATE	SIG

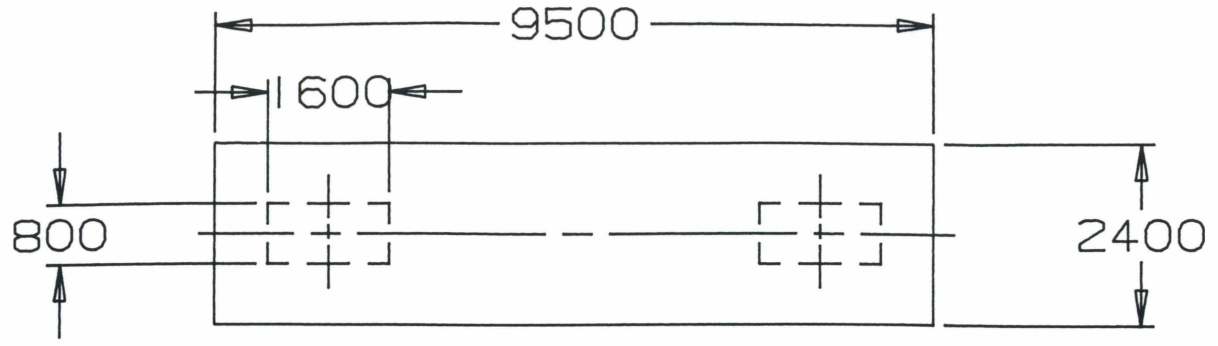

@ SIMPLE SUPPORT

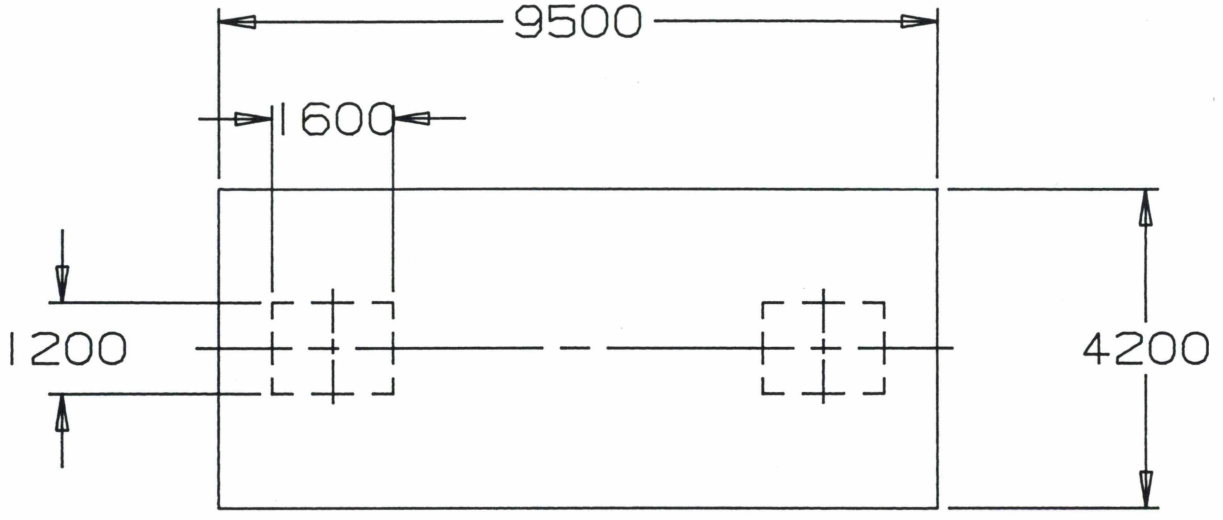

@ CONT. SUPPORT

FOOTING DETAILS
(TYPICAL)

UNLESS OTHERWISE SPECIFIED	DRAWN	FOSTER-MILLER, INC.
BREAK CORNERS .005-.015	CHECKED	350 SECOND AVENUE WALTHAM, MA 02254
FRACT. ± / .X ± / .XX ± / .XXX ±	APPROVED	ELEVATED GUIDEWAY DETAILS
ANGLES ± / MACH. SURF. ✓ MAX.	APPLICATION	
MATERIAL	NEXT ASSY	
HEAT TREATMENT	FINAL ASSY	SIZE A / FSCM 30233 / 9399106 / REV
FINISH	MACHINE	
	PROJECT NO	SCALE 1/100 / WEIGHT / SHEET 1 OF 1

REVISIONS				
ZONE	REV	DESCRIPTION	DATE	SIG

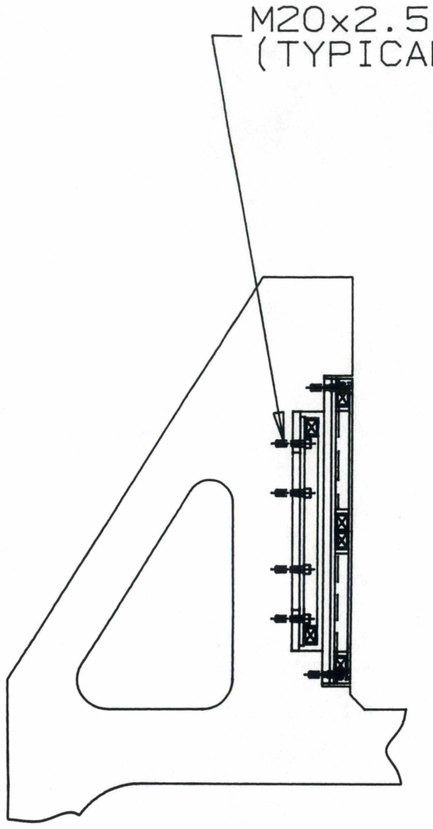

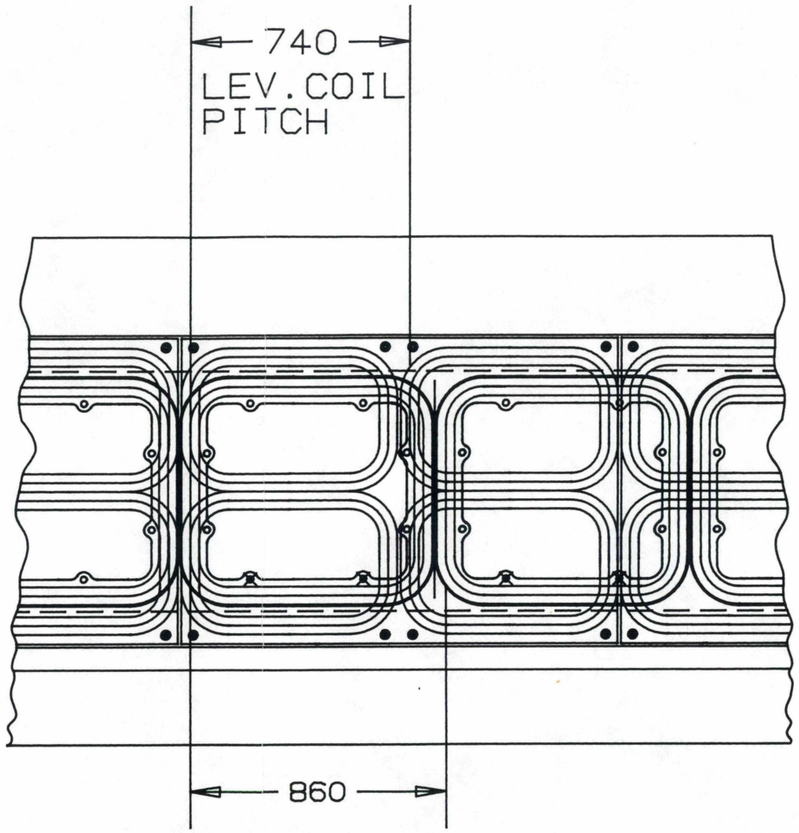

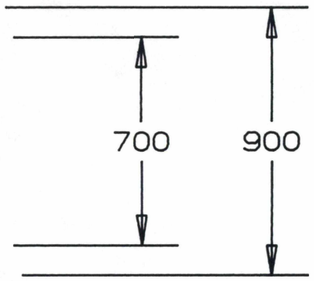

DESTROY ALL
NOV 0 9 1992
PREVIOUS PRINTS

UNLESS OTHERWISE SPECIFIED				DRAWN		
BREAK CORNERS .005-.015				CHECKED		
FRACT. ±	.X ±	.XX ±	.XXX ±	APPROVED		
ANGLES ±	MACH. SURF. ✓ MAX.			APPLICATION		
MATERIAL				NEXT ASSY		
HEAT TREATMENT				FINAL ASSY		
FINISH				MACHINE		
				PROJECT NO		

FOSTER-MILLER, INC.
350 SECOND AVENUE WALTHAM, MA 02254

GROUND COIL MOUNT DETAIL

SIZE	FSCM		REV
B	30233	9399107	1
SCALE 1/20	WEIGHT	SHEET 1 OF 1	

REVISIONS				
ZONE	REV	DESCRIPTION	DATE	SIG

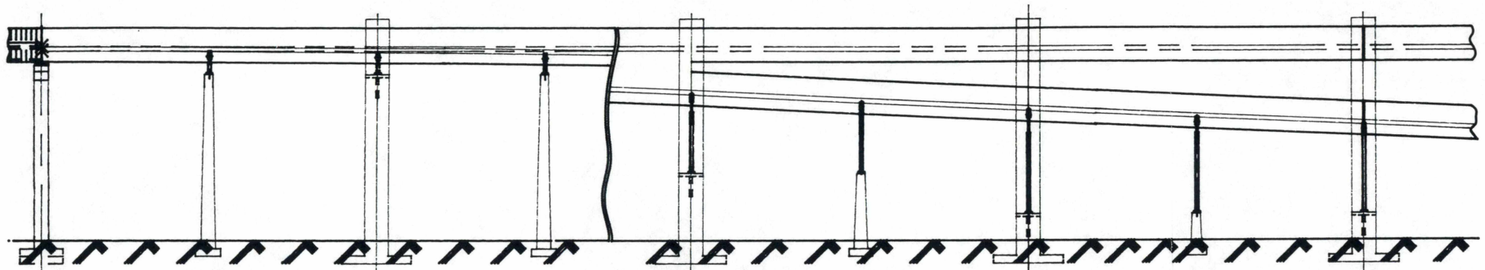

Sta. 0+00 | Sta. 0+22.50 | Sta. 1+35.00 | Sta. 1+57.50 | Sta. 1+80.00

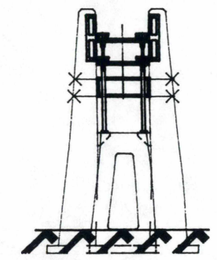

CROSS SECTION (TYPICAL)

UNLESS OTHERWISE SPECIFIED	DRAWN		
BREAK CORNERS .005-.015	CHECKED		
FRACT. ± / .X ± / .XX ± / .XXX ±	APPROVED		
ANGLES ± / MACH. SURF. ✓ MAX.	APPLICATION		
MATERIAL	NEXT ASSY		
HEAT TREATMENT	FINAL ASSY		
FINISH	MACHINE		
	PROJECT NO		

FOSTER-MILLER, INC.
350 SECOND AVENUE WALTHAM, MA 02254

ELEVATED GUIDEWAY VERTICAL SWITCH

SIZE	FSCM		REV
B	30233	9399200	
SCALE 1/400	WEIGHT	SHEET 1 OF 1	

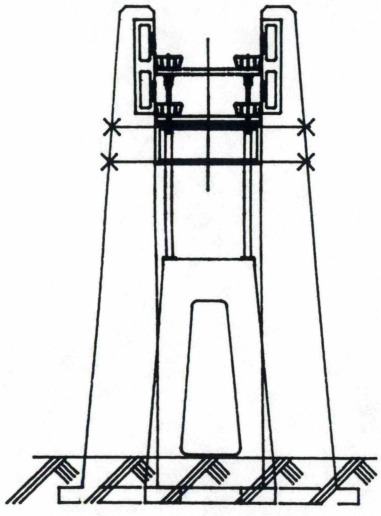

Sta 0+11.25

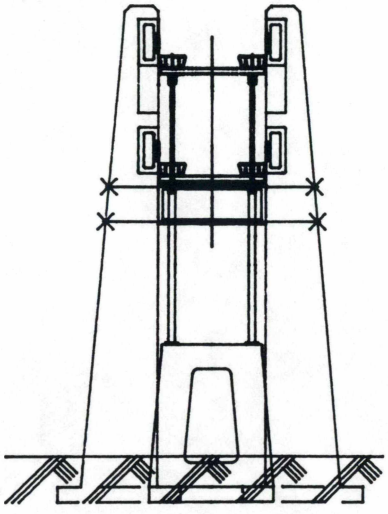

Sta 1+46.25

2 1

REVISIONS				
ZONE	REV	DESCRIPTION	DATE	SIG

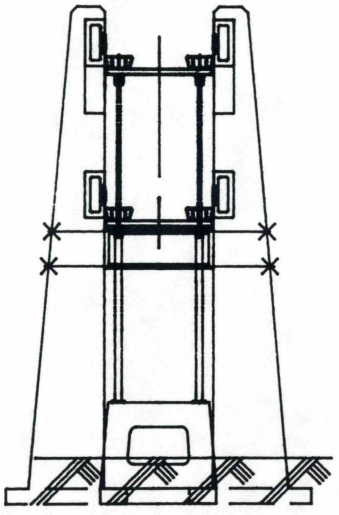

Sta 1+68.75

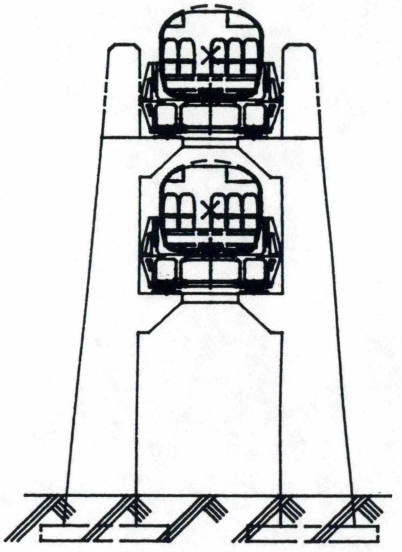

STA 1+80

UNLESS OTHERWISE SPECIFIED				DRAWN	
BREAK CORNERS .005-.015				CHECKED	
FRACT. ±	.X ±	.XX ±	.XXX ±	APPROVED	
ANGLES ±	MACH. SURF. ✓ MAX.			APPLICATION	
MATERIAL				NEXT ASSY	
HEAT TREATMENT				FINAL ASSY	
FINISH				MACHINE	
				PROJECT NO	

FOSTER-MILLER, INC.
350 SECOND AVENUE WALTHAM, MA 02254

VERTICAL SWITCH CROSS SECTION

SIZE	FSCM		REV
B	30233	9399201	

SCALE	WEIGHT	SHEET	OF
1/250		1	1

2 1

REVISIONS				
ZONE	REV	DESCRIPTION	DATE	SIG

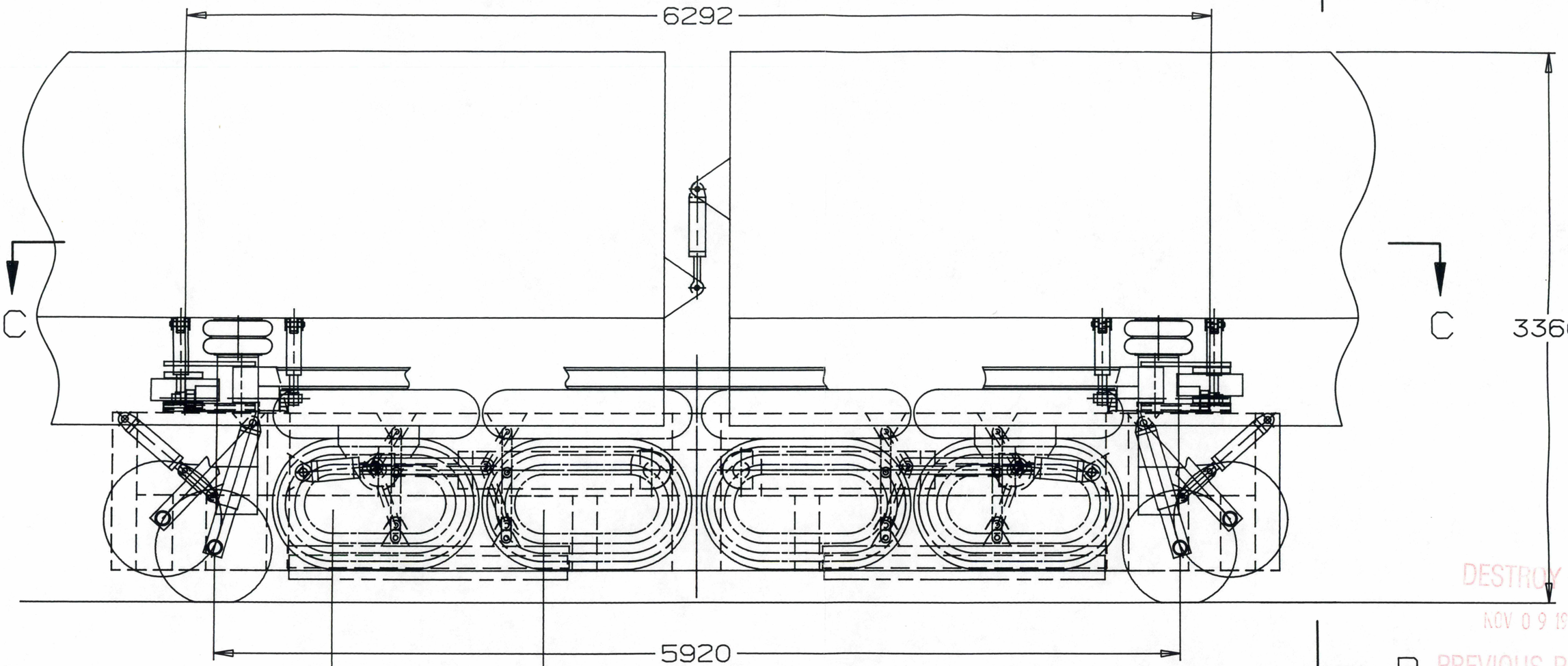

UNLESS OTHERWISE SPECIFIED				DRAWN		
BREAK CORNERS .005-.015				CHECKED		
FRACT. ±	.X ±	.XX ±	.XXX ±	APPROVED		
ANGLES ±	MACH. SURF. ✓ MAX.			APPLICATION		
MATERIAL				NEXT ASSY		
HEAT TREATMENT				FINAL ASSY		
FINISH				MACHINE		
				PROJECT NO		

FOSTER-MILLER, INC.
350 SECOND AVENUE WALTHAM, MA 02254

INSTALLED BOGIE ASSEMBLY

SIZE	FSCM		REV
B	30233	9399300	1
SCALE 1/25	WEIGHT	SHEET 1 OF 6	

REVISIONS				
ZONE	REV	DESCRIPTION	DATE	SIG

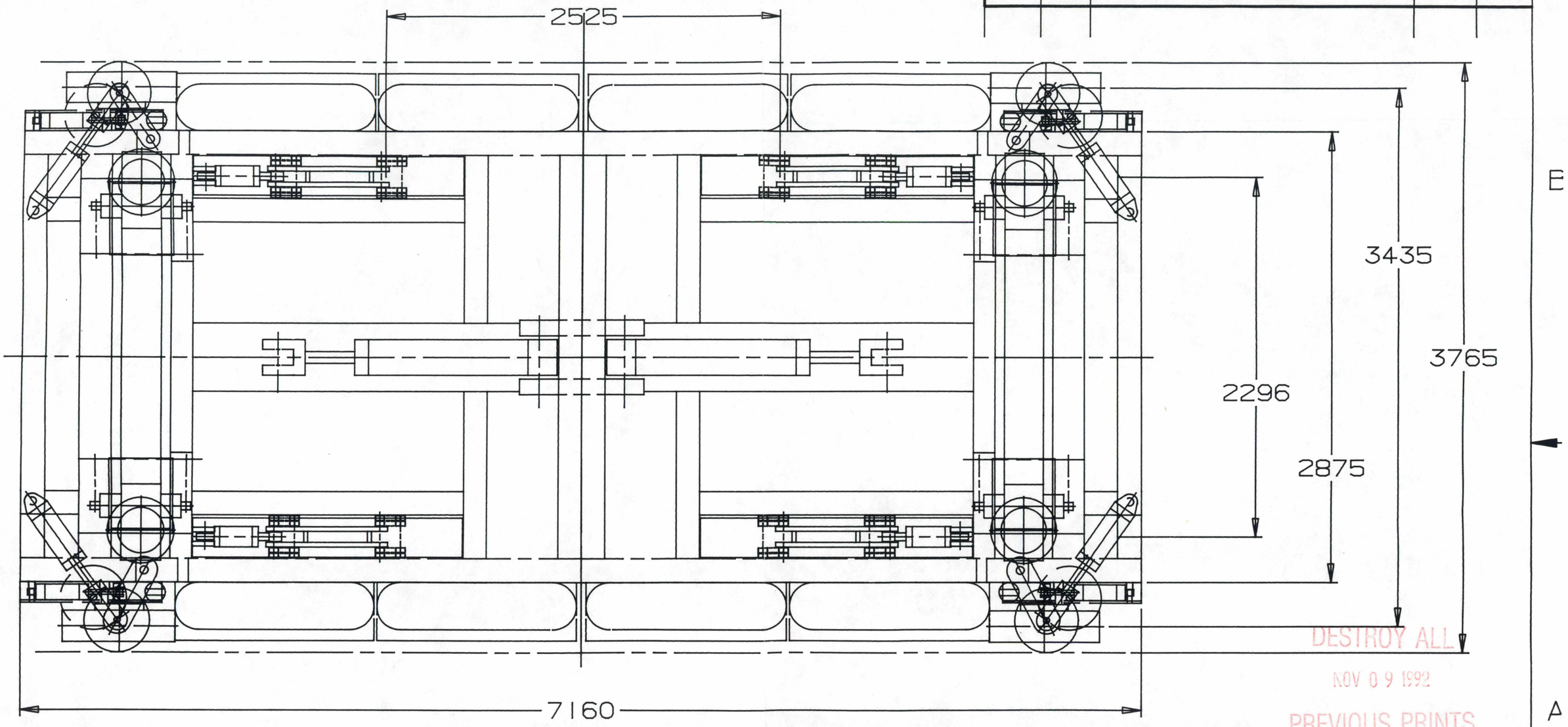

SECTION C-C

UNLESS OTHERWISE SPECIFIED			DRAWN	
BREAK CORNERS .005-.015			CHECKED	
FRACT. ±	.X ±	.XX ±	.XXX ±	APPROVED
ANGLES ±	MACH. SURF. ✓ MAX.			APPLICATION
MATERIAL			NEXT ASSY	
HEAT TREATMENT			FINAL ASSY	
FINISH			MACHINE	
			PROJECT NO	

FOSTER-MILLER, INC.
350 SECOND AVENUE WALTHAM, MA 02254

INSTALLED BOGIE ASSEMBLY

SIZE	FSCM		REV
B	30233	9399300	1
SCALE 1/25	WEIGHT		SHEET 2 OF 6

REVISIONS				
ZONE	REV	DESCRIPTION	DATE	SIG

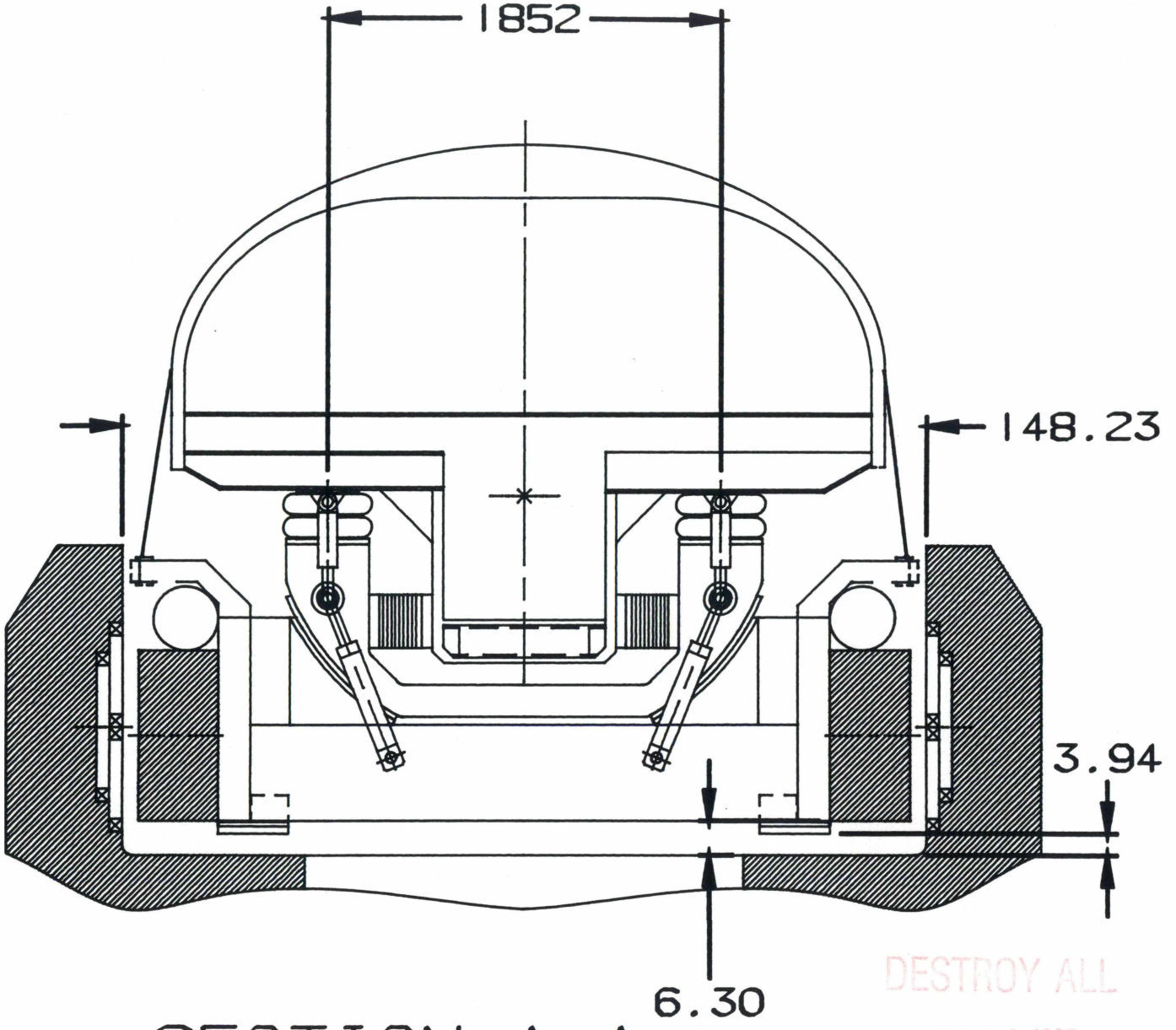

SECTION A-A

UNLESS OTHERWISE SPECIFIED	DRAWN	
BREAK CORNERS .005-.015	CHECKED	
FRACT. ± / .X ± / .XX ± / .XXX ±	APPROVED	
ANGLES ± / MACH. SURF. ✓ MAX.	APPLICATION	
MATERIAL	NEXT ASSY	
HEAT TREATMENT	FINAL ASSY	
FINISH	MACHINE	
	PROJECT NO	

FOSTER-MILLER, INC.
350 SECOND AVENUE WALTHAM, MA 02254

INSTALLED BOGIE ASSEMBLY

SIZE	FSCM		REV
A	30233	9399300	

SCALE 1/30 | WEIGHT | SHEET 3 OF 6

REVISIONS				
ZONE	REV	DESCRIPTION	DATE	SIG

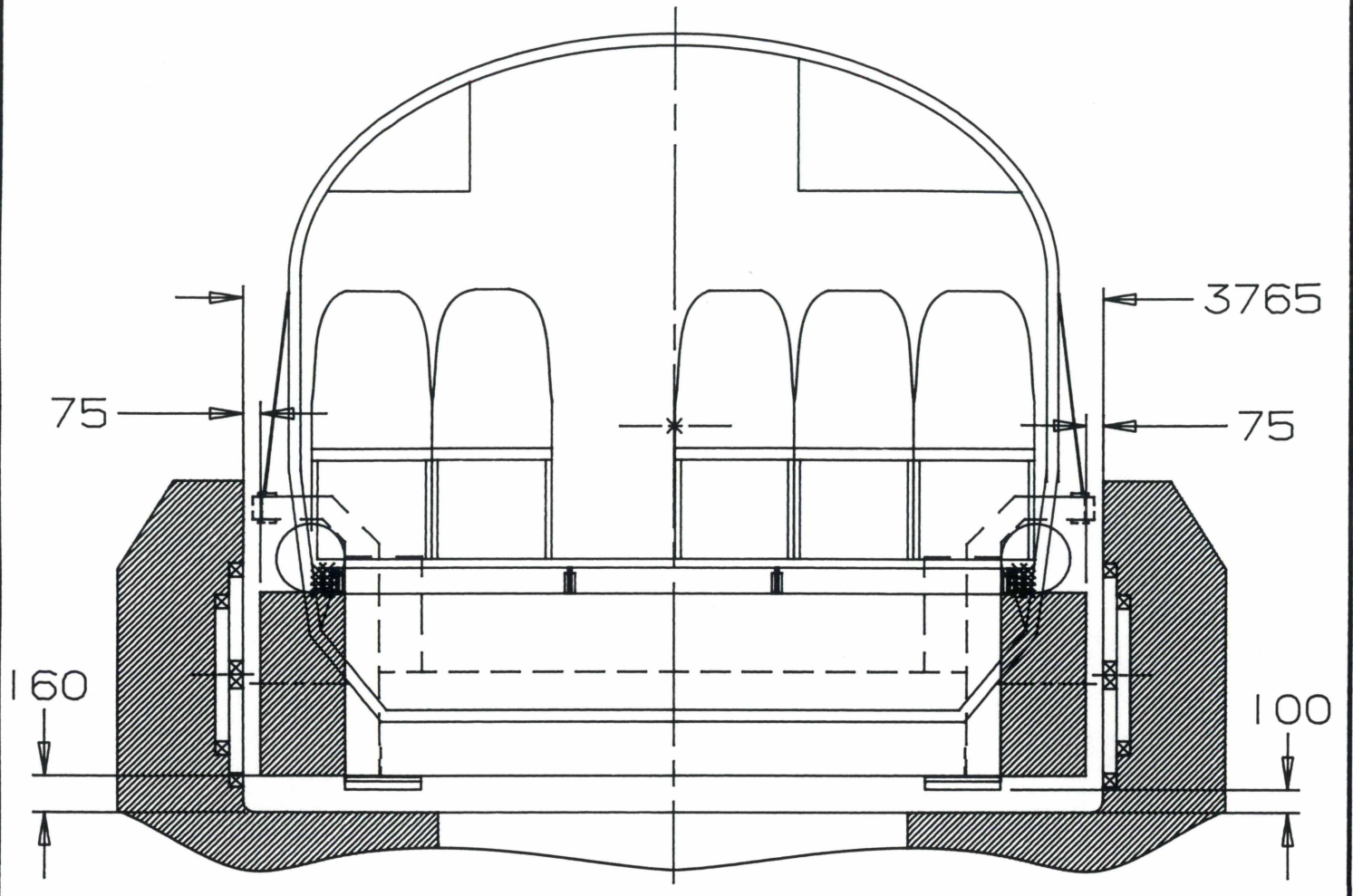

SECTION B-B

UNLESS OTHERWISE SPECIFIED	DRAWN	FOSTER-MILLER, INC.
BREAK CORNERS .005-.015	CHECKED	350 SECOND AVENUE WALTHAM, MA 02254
FRACT. ± / .X ± / .XX ± / .XXX ±	APPROVED	INSTALLED BOGIE ASSEMBLY
ANGLES ± / MACH. SURF. ✓ MAX.	APPLICATION	
MATERIAL	NEXT ASSY	SIZE A / FSCM 30233 / 9399300 / REV 1
HEAT TREATMENT	FINAL ASSY	
FINISH	MACHINE	
	PROJECT NO	SCALE 1/30 / WEIGHT / SHEET 4 OF 6

REVISIONS				
ZONE	REV	DESCRIPTION	DATE	SIG
	1	CAR BODY MODIFIED	10/6/92	

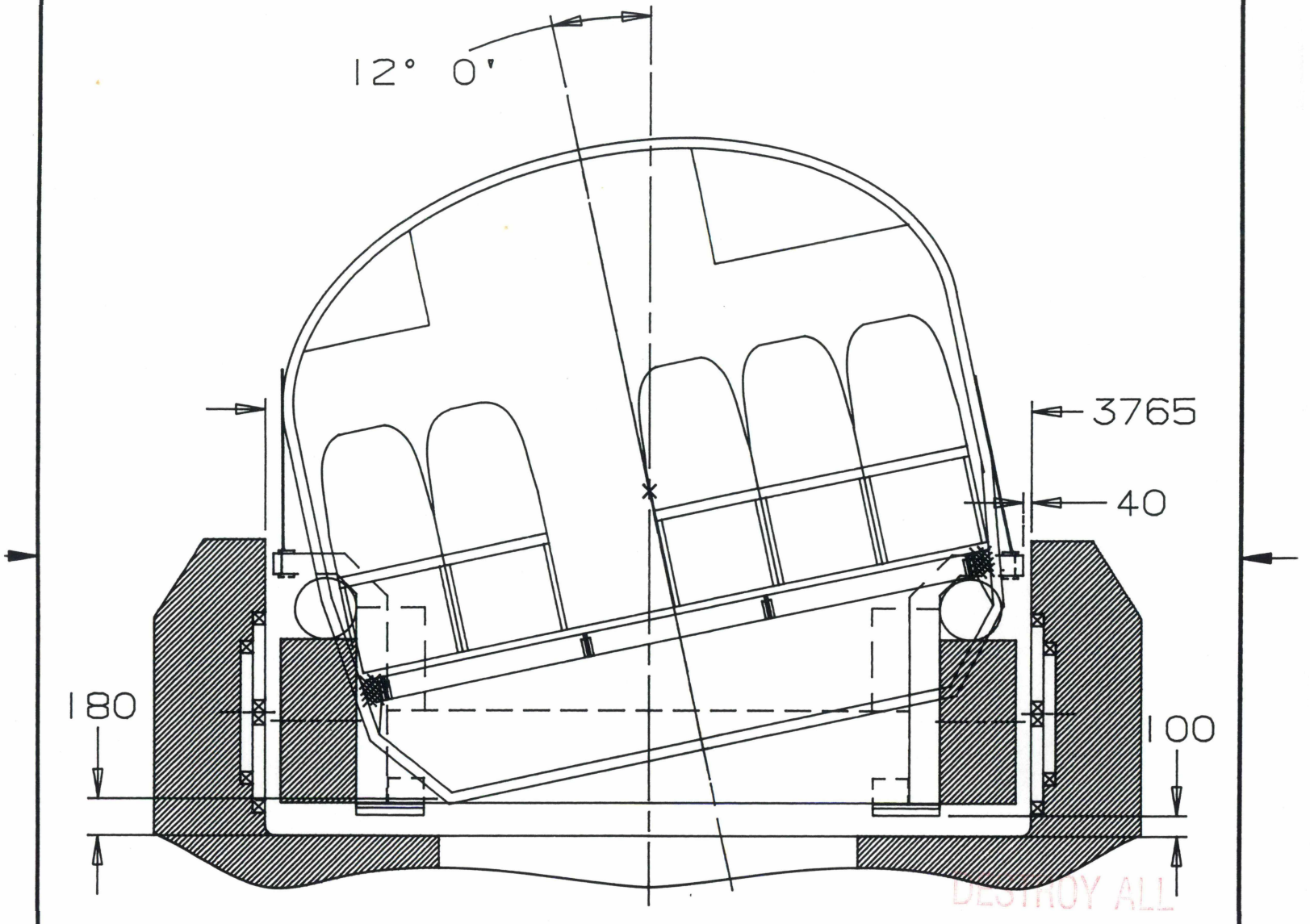

SECTION B-B
(AT FULL TILT)

UNLESS OTHERWISE SPECIFIED	DRAWN	
BREAK CORNERS .005-.015	CHECKED	
FRACT. ± / .X ± / .XX ± / .XXX ±	APPROVED	
ANGLES ± / MACH. SURF. ✓ MAX.	APPLICATION	
MATERIAL	NEXT ASSY	
HEAT TREATMENT	FINAL ASSY	
FINISH	MACHINE	
	PROJECT NO	

FOSTER-MILLER, INC.
350 SECOND AVENUE WALTHAM, MA 02254

INSTALLED BOGIE ASSEMBLY

SIZE	FSCM		REV
A	30233	9399300	1

SCALE 1/30 | WEIGHT | SHEET 5 OF 6

REVISIONS				
ZONE	REV	DESCRIPTION	DATE	SIG

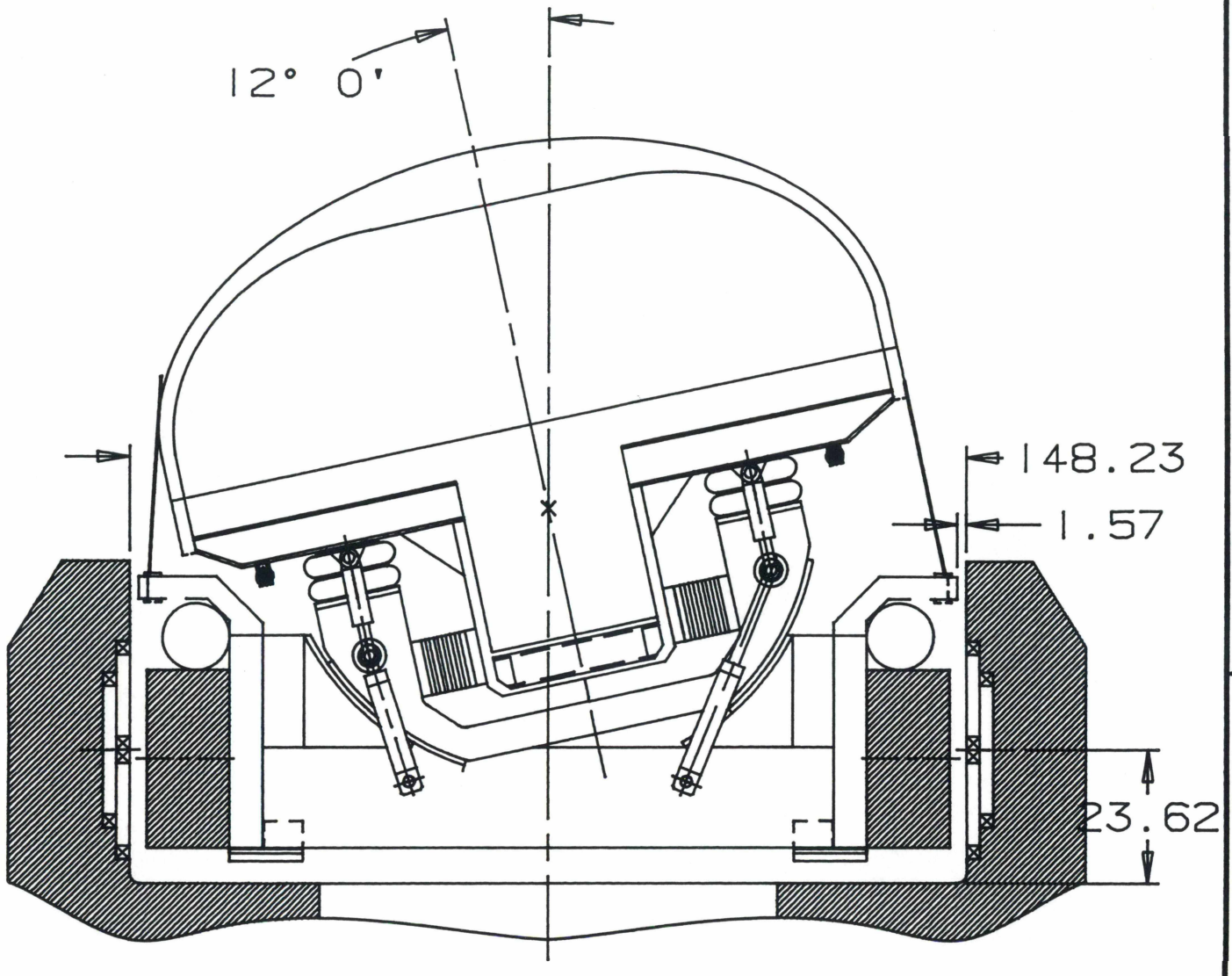

SECTION A-A

(AT FULL TILT)

UNLESS OTHERWISE SPECIFIED		DRAWN			FOSTER-MILLER, INC. 350 SECOND AVENUE WALTHAM, MA 02254
BREAK CORNERS .005-.015		CHECKED			
FRACT. ±	.X ±	APPROVED			INSTALLED BOGIE ASSEMBLY
.XX ±	.XXX ±	APPLICATION			
ANGLES ±	MACH. SURF. ✓ MAX.	NEXT ASSY			SIZE A | FSCM 30233 | 9399300 | REV
MATERIAL		FINAL ASSY			
HEAT TREATMENT		MACHINE			SCALE 1/30 | WEIGHT | SHEET 6 OF 6
FINISH		PROJECT NO			

REVISIONS				
ZONE	REV	DESCRIPTION	DATE	SIG

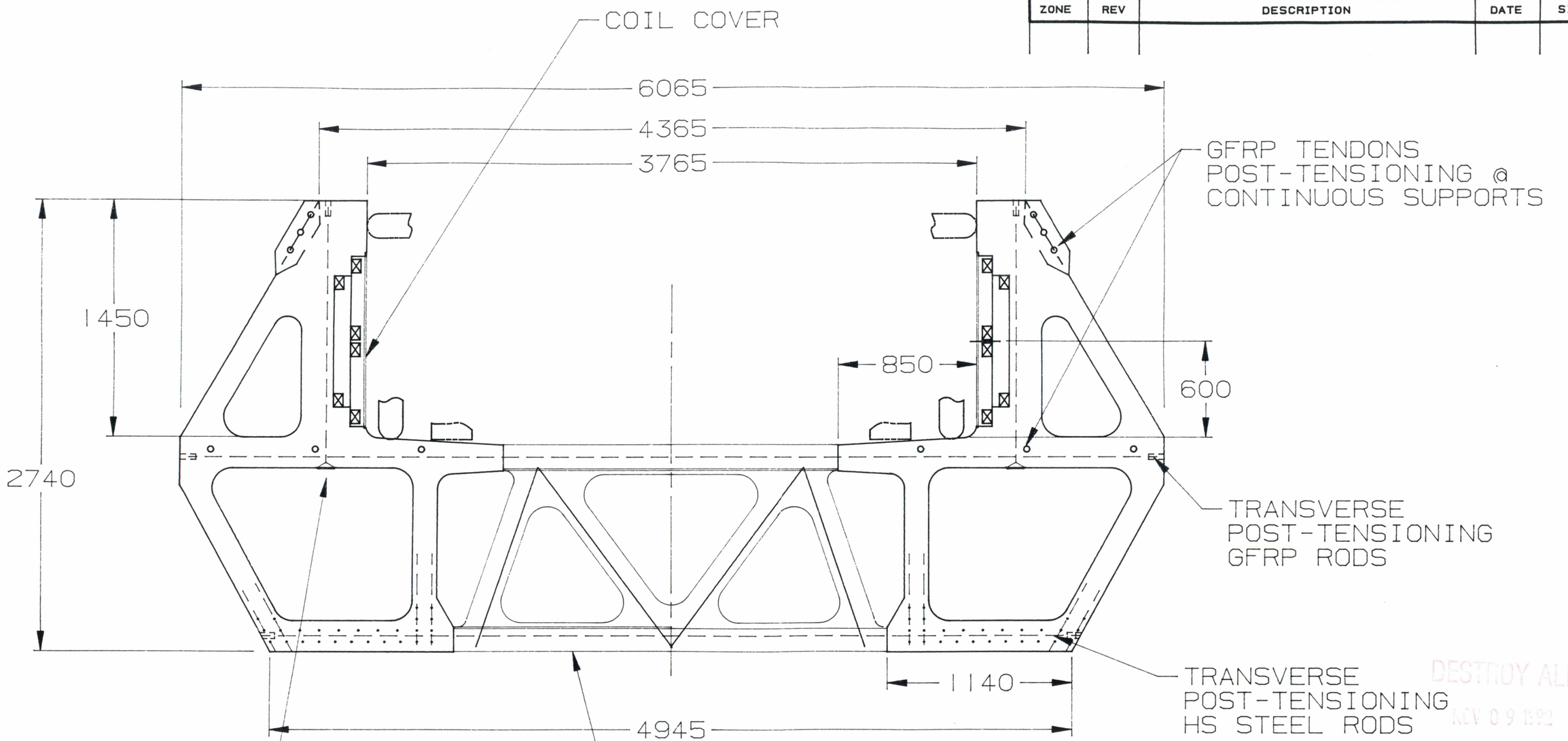

DIMENSIONS IN mm

UNLESS OTHERWISE SPECIFIED			DRAWN		
BREAK CORNERS .005-.015			CHECKED		
FRACT. ±	.X ±	.XX ±	.XXX ±	APPROVED	
ANGLES ±	MACH. SURF. ✓ MAX.			APPLICATION	
MATERIAL				NEXT ASSY	
HEAT TREATMENT				FINAL ASSY	
FINISH				MACHINE	
				PROJECT NO	

FOSTER-MILLER, INC.
350 SECOND AVENUE WALTHAM, MA 02254

ELEVATED GUIDEWAY ASSEMBLY SECTION

SIZE	FSCM		REV
B	30233	9399101	
SCALE 1/25	WEIGHT	SHEET 1 OF 1	

REVISIONS				
ZONE	REV	DESCRIPTION	DATE	SIG

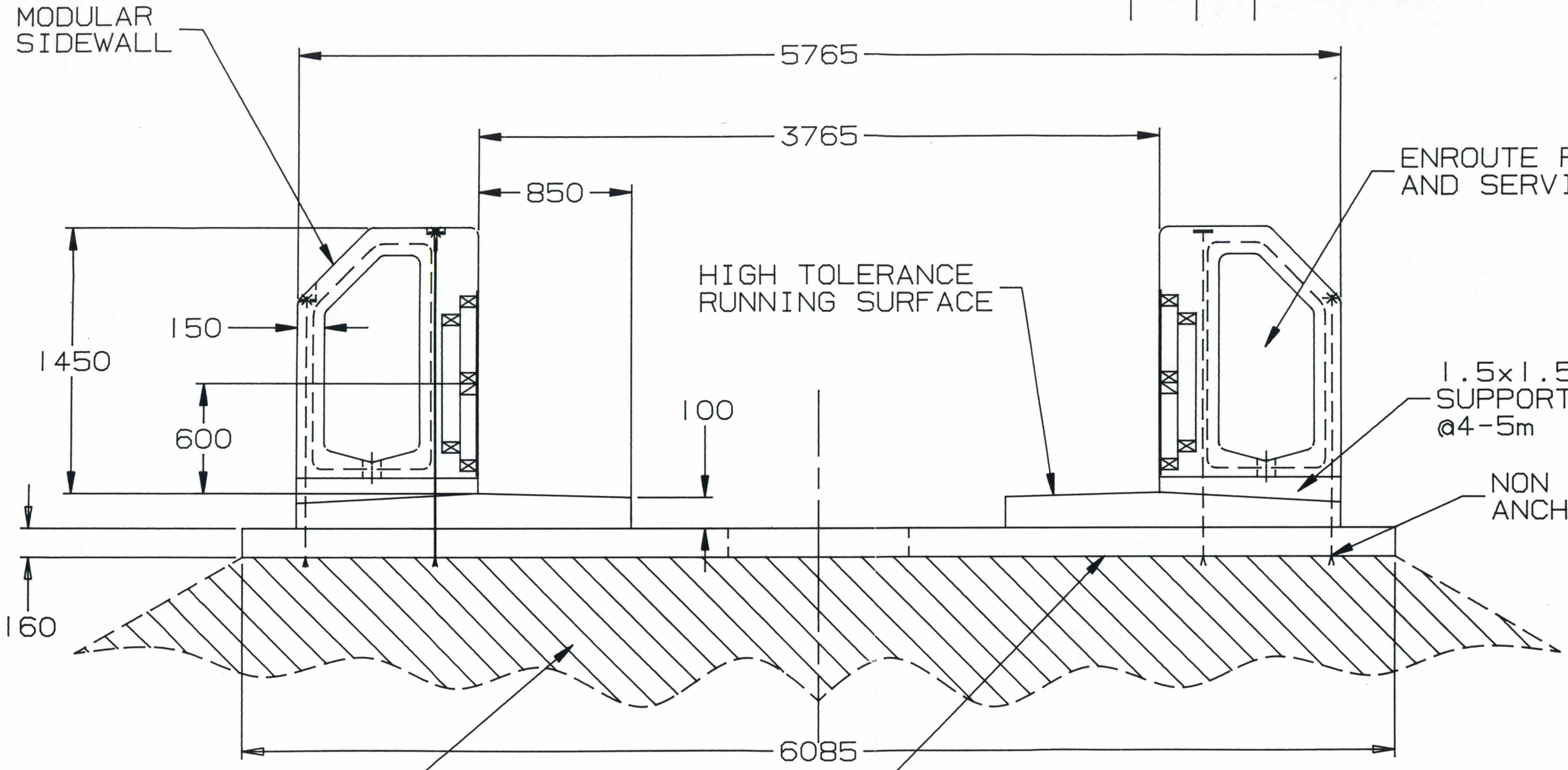

UNLESS OTHERWISE SPECIFIED	DRAWN	FOSTER-MILLER, INC.
BREAK CORNERS .005-.015	CHECKED	350 SECOND AVENUE WALTHAM, MA 02254
FRACT. ± / .X ± / .XX ± / .XXX ±	APPROVED	AT-GRADE GUIDEWAY CROSS SECTION
ANGLES ± / MACH. SURF. ✓ MAX.	APPLICATION	
MATERIAL	NEXT ASSY	SIZE B / FSCM 30233 / 9399102 / REV
HEAT TREATMENT	FINAL ASSY	
FINISH	MACHINE	SCALE 1/25 / WEIGHT / SHEET 1 OF 1
	PROJECT NO	

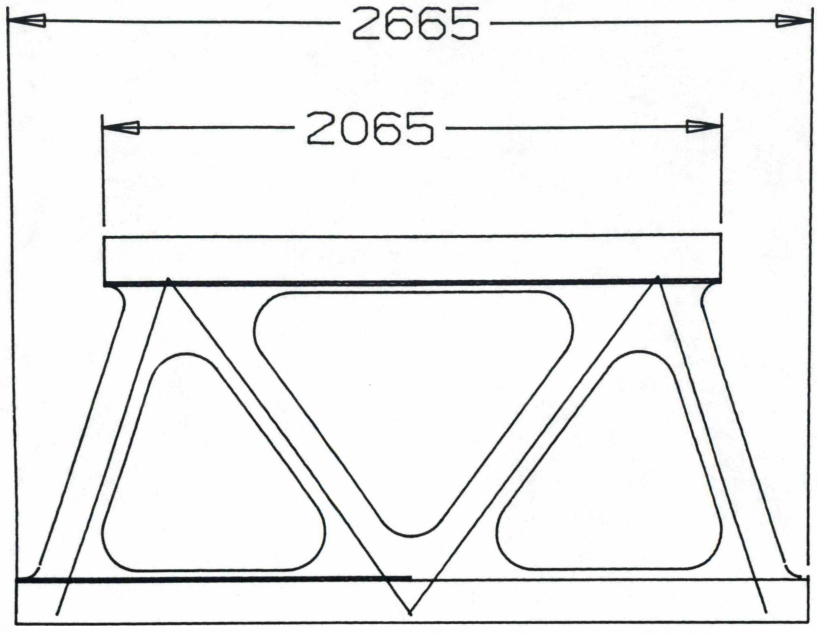

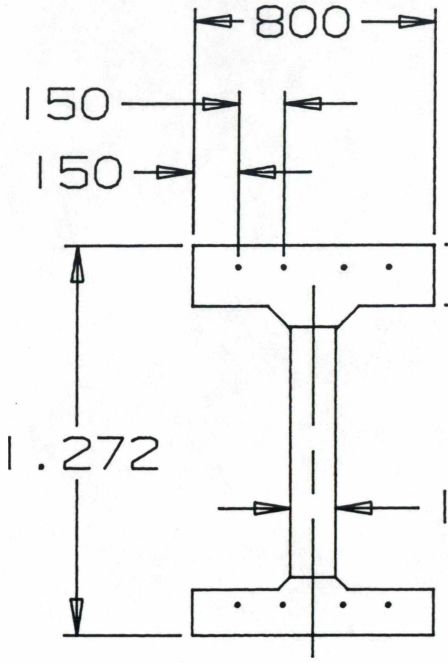

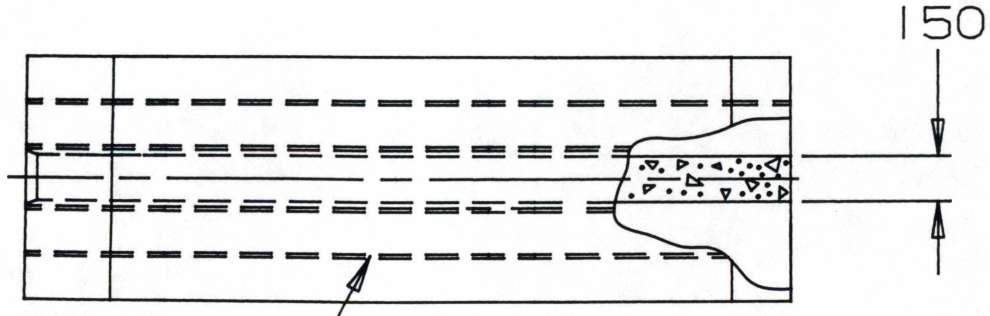

DIAPHRAGM

Ø12mm SHEATH FOR
Ø7.5mm GFRP RODS

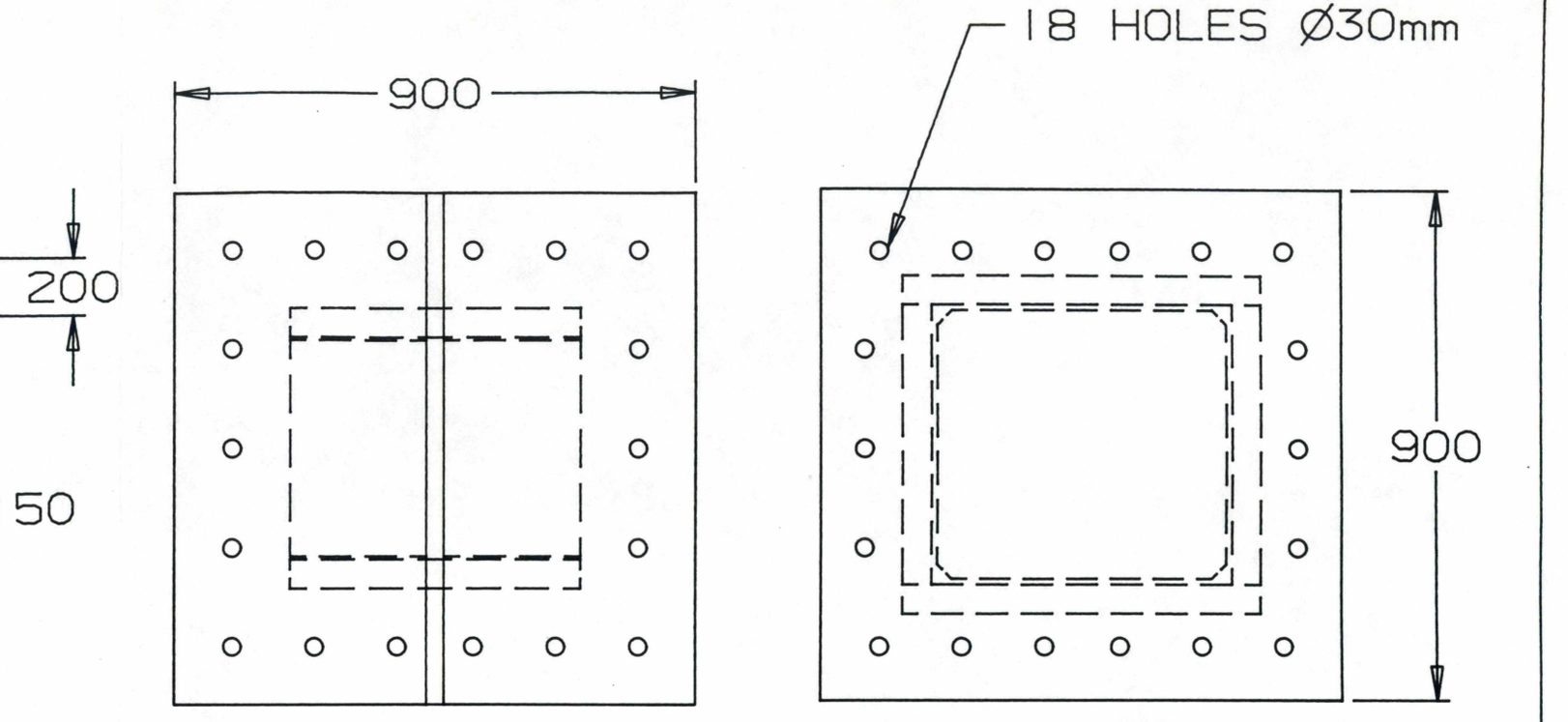

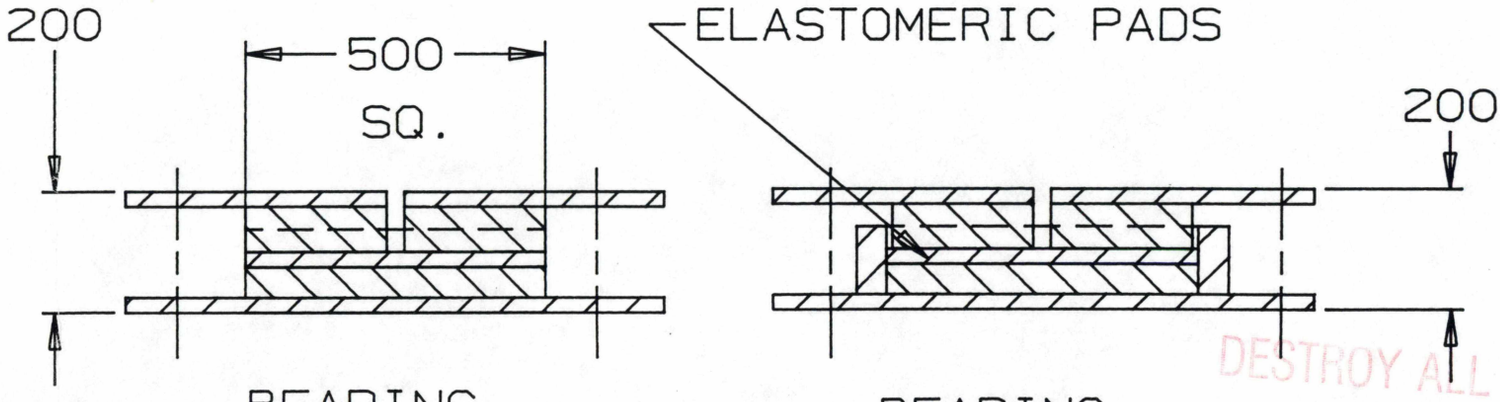

BEARING
@ S. SUPPORT

BEARING
@C. SUPPORT

UNLESS OTHERWISE SPECIFIED	DRAWN		
BREAK CORNERS .005-.015	CHECKED		
FRACT. ± / .X ± / .XX ± / .XXX ±	APPROVED		
ANGLES ± / MACH. SURF. ✓ MAX.	APPLICATION		
MATERIAL	NEXT ASSY		
HEAT TREATMENT	FINAL ASSY		
FINISH	MACHINE		
	PROJECT NO		

FOSTER-MILLER, INC.
350 SECOND AVENUE WALTHAM, MA 02254

ELEVATED GUIDEWAY DETAILS

SIZE	FSCM		REV
B	30233	9399103	
SCALE 1/25	WEIGHT	SHEET	OF

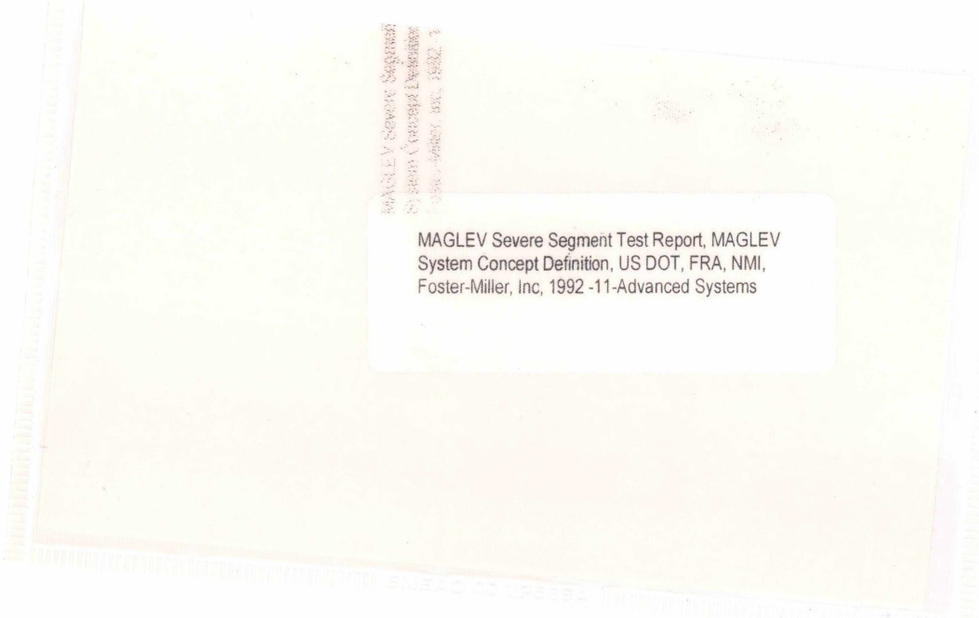

MAGLEV Severe Segment Test Report, MAGLEV System Concept Definition, US DOT, FRA, NMI, Foster-Miller, Inc, 1992 -11-Advanced Systems